Studies on Continuous Pre- to Post-Reperfusion Intra-Carotid Artery Cold Infusion for Neuroprotection in a Rodent Model of Acute Ischemic Stroke

Dissertation

zur Erlangung des Grades eines
Doktors der Naturwissenschaften

der Mathematisch-Naturwissenschaftlichen Fakultät
und
der Medizinischen Fakultät
der Eberhard-Karls-Universität Tübingen

vorgelegt
von

Yi Wang
aus *Chongqing*, *Volksrepublik China*

2026

Tag der mündlichen Prüfung: .....06.02.2026.....

Dekan der Math.-Nat. Fakultät: Prof. Dr. Thilo Stehle
Dekan der Medizinischen Fakultät: Prof. Dr. med. Sara Y. Brucker

1. Berichterstatter: Prof. Dr. Sven Poli

2. Berichterstatter: Prof. Dr. Jonas Neher

Prüfungskommission: Prof. Dr. Sven Poli

Prof. Dr. Jonas Neher

Prof. Dr. Constantin Roder

Prof. Dr. Cornelius Schwarz

Erklärung / Declaration:

Ich erkläre, dass ich die zur Promotion eingereichte Arbeit mit dem Titel:

„Studies on Continuous Pre- to Post-Reperfusion Intra-Carotid Artery Cold Infusion for Neuroprotection in a Rodent Model of Acute Ischemic Stroke“

selbständig verfasst, nur die angegebenen Quellen und Hilfsmittel benutzt und wörtlich oder inhaltlich übernommene Stellen als solche gekennzeichnet habe. Ich versichere an Eides statt, dass diese Angaben wahr sind und dass ich nichts verschwiegen habe. Mir ist bekannt, dass die falsche Abgabe einer Versicherung an Eides statt mit Freiheitsstrafe bis zu drei Jahren oder mit Geldstrafe bestraft wird.

I hereby declare that I have produced the work entitled “ Studies on Continuous Pre- to Post-Reperfusion Intra-Carotid Artery Cold Infusion for Neuroprotection in a Rodent Model of Acute Ischemic Stroke ”, submitted for the award of a doctorate, on my own (without external help), have used only the sources and aids indicated and have marked passages included from other works, whether verbatim or in content, as such. I swear upon oath that these statements are true and that I have not concealed anything. I am aware that making a false declaration under oath is punishable by a term of imprisonment of up to three years or by a fine.

Tübingen, den ....

Datum / Date Unterschrift /Signature

Table of Content

Summary

Background

Systemic hypothermia is so far the only proven effective neuroprotective strategy in neonatal hypoxia brain disease. In acute ischemic stroke the low cooling efficacy as well as the adverse side effects of whole-body cooling limited its clinical translation. Supported by numerous animal studies, local hypothermia via selective brain cooling methods could achieve comparable neuroprotective effects in acute ischemic stroke. Due to thicker cranial structure and large cerebral blood flow, conventional cooling devices / methods could hardly induce local therapeutic hypothermia in human.

By taking advantage of the large cerebral blood flow, intra-carotid cold infusion (ICCI) has been proven the most efficient strategy for local brain hypothermia induction. Its easy implementation into endovascular treatment (EVT) of acute ischemic stroke has been also confirmed in several recent clinical pilot studies. In middle cerebral artery occlusion rodent studies, ICCI administered either pre- or post-reperfusion has showed its neuroprotective effects. However, whether continuous pre- to post-reperfusion, i.e., hypothermia is initiated as soon as the first catheter pathway is established and throughout the whole EVT process, brings more pronounced neuroprotective effects is unclear. Rodent models that allow for testing pre- to post-reperfusion ICCI are also absent.

Objectives

The objectives of this study are therefore 1) To establish a novel infusion system that permits continuous pre- to post-reperfusion cold fluid delivery via carotid artery in a filament middle cerebral artery occlusion rat model. 2) To establish a reproducible cold infusion protocol for maintaining moderate local brain hypothermia of around 32 °C during the whole infusion period. 3) To evaluate the impact of continuous pre- to post-reperfusion ICCI on infarct volume, brain edema and neurofunction. 4) To investigate the impact of continuous pre- to post-reperfusion ICCI on hemorrhagic infarct transformation, systemic physiological parameters, the cerebral blood flow and blood parameters.

Methods

In this study, middle cerebral artery occlusion models were established in adult male Sprague-Dawley rats with filament method. In experiment part I, firstly, an infusion port was designed with a 21Gauge infusion cannula. Which was bent and close to its tip a side hole was

drilled. The connection part of the infusion port was further coated with elastic silicone. A longitudinal concavity was molded by imprinting of the filament thread into the elastic silicone on the convex surface in order to further avoid fluid leakage during infusion. A commercially available SC-20 heater/cooler was used for cooling the infusate (target temperature: 0 °C to 1 °C). To prevent the rewarming effect of ambient room temperature on cooled infusate, a secondary closed loop was integrated between the outlet of the SC-20 heater/cooler and the connection part of the infusion port. Further, cooling performance of the modified infusion system at a range of infusion rates (0.2 mL/min to 2.0 mL/min) was tested by directly monitoring bilateral cortical and striatal brain temperatures. Based on the brain temperature drop, a continuous pre- to post-reperfusion infusion protocol with total saline volume corresponding to half of the total circulatory blood volume (i.e. 30 mL/kg of body weight) was established and its reproducibility was tested.

In experiment part II, middle cerebral artery occlusion of 100 minutes was exerted on rats from four groups, including control group (CTRL), ICCI, intra-carotid artery warm infusion group (ICWI, saline temperature 37°C) and intra-venous cold infusion group (number of animals, n = 23 / group). Cerebral blood flow was continuously monitored with laser Doppler flowmetry (LDF) during the whole experiment period. Rats with residual LDF value lower than 40% of baseline were considered as successful middle cerebral artery occlusion and randomized for flowing treatment. All the infusion groups received the same infusion protocol with the modified cooling system. At 24 hours after treatment, brains were collected and stained with 2% 2, 3, 5 - triphenyltetrazolium chloride (TTC) for infarct volume and brain edema evaluation. Neurofunctional tests were performed at 1 hour before operation and at 24 hours after treatment. Blood parameters were measured at 20 minutes before, 50 minutes after middle cerebral artery occlusion, and immediately after infusion.

In experiment part III, rats received 60-minute middle cerebral artery occlusion and baseline cerebral ischemia was controlled with MRI (ADC maps, perfusion-MRI, T2-MRI) before randomized to ICCI group or CTRL (n = 13 / group). The same infusion protocol/cooling system was applied as in experiment Parts I and II. Another two sessions of MRI scanning were performed at 24 hours and 2 weeks after treatment. With PMOD software, thresholds that predict the lesion volume at 24-hour ADC maps, infarct volume on 2-week T2-MRI were determined in control group. Those thresholds were then applied in ICCI group for generating the predictive lesion and infarct volumes, which were then compared with actually

measured lesion volume and infarct volume on 24-hour ADC maps and 2-week T2-MRI respectively. Cerebral edema was measured at 24 hours post-reperfusion and neurofunctional tests were performed before middle cerebral artery occlusion, on day 2, 4, 6, 9, 13 after treatment.

Results

With our infusion system, continuous pre- to post-reperfusion ICCI could be successfully realized in rats. Normal saline (~ 0 °C) was successfully delivered into the internal carotid artery without interruption of middle cerebral artery occlusion. The time point of reperfusion could be also easily controlled by simply withdraw the filament end. Maximum brain cooling rate before reperfusion was achieved with ICCI at 0.5 mL/min. Ischemic striatal temperature was decreased by 2.3 ± 0.3 °C within 2 minutes. After reperfusion, ICCI was increased to 2 mL/min for 42 seconds to prevent the rewarming effect of restored cerebral blood flow. Based on which, brain temperature could be further maintained at 32.1 ± 0.3 °C at 0.7 mL/min ICCI over a duration of 14.6 ± 0.8 min.

At 24 hours after reperfusion / treatment, neither infarct volume nor brain edema evaluated on TTC staining exhibited inter-group difference ($P > 0.05$). In the post-hoc analysis, moderate ischemic rats (residual LDF value > 25% of baseline) were found with smaller infarct volume, less extent of edema and better preserved neurofunction in ICCI group in comparison with other groups, however no statistical significance was achieved. In experiment part III, lesion volume on 24-hour ADC maps and final infarct volume on 2-week T2-MRI were respectively 47.1 ± 37.7 mm^3 , 51.6 ± 45.6 mm^3, they were significant smaller than the predictive infarct volume generated on baseline ADC maps (versus predictive volume 71.0 ± 40.1 mm^3, $p = 0.011$ and $p = 0.007$, respectively) . No significant lesion or infarct volume decrease was found in striatum, but a less extent of edema was observed (41.8 ± 15.9% versus 27.6 ± 14.5% in the striatum ($p = 0.021$). ICCI treated rats tended to have better neurofunctional performance, however statistical significance could not be concluded at majority of the evaluation time points.

In the physiological parameters measurement, core body temperature decreased (versus baseline) by 0.7 ± 1.0 °C and 2.5 ± 0.5 °C in ICCI group and intra-venous cold infusion group respectively. But ICCI exerted more obvious impact on regional cerebral blood flow and mean arterial pressure during the pre-reperfusion phase. ICCI had minor impact on blood gas in

contrast to intra-venous cold infusion group. In addition, hemorrhagic transformation was observed in 2 out of 10 rats in the control group and in 5 out of 11 rats in the ICCI group on MRI at 2-week post-reperfusion.

Conclusion

In conclusion, with our infusion system, continuous pre- to post-reperfusion ICCI via intra-carotid artery could be easily realized. The neuroprotective effects of ICCI under the infusion protocol applied in the present study could only be observed in the cortex after shorter ischemia duration (60 minutes). It implies that patients with larger malignant infarction should be excluded in future clinical studies. In comparison with intra-venous cold infusion, ICCI has less systemic adverse effects. Its impact on regional cerebral blood flow, and incidence of hemorrhagic transformation should be further studied.

Introduction

Acute ischemic stroke, a global problem

Despite enormous efforts and progress in stroke prevention, diagnosis and the development of novel treatment strategies, stroke remains one of the major global health care problems [1]. According to a recent systematic analysis, age-standardized rates of stroke incidence and prevalence have decreased over the last two decades (from 1990 to 2019), whereas the absolute numbers of incident and prevalent strokes increased by 70% and 85%, respectively [1]. Especially in young populations below 70 years of age, the burden of stroke is rising, with increases of incidence and prevalence of stroke by 15% and 22%, respectively [1].

Stroke continues to be the second leading cause of death and the third leading cause of disability among adults globally [1, 2]. It was estimated that more than six million people died from stroke in 2019, accounting for about 11.6% of all the deaths. Furthermore, more than 140 million stroke-related disability-adjusted-life-years (DALYs) can be attributed to stroke [1]. The situation is even worse in low-income countries. Both age-standardized stroke-related mortality rate and stroke-related DALYs are more than 3 times higher than those in high-income countries [1].

Classification of stroke, pathology of acute ischemic stroke

Stroke could be generally classified into hemorrhagic and ischemic stroke, which results primarily either from the rupture of cerebral vessels or blockage of cerebral blood flow by thrombosis in situ or emboli from other sources. Notably, ischemic stroke constitutes more than 60% of all the new stroke cases at the global level [1].

Targeting ischemic stroke is therefore of great significance in the fight against stroke.

Many pivotal molecules and pathways of brain damage mechanisms after acute ischemic stroke have been explored and reported. Instead of independently influencing the fate of ischemic brain tissue, those pathological mechanisms seem to interact with each other and they synergistically contribute to brain damage [3]. However, in a simplified overview, energy failure, excessive release of excitatory neurotransmitters, overproduction of reactive oxygen species, neuroinflammation and apoptosis could be summarized as the main contributors to brain damage in acute ischemic stroke [4].

As a result of energy failure, adenosine triphosphate-dependent ionic pumps or channels stop working properly, which incurs disruption of intercellular ionic homeostasis, following cell membrane depolarization, and excessive release of excitatory amino acids [5]. Especially, glutamate, a well-studied excitatory transmitter, has been proven not only to have direct neurotoxic effects on neurons, but it also activates ionotropic glutamate receptors (e.g., the N-methyl-D-aspartate receptor, the α-amino-3-hydroxy-5-methyl-4-isoxazolepropionic acid receptor, and the kainite receptor) [6]. This further deteriorates the disrupted ionic homeostasis as a result of large influx of sodium, potassium, calcium, chloride into affected cells [6]. Increased intracellular osmolarity leads to intracellular water retention finally leading to cytotoxic edema in the affected cells [6].

Under ischemia, brain tissue turns to anaerobic metabolism leading to lactic acidosis. The increased intracellular hydrogen replaces calcium binding to proteins [5]. Together with the calcium released from organelles and calcium influx via various calcium channels, sodium-calcium ion exchanger, level of intracellular calcium could significantly increase [7]. The dysfunction of calcium discharge due to failure of sodium-potassium adenosine triphosphate-dependent pumps and adenosine triphosphate-dependent channels following energy failure further enhances intracellular accumulation of calcium [5].

Overload of intracellular calcium is an important trigger of a series of pathological processes after acute ischemic stroke. On the one hand, calcium functions as an activator of proteases, lipases and endonucleases that destruct cellular protein, membrane and deoxyribonucleic acid [6]. On the other hand, it causes mitochondrial dysfunction, which is one of the main sources of reactive oxygen species in acute ischemic stroke. Especially after recanalization, in the post-ischemia reperfusion injury phase, reactive oxygen species production is dramatically increased and leads to more extensive and deleterious oxidation of lipids, deoxyribonucleic acid and proteins [7].

Increased intracellular calcium, overproduction of free radicals, and hypoxia, together trigger the inflammatory response within the ischemic brain territory. The elevated expression of pro-inflammatory genes and overproduction of inflammation mediators such as tumor necrosis factor-alpha and interleukin-1 beta induce the expression of adhesion molecules on the surface of endothelial cells, which facilitates the anchoring and infiltration of neutrophils, macrophages and monocytes. Cerebral microcirculation could be potentially impaired by

aggregated leukocytes within the microvasculature [3]. Infiltrated leukocytes, as well as resident activated microglia further promote inflammation and leukocytes recruitment by producing free radicals and matrix metalloproteases [8]. Furthermore, matrix metalloproteases are important enzymes that disrupt the blood brain barrier integrity leading to vasogenic edema and hemorrhagic transformation of acute ischemic stroke [9].

Depending on the intensity of those adverse stimuli, namely, the severity of ischemia, brain tissue will be lost as the result of necrosis, which typically occurs in the ischemic core where brain tissue is extremely hypo-perfused, or apoptosis in the surrounding brain territory (known as the ischemic "penumbra") which is under critical but less severe ischemia. Both numerous animal studies and histopathological studies of human specimens [3, 10, 11], have proven the different fate of neurons in the ischemic core and the ischemic penumbra.

"Time is brain" is a widely known maxim in acute ischemic stroke treatment. It was estimated that about 1.9 million neurons will be lost with each hour of delay of reperfusion [12]. Today, recanalization is therefore the most important strategy in acute ischemic stroke treatment. It not only prevents the further expansion of the ischemic core [13], but also minimizes the activation of cerebral damage cascades that contribute to delayed apoptosis of neurons in the ischemic penumbra.

Progress in reperfusion treatment and patient management - the advent of endovascular mechanical thrombectomy

Intra-venous thrombolysis with recombinant tissue plasminogen (alteplase) has been the only proven strategy for promoting recanalization in acute ischemic stroke before 2015. However, due to its narrow therapeutic time window of only 4.5 hours and strict contraindications, it was estimated that only about five percent of acute ischemic stroke patients are eligible to receive intra-venous thrombolysis [14]. The number of acute ischemic stroke patients that could benefit from intra-venous thrombolysis is further minimized depending on the site of arterial vessel occlusion, features of the clot such as length and composition, and the extent of residual cerebral blood flow via collaterals or through plasma flow penetrating the clot itself, because all these factors are known to affect the thrombolytic efficacy of alteplase. It was found that intra-venous thrombolysis is much less effective in cases where the responsible clot is longer than eight millimeters or if no residual cerebral blood flow across the site of vessel occlusion exists [15, 16].

In contrast to intra-venous thrombolysis, endovascular mechanical thrombectomy of larger sized proximal brain-supplying arteries is a more straightforward strategy for recanalization in acute ischemic stroke. In 2015, five randomized controlled clinical trials reported the superior recanalization rate and better neurological outcomes brought by endovascular mechanical thrombectomy in anterior large vessel occlusion in patients within six, eight and twelve hours after stroke onset [17]. Moreover, endovascular mechanical thrombectomy has a wider therapeutic time window, which has been extended to 24 hours after stroke onset in patients with favorable perfusion status [18, 19], and even beyond [20]. Recently published randomized controlled trials have reported the efficacy of endovascular mechanical thrombectomy in patients with large-volume brain infarction [21], comparable treatment effects of direct endovascular mechanical thrombectomy to that of combined endovascular mechanical thrombectomy and intra-venous thrombolysis [22, 23], as well as favorable neurological outcomes in patients who underwent endovascular mechanical thrombectomy for basilar artery occlusion within up to 24 hours after stroke symptom onset [19, 24, 25].

In summary, endovascular mechanical thrombectomy has joined intra-venous thrombolysis as an established reperfusion treatment for acute ischemic stroke.

Aside from improving recanalization rate via developing novel endovascular thrombectomy devices or more effective thrombolytic drugs such as tenecteplase, which was recently approved in Europe for treating acute ischemic stroke [26], optimizing overall acute stroke patient management is an equally important strategy to improve outcomes by further shortening the time from stroke onset to successful reperfusion.

It was estimated that an extra extension of 1.8 and 4.2 days of healthy life could be granted to patients by every single saved minute in initiating intra-venous thrombolysis and endovascular mechanical thrombectomy, respectively, after stroke symptom onset [27, 28].

In a systematic review, from 1981 to 2007, an estimated 6.0% annual reduction in hours per year for prehospital delay was reported. Similarly, in-hospital delay of acute ischemic stroke treatment was also reduced with the establishment of specialized stroke units [29]. Mobile stroke units (i.e., ambulances that are equipped with a small CT scanner, a point-of-care laboratory, and, most importantly, an expert team that is trained for diagnosing and treating stroke) are emerging as a new trend in pre-hospital stroke care. Since mobile stroke units allow

for on-site brain and vessel imaging as well as laboratory testing, exclusion of intracranial hemorrhage and contraindications and detection of large vessel occlusions are accelerated. This enables the rapid initiation of intra-venous thrombolysis and optimized prehospital triage, including redirecting patients to centers capable of endovascular mechanical thrombectomy. This consequently translates into higher rates of early and successful recanalization [30, 31]. According to a recent study report, mobile stroke unit-based pre-hospital acute ischemic stroke management could save 40 and 50 minutes from dispatch to thrombolysis and endovascular treatment, respectively [32]. Although the net benefit appears to remain even when considering the enormous economic investment required for mobile stroke units, from a technical point of view, the bottleneck for achieving better clinical outcomes has been only met by optimizing stroke management workflow [33].

Unfortunately, if instant endovascular mechanical thrombectomy cannot be performed in the prehospital setting, patients' transfer to endovascular treatment-ready hospitals will always cause a critical loss of time until reperfusion can be established. In addition, the endovascular mechanical thrombectomy procedure itself also takes time, and reaching the clot may be significantly protracted depending on vessel morphology.

Pharmacological neuroprotection and hypothermia: buying time for the endangered ischemic penumbra

Taking measures to slow down or even to halt the pathological progress of acute ischemic stroke before reperfusion, and to additionally promote brain tissue survival in the penumbra after recanalization is the ultimate goal in the realm of neuroprotection research. In correspondence to the aforementioned pathological mechanisms that contribute to brain damage after acute ischemic stroke, there are more than 1,000 potential agents that have been tested in preclinical studies for their potential neuroprotective effects [34]. A significant number of these agents have also been evaluated in clinical trials, such as N-methyl-D-aspartate receptor antagonists, calcium channel blockers, free radical scavengers and most recently Nerinetide, a post-synaptic density protein inhibitor that reduces generation of toxic nitric oxide [35-37]. However, large randomized controlled trials that could prove the efficacy of any neuroprotective drug are still missing.

In contrast to pharmacological strategies, which selectively target one or a few molecules contributing to the brain damaging cascades, hypothermia influences almost all of these adverse mechanisms [4].

Firstly, hypothermia decreases cerebral metabolism. It was estimated that every 1 °C of brain temperature decrease results in a five percent decline in oxygen and glucose consumption [38]. The decreased metabolic rate could therefore result in increased hypoxia tolerance of hypo-perfused brain tissue before recanalization. Secondly, hypothermia mitigates other ischemia induced mechanisms of brain damage such as glutamate release, generation of reactive oxygen species, oxidation of the deoxyribonucleic acid, lipids and proteins, and activation of proteases [4]. Finally, extended hypothermia after reperfusion could potentially inhibit the apoptotic pathway, suppress neuroinflammation and maintain blood-brain-barrier integrity [4].

Targeted temperature management including hypothermia is already an established method for neuroprotection in global cerebral ischemia after cardiac arrest and in hypoxic-ischemic encephalopathy of the newborn [39-41].

Supported by numerous animal studies, hypothermia appears to be the most promising candidate strategy for promoting neuroprotection in acute ischemic stroke. In a meta-analysis of preclinical studies, an average reduction of infarct volume by 44% was reported in hypothermia treated rodents suffering from focal cerebral ischemic compared to non-hypothermia treated animals [42].

Whole-body cooling for achieving systemic hypothermia

For the clinical translation of hypothermia in acute ischemic stroke, so far, a number of cooling methods have been developed and tested in clinical studies. Depending on whether the respective method aimed at cooling the whole body or selectively just the brain, those methods could be generally classified into systemic hypothermia and organ-specific, local hypothermia approach[43].

Systemic hypothermia has been induced in acute ischemic stroke patients using surface cooling devices with active or passive cooling blankets or pads [44, 45], or, alternatively, an intra-venous approach with either closed-loop heat transfer elements (mostly, cold water that

circulates in balloons surrounding a dedicated central venous catheter) [46-48] or with direct intra-venous cold fluid infusion [49].

Surface cooling methods have the advantages of being available at low cost and being non-invasive and easy to apply even in the prehospital field. However, due to the large human body mass, the low surface-volume ratio, and method inherent limitations of heat transfer efficiency, whole-body surface cooling has the critical drawback of limited cooling efficacy. In a study by S Schwab et al. [50], as long as 3.5 to 11 hours were required for obtaining moderate hypothermia (< 33 °C) in sedated patients.

Intra-venous cooling methods could be potentially more efficient. Modern closed-loop central venous cooling catheters may achieve the targeted mild hypothermia within less time compared to surface cooling devices [46], however, even with a massive volume load of cold fluids being directly infused into the venous system at a high infusion rate, more than 30 minutes were required for induction of mild hypothermia. And due to its transient temperature-lowering effect, additional measures are usually required to assure seamless maintenance of hypothermia and avoid rebound of core body temperature [43, 51].

In contrast to cardiac arrest patients with global cerebral ischemia, the vast majority of acute ischemic stroke patients are awake, fully conscious, and not anesthetized, intubated, or mechanically ventilated [39, 52, 53]. The pain and temperature perception, as well as thermoregulatory reflexes are still intact. During whole body cooling, inner thermogenesis could be activated when there is core body temperature drop. This not only extends hypothermia induction [54], but also incurs failure of inducting deeper hypothermia [55]. In the COOLIST trial, no patients were successfully cooled to 34 °C with directly infused cold saline [55] . In another study by Christoph Testori et al. [45], systemic hypothermia was conducted in awake healthy volunteers with surface cooling method. Although core body temperature (Esophageal) could be decreased to 35 °C after 38 to 102 minutes cooling, deeper hypothermia seems hard to reach. Only in 6 of 16 volunteers were induced with core body temperature below 34C°.

Missing the time window for neuroprotection due to the limited cooling rate of any of the whole-body cooling approaches is probably one of the main reasons accounting for the negative findings in previous clinical trials [49, 56]. Furthermore, whole-body cooling related

extensive systemic side effects, such as cold shivering, immunosuppression [57], coagulation dysfunction [58, 59] and electrolyte imbalances [43] , which result from core body temperature drop, represent additional barriers to its successful clinical translation.

Cold shivering, functions as one of the main thermogenesis mechanisms in human, has been commonly reported in whole body cooling clinical trials [44, 46, 55, 60]. Aside from hindering hypothermia induction, shivering also markedly increases oxygen consumption [61, 62]. Although it has minor impact on arterial partial oxygen pressure in healthy cohorts, hypoxia could be incurred in cases with impaired respiratory or cardiac function [63, 64]. Ischemia-hypoxic condition within affected hemisphere could be therefore further aggravated in those patients.

Combination of meperidine and buspirone has been an established pharmacological strategy for controlling shivering and to enhance compliance with the whole-body hypothermia treatment in clinical trials. The high doses of meperidine of up to over 1,000 mg per day [46, 54] (i.e., more than twice the recommended maximum daily dose treatment) are known to attenuate protective gag and cough reflexes and thereby may increase the risk of pneumonia [65], which itself is a frequently occurring complication after stroke as a result of immunosuppression [66, 67].

In addition, hypothermia is also widely recognized as having anti-inflammatory capability via multiple mechanisms [68], but this property could also compromise the host immune defenses when hypothermia is applied systemically (whole body) , leading to infection [69] . Two recent large multicenter clinic trials, the international ICTuS-2/3 trial and the European counterpart EuroHYP-1, that had been initiated with the idea to finally confirm the efficacy of hypothermia in acute ischemic stroke, were both prematurely terminated mainly because of the high number of pneumonia cases in the hypothermia treatment arms, and also the very low feasibility of whole body cooling with the requirement of excessive nursing care ultimately leading to a very slow recruitment [49, 56].

Head- and neck or nasopharyngeal cooling for achieving selective brain hypothermia

Based on positive experiences of hypothermia-mediated isolated organ preservation in transplant medicine [70], as well as on pre-clinical findings indicating protective effects of organ-specific local hypothermia [71-73], it was concluded that local therapeutic hypothermia achieved by selective cooling of the brain may also be suited to protect the vulnerable ischemic-hypoxic

brain tissue during acute ischemic stroke. Compared with whole-body cooling, selective brain cooling targets a significantly smaller tissue volume and thus may only minimally affect core body temperature [43]. Therefore, it may be assumed that faster brain hypothermia induction with less systemic adverse side effects could be realized by means of selective brain cooling.

Surface cooling on head with liquid nitrogen vapor, ice packs, cooling pads [57,74, 75], and even with electric Peltier elements that require craniotomy to be placed directly on the brain surface have been investigated in animals [76]. As with whole-body hypothermia, neuroprotective effects including significantly reduced infarct volumes and improved neurofunction have been consistently reported by these small animal studies [57,74-76].

Non-invasive surface local cooling devices such as cooling helmets [77, 78] or systems for nasopharyngeal cooling with air [79, 80] or with perfluorocarbon [51, 81] have been also developed for human use and tested in a number of clinical studies. Interestingly and similar to the findings in the aforementioned clinical whole-body cooling studies, none of them was able to show neuroprotective effects of brain-specific local hypothermia in acute ischemic stroke patients [51, 78-81].

One of the reasons behind the negative findings in clinical studies may have been the lack of achieving effective therapeutic hypothermia levels in those brain regions that were affected by ischemia-hypoxia in human stroke. Skull and brain anatomy of humans critically differ from that of animals [81] and studies that included invasive brain temperature measurement have clearly shown that brain cooling with some devices may be insufficient and restricted to superficial cortical layers or even absent [78].

In comparison to rodent animals, humans have obviously larger brain and much thicker cranial structure. It was reported that the distance between scalp and cortex is more than 14 mm in adults human [82, 83] and less than 2 mm in rats or mouse [84, 85] . Rodent and human brains are similarly supplied with an abundant blood flow at core body temperature, and the temperature gradient between the brain surface (which is normally less than 1 °C higher than core body temperature [86]) and an externally applied cold surface (such as an ice pack at 0 °C) is relatively fixed. Based on the law of heat transfer [87], deeper brain regions may not effectively be cooled with head surface cooling devices, especially in human with larger brains volumes.

The only possibility of improving cooling efficacy of head surface brain cooling would be to increase the contact surface which is, however, limited by anatomy, or by using active devices that are capable of maintaining the temperature gradient for prolonged cooling. Interestingly, passive head cooling in adult stroke patients was insufficient for brain cooling even when the cooled surface involved the neck [78]. In stroke patients, who were equipped with an invasive intracranial pressure and temperature brain probe, subcortical brain tissue temperature was only reduced by 0.4 °C after 49 minutes of cooling [78]. In contrast, cooling efficacy of an active cooling helmet was much greater [77]. Superficial brain tissue temperature could be decreased by as much as 1.8 °C after one hour of continuous active head cooling, and brain temperature further decreased to below 34 °C after 3.4 hours of cooling. Importantly, this more pronounced decrease of brain temperature was accompanied by a similar decrease of core body temperature, i.e., systemic whole-body hypothermia [77].

Local nasopharyngeal cooling devices were postulated to also enable cooling of deeper brain regions by taking advantage of the dense vasculature network within the nasal cavity walls and the proximity of the roof of the nasal cavity to the frontal brain. As shown in clinical studies, the choice of the coolant that is used for nasopharyngeal cooling is crucial and largely determines the cooling efficacy. In a study in which the nasopharynx was ventilated with cold air, no significant brain temperature reduction could be observed [79, 80]. On the other side, studies evaluating the Rhino Chill® device, which uses evaporable perfluorocarbon that is sprayed onto the nasal cavity walls, have shown a significant drop of brain temperature in the frontal lobe of 1.2 to 1.4 °C after one hour of active cooling [51, 81, 88]. Unfortunately, this latter method potentially caused immediate and steep increases in blood pressure of up to 60 mmHg in some patients [81].

In summary, head- and neck cooling devices provide limited brain cooling efficacy with regard to speed of hypothermia induction and the extent [78], and most importantly, lead to systemic whole-body hypothermia when applied for a longer period [77]. Although nasopharyngeal cooling using perfluorocarbon vapor as the coolant instead of cold air showed comparatively higher cooling performance, it was associated with critical blood pressure increases [79-81].

The intra-arterial cooling approach for achieving selective brain hypothermia

Human brain shares only two to three percent of the body weight, while its blood supply accounts for as much as 12% of the total cardiac output [89]. Thus, selective brain cooling by lowering the temperature of the blood that flows into the cerebral circulation could represent a highly efficient method for rapidly inducing local hypothermia of the brain. In this process, adequate heat transfer would take place directly between the brain tissue and the cold blood distributed via the cerebral arterial tree. Furthermore, in acute ischemic stroke patients, intra-arterial cooling devices can take advantage of the access to brain-supplying arteries that is routinely established during endovascular mechanical thrombectomy.

The first key technical challenge that needs to be solved, is to decrease the temperature of the blood flowing into the cerebral circulation as much and as fast as possible without affecting the cerebral hemodynamics, especially the collateral blood flow to the penumbra in a way that may contribute to brain damage. So far, only few heat exchange catheters, e.g., the consecutive work by Cattaneo et al. [90-92] and direct intra-arterial cold fluid infusion strategies [93-96] have been investigated. The former has been realized with a closed-loop balloon catheter system, which is placed into the common carotid artery. Within the closed-loop balloon system, cold physiological saline is circulated similar to the aforementioned endovascular cooling catheters that are placed into a central vein for inducing whole-body hypothermia [90]. Because of the high flow rate of blood circulating through the carotid artery which ranges between 325 mL/minute and 536 ml/minute (see summary by Nigel Ackroyd et al. [97]), limited length and small surface of the balloons surrounding the catheter, the duration of contact (i.e., the time available for heat exchange) between the warm arterial blood and the small cold balloon surface is likely to be too short for a sufficient cooling performance. Such a closed-loop balloon system was tested in two large animal studies involving canines. A coolant temperature of 6 °C and a balloon system measuring 80 mm in length and 4 mm in diameter allowed ipsilateral cortex temperature to be reduced by 2 °C within 29 minutes and by 3 °C within 80 minutes [90, 91].

On the other hand, direct infusion of cold fluid into the cerebral arteries appears to be a far more effective cooling strategy, as shown in several theoretical and practical simulations [93, 98, 99] . Moreover, speed and depth of hypothermia induction could be easily controlled by adjusting either the temperature of the cold infusate, infusion rate, or both. It was estimated by several computer simulations that target hypothermia levels of even lower than 34 °C could be reached in the brain within only a few minutes depending on the infusion rate, the temperature

of infused fluid and targeted brain tissue volume [43]. The Latter is determined by the volume of the vascular circulation that is supplied by the respective artery in which the cold fluid will be infused. Cold infusion into the internal carotid artery would affect the volume of the whole anterior hemispheric circulation involving both the territories of the middle cerebral artery and the anterior cerebral artery. Cold infusion that is administered solely into the middle cerebral artery and distal to the vessel-occluding clot would further reduce the volume of the targeted brain tissue [43].

Two different approaches for cold fluid delivery are imaginable when considering using the same catheter pathways as they are routinely established during endovascular mechanical thrombectomy: The first approach would be to deliver cold fluid via the microcatheter. Cold infusion could be started as soon as the microcatheter has penetrated the clot and the micro wire has been withdrawn. This would be just before clot retrieval and recanalization. Direct access to the vasculature downstream of the occlusion site would allow the cold infusate to directly hit the ischemic target tissue without being diluted by any warm blood and thus, resulting in most rapid cooling. Harmful metabolic products, which potentially aggravate reperfusion injury, could also be washed out by the cold infusate before recanalization.

The second approach would be to use the large lumen guide catheter to infuse cold fluid into the internal carotid artery. Cold infusion into the internal carotid artery could theoretically be started as soon as the guide catheter is placed into the internal carotid artery. This is usually much earlier during the endovascular mechanical thrombectomy procedure than the penetration of the vessel occluding blood clot with the microcatheter. Before clot removal, however, the cold infusate would only be able to reach and cool the ischemic target tissue indirectly via collateral vessels. Compared to the microcatheter approach, the impact of cold infusion on target brain tissue temperature may thus be assumable less important when applied into the internal carotid artery due to only indirectly flowing into a larger tissue volume.

So far, most preclinical studies have simulated the ‘microcatheter approach’ (**see Figure 1A**, **Table 1**). Mild to moderate hypothermia of around 34 °C to 31 °C could be reached as fast as within three to ten minutes depending on the respective infusion protocol, i.e., fluid temperature and infusion rate (**see Table 1**). Importantly, in all small animal studies, it was not possible to initiate cold infusion before vessel recanalization, as the ‘microcatheter approach’ would suggest. This limitation arose because these models relied on an infusion tube for vessel

occlusion. Cold infusion could only be initiated after the tube was retracted, allowing partial reperfusion through arterial crossflow via the Circle of Willis and the anterior cerebral artery to be reestablished. The key technical challenge lies in the tiny lumen of intracranial vessels in rats. To more accurately simulate the clinical scenario in patients, a thromboembolic clot model and a catheter small enough to penetrate the clot for administering cold intra-arterial infusion directly would be required - an approach that is technically unfeasible in small animals.

Relatively less studies have chosen the 'guide catheter approach' with infusion of cold saline into the carotid artery (**Figure 1B, 1C**). Importantly, however, none of the rodent studies took full advantage of the 'guide catheter approach' as it could be applied in the real-life setting of clinical endovascular mechanical thrombectomy, i.e., with starting of the cold infusion much earlier before recanalization and continuation during and after reperfusion (**see Figure 2**). Cold infusion was either given either before reperfusion or with a significant delay after reperfusion (**Table 2**). Despite these procedural drawbacks, studies using direct brain temperature monitoring [100-105] also consistently reported high brain cooling efficacy for intra-carotid artery cold infusion (ICCI). Targeted hypothermic brain temperature of 33 to 34 °C was reached within 5 to 10 minutes in case of pre-reperfusion ICCI [100] and within 20 minutes in case of only post-reperfusion ICCI [104].

As to the neuroprotection effect, intra-arterial cold infusion started either before or after reperfusion has been reported to reduce infarct volume and improve neurofunctional integrity in transient focal cerebral ischemia models in rodents (**Table 1, Table 2**) and in non-human primates with their relatively larger brains **(Table 3).**

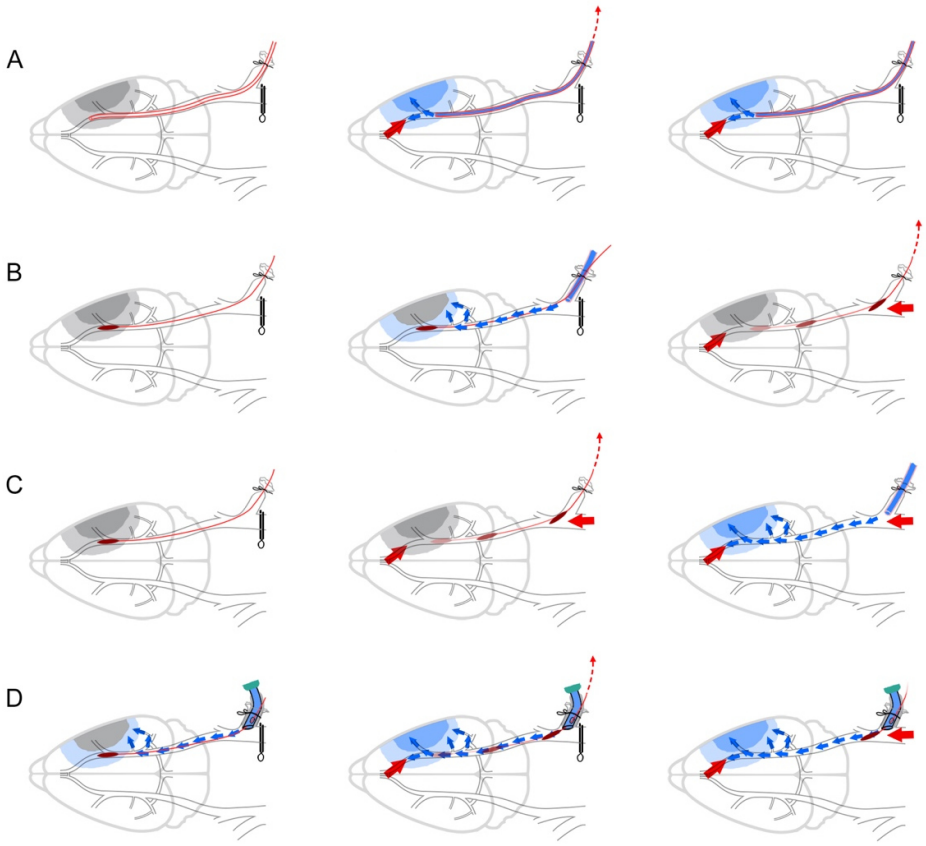

Figure 1 Existing (**A, B, C**) and our (**D**) experimental setups for testing intra-arterial cold infusion in small animal stroke models. (**A**) the microcatheter approach, a modified polyethylene-50 tube firstly was used for middle cerebral artery occlusion (left), at designated time point the catheter was withdrawn by a few millimeters. Together with the retrograde blood flow (reperfusion, red arrow) from anterior communicating artery, cold fluid was delivered into middle cerebral artery. (**B**) pre-reperfusion ICCI via the guide catheter approach. A polyethylene-50 tube was inserted into the carotid bifurcation for cold fluid delivery before removing the filament. (**C**) conventional post-reperfusion ICCI setup. Cold fluid infusion was initiated after complete reperfusion and there is potential delay due to the time required for filament removal and connecting the tube. (**D**) the guide catheter approach developed and applied in our study. By modifying the connection between infusion port and external carotid artery, ICCI could be initiated at any time during the ischemia (**left**). Thus, the ischemic penumbra could be cooled by residual collateral cerebral blood (e.g., anterior choroidal artery or leptomeningeal collaterals) before reperfusion. Reperfusion was easily controlled by simply retracting the filament (red dashed line) and opening the clip around common carotid artery (middle). *(modified from Figure 6, Wang Yi, et al. Transl Stroke Res. 2021 Aug;12(4):676-687)*

Table 1 Studies testing intra-arterial cold infusion in small animal ischemic stroke models using the 'microcatheter approach' (see Figure 1C). In all studies, Sprague-Dawley rats were used, and cold infusion was administered into the middle cerebral artery.

Study, Year	Infusate (volume)	Infusion rate (duration)	Cortical / striatal / core body temperature	Time to target Temp (min)	Duration of focal cerebral ischemia (h)	Infarct volume decrease (versus Control, at 48h post treatment)	Time point of cooling
Ding et al. [106], 2002	23.0 °C heparinized saline (8.0 - 10.0 mL)	3 mL/min (3.0 to 4.0 min)	32.4 °C / 33.0 °C / 37.5 °C	3 – 4	2.0	–75%	After partial reperfusion (see Figure 1A)
Ding et al. [107], 2002	23.0 °C saline (7.0 mL)	2 mL/min (3.0 to 4.0 min)	32.0 – 33.0 °C / 32.0 – 33.0 °C / Not reported	3 – 4	2.0	–73%	After partial reperfusion (see Figure 1A)
Ding et al. [108], 2004	20.0 °C saline (6.0 mL)	0.6 mL/min (10.0 min)	33.4 °C / 33.9 °C / > 36.0 °C	Not reported	3.0	–90%	After partial reperfusion (see Figure 1A)
Luan et al. [109], 2004	20.0 °C saline (6.0 mL)	0.6 mL/min (10.0 min)	33.4 °C / 33.9 °C / > 36.0 °C	≤ 10	3.0	Not reported	After partial reperfusion (see Figure 1A)
Li et al. [110], 2004	20.0 °C saline (6.0 mL)	0.6 mL/min (10.0 min)	Not reported	Not reported	3.0	–57% *	After partial reperfusion (see Figure 1A)
Zhao et al. [111], 2009	20.0 °C saline (6.0 mL)	0.6 mL/min (10.0 min)	32.8 °C / 33.2 °C / 37.0 °C 33.1 °C / 33.3 °C / 37.1 °C 33.2 °C / 33.3 °C / 37.1 °C 32.9 °C / 33.2 °C /37.0 °C	≤ 10 ≤ 10 ≤ 10 ≤ 10	1.5 2.0 2.5 3.0	–44% –33% –47% No difference	After partial reperfusion (see Figure 1A)
Chen et al. [112], 2013	0 °C saline (2.5 mL) 0 °C albumin saline (2.5 mL)	Not reported Not reported	30.5 °C / 30.8 °C / 37.0 °C 30.5 °C / 30.8 °C / 37.0 °C	< 3 < 3	2.0 2.0	–32% –67%	After partial reperfusion (see Figure 1A)
Chen et al. [113], 2015	0 °C saline (2.5 mL)	0.25 mL/min (10.0 min)	30.7 °C / 30.9 °C / > 36.0 °C	< 5	2.0	–34%	After partial reperfusion (see Figure 1A)
Wei et al. [114], 2019	4 °C saline (3.0 mL)	0.6 mL/min (5.0 min)	Not reported	Not reported	1.5	–33% **	After partial reperfusion (see Figure 1A)

* Compared at 28 days after treatment

** Compared at 24 hours after treatment

Table 2 Studies testing intra-carotid artery cold infusion (ICCI) in small animal ischemic stroke models using the 'guide catheter approach'. In all studies, Sprague-Dawley rats were used

Study, year	Infusate (volume)	Infusion rate (duration)	Cortical / striatal / core body temperature	Time to target Temp (min)	Duration of focal cerebral ischemia (h)	Infarct volume decrease (versus Control, at 48h post treatment)	Time point of cooling
Song et al. [100], 2004	15 °C saline (8.0 mL)	0.40 mL/min (20 min)	33.0 – 34.0 °C / 33.0 – 34.0 °C / 37.0 °C	5 –10	3	–48%	Before reperfusion (see Figure 1B)
	15 °C saline (MgSO4) (8.0 mL)	0.4 mL/min (20 min)	33.0 – 34.0 °C / 33.0 – 34.0 °C / 37.0 °C	5 – 10	3	–65%	Before reperfusion (see Figure 1B)
Ji et al. [102], 2012	10 °C saline	0.25 mL/min (30 min)	< 36.5 °C / not reported / 37.0 °C	6	3	–33%	After reperfusion (see Figure 1C)
	(7.5 mL)	0.25 mL/min (10 min × 3)	< 36.5 °C / not reported / 37.0 °C	6	3	–32%	
Ji et al. [103], 2012	10 °C saline (NR)	0.17 – 0.42 mL/min (20 min)	33.0 – 34.0 °C / not reported / 37.0 °C	Not reported	2	–56%	After reperfusion (see Figure 1C)
	10 °C saline (not reported)	0.17 – 0.42 mL/min (20 min)	33.0 – 34.0 °C / not reported / 37.0 °C	Not reported	2	–42%	1 hour after reperfusion (see Figure 1C)
	10 °C saline (not reported)	0.17 – 0.42 mL/min (20 min)	33.0 – 34.0 °C / not reported / 37.0 °C	Not reported	2	–31%	2 hours after reperfusion (see Figure 1C)
Kurisu et al. [101], 2016	10 °C saline (4.8 – 6.2 mL*)	0.32 – 0.41 mL/min‡ (15 min)	34.8 °C / 35.4 °C / 37.0 °C	Not reported	2	–72% ‡	Before reperfusion (see Figure 1B)
Kurisu et al. [105], 2016	4 °C saline (4.2 – 5.6 mL *)	0.28 – 0.37 mL/min ‡ (15 min)	32.5 °C / 34.3 °C / 37.0 °C	Not reported	Permanent **	–77%	At the onset of bilateral CCA occlusion
	4 °C saline (4.2 – 5.6 mL*)	0.28 – 0.37 mL/min ‡ (15 min)	32.5 °C / 34.3 °C / 37.0 °C	Not reported	Permanent **	–55%	After bilateral CCA occlusion
Corey et al. [115], 2019	6 °C saline (5.0 mL)	1.0 mL/min (5 min)	Not reported	Not reported	1	Not reported	Before middle cerebral artery occlusion
Duan et al. [104], 2020	0 °C saline (6.0 mL)	0.2 mL/min (30 min)	34.0 °C / 34.8 °C / 36.0 °C	20	2	–29% ‡	After reperfusion (see Figure 1C)

* Estimated infusate volume by referring to reported rat body weight and infusion volume (i.e., 20 mL/kg)

** Permanent ligation of the middle cerebral artery with 1 hour of bilateral common carotid artery (CCA) occlusion.

‡ Versus Control, at 24 hours after treatment

Table 3 Studies testing intra-arterial cold infusion in healthy or ischemic stroke large animals using microcatheter for cold fluid delivery

Study, year	Infusate (volume)	Infusion rate (duration)	Cortical / striatal / core body temperature	Time to target Temp (min)	Duration of focal cerebral ischemia (h)	Infarct volume decrease (at 24h)	Time point of cooling and catheter approach
Non-human primates							
Wang et al. [116], 2016	0 °C Ringer solution (100 mL)	5 mL/min (20 min)	< 35 °C / < 35 °C / 37.1 °C	10	No ischemia	Not reported	Infusion via microcatheter placed in proximal middle cerebral artery
Wu et al. [117], 2020 *	0 – 4.0 °C Ringer solution (100 mL)	5 mL/min (20 min)	< 35 °C / < 35 °C / 37.1 °C **	10	Permanent	No decrease was observed	No reperfusion, infusion via microcatheter placed in proximal middle cerebral artery
					2.50	–25% ‡	In adult rhesus macaques with partial reperfusion, infusion via microcatheter placed in proximal middle cerebral artery
					2.50	–38% ‡	In adult rhesus macaques with total reperfusion, infusion via microcatheter placed in proximal middle cerebral artery
Wu et al. [118], 2020 *	0 – 4.0 °C Ringer solution (100 mL)	5 mL/min (20 min)	< 35 °C / < 35 °C / 37.1 °C **	10	2.50	Not reported	After partial reperfusion, infusion via microcatheter placed in proximal middle cerebral artery
Canine							
Caroff et al. [119], 2020 §	4.5 °C saline (550 mL)	22 mL/min (25 min)	31 – 32 °C / Not reported / 37.2 °C	Not reported	0.75	–95% §§	Continuous pre- to post-reperfusion ICCI (see Figure 1D), cold fluid was delivered via microcatheter

* Middle cerebral artery occlusion was established with a thrombus in rhesus monkeys. After 2.5 hours of focal cerebral ischemia, intra-arterial local thrombolysis was given, leading to no reperfusion (permanent focal cerebral ischemia), partial reperfusion, or complete reperfusion.

** Values were not reported in the original article and estimated from a feasibility study from the same research group using the same infusion protocol.

‡ Compared with subjects with the same reperfusion status after thrombolysis; value was not reported in the original article, but estimated on the basis of published diagrams.

§ Intra-carotid artery cold infusion (ICCI) was given via microcatheter at 5 min before reperfusion and continued for 20 after reperfusion.

§§ Infarct volumes were evaluated on magnetic resonance imaging apparent diffusion coefficient (ADC) maps immediately after treatment.

In one human pilot study, cold infusion was delivered into the internal carotid artery via a standard guide catheter in patients who underwent routine diagnostic digital subtraction angiography as follow-up after treatment of a vascular malformation or aneurysm [93]. Brain temperature reflected by jugular venous bulb temperature was found to drop by 0.84 °C after 10 minutes of cold isotonic saline infusion at a temperature of 4 to 17 °C and an infusion rate of 33 mL per minute [93]. No adverse side effects were observed in this pilot study in more or less healthy subjects [93].

In three clinical studies conducted in acute ischemic stroke patients undergoing endovascular mechanical thrombectomy for treatment of acute proximal vessel occlusion [94-96], cold infusion was initiated after clot penetration and administered into the downstream middle cerebral artery territory via the conventional non-insulated microcatheter that is routinely used for delivery of the stent retriever during endovascular mechanical thrombectomy [94-96]. In two studies, respectively conducted by Chen J et al. [95] and Wu C et al. [96], additional volume of cold infusion was applied after the retrieval of the blood clot. All three clinical studies proved the feasibility and safety of intra-arterial cold infusion in acute ischemic patients. Two of the clinical studies [94, 96] even reported the positive neuroprotective effects of intra cerebral artery cold infusion in contrast to patients who received only recanalization therapy (see **Table 4**).

Unfortunately, the lack of a brain temperature surrogate (e.g., jugular venous bulb temperature) in all three acute ischemic stroke studies did not allow any conclusions on a potential dose (brain temperature decrease) dependent efficacy relation.

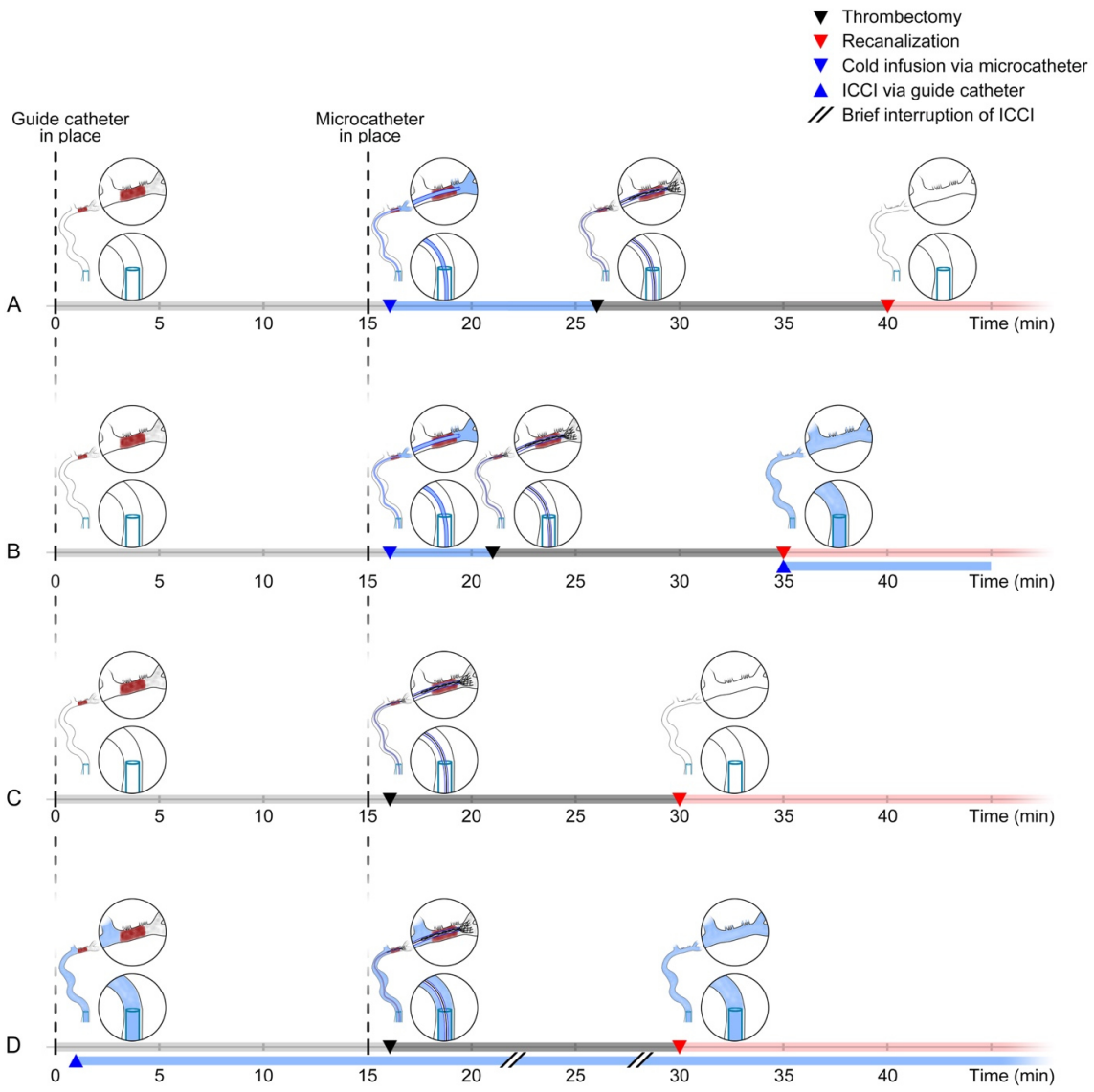

Figure 2 Existing studies (**A, B**) integrating intra-arterial cold infusions into the clinical workflow of endovascular thrombectomy (EVT) with stent retriever (**C**) in large vessel acute ischemic stroke. One clinical pilot study by Peng et al. [94] that applied the microcatheter approach for delivering cold fluid (**A**) and another two studies by Chen et al. [95]. and Wu et al. [96], in which the guide catheter was further used for intra-carotid artery cold infusion (ICCI) after clot removal aside from the pre-reperfusion microcatheter based cold fluid delivery (**B**). **(D)** The absent continuous pre- to post-reperfusion cold infusion via guide catheter, i.e., the "guide catheter approach" that would be simulated in the present study. ICCI could be started as soon as the guide catheter is placed in the internal carotid artery and does not interrupt EVT. Brief interruption of ICCI may be necessary during the retrieval of clot for avoiding the danger of clot detachment from stent. *(Figure was modified from Figure 1, Wang Yi, et al. Transl Stroke Res. 2021 Aug;12(4):676-687)*

Table 4 Studies testing intra-arterial cold infusion in healthy human subjects or ischemic stroke patients using either the 'microcatheter approach' or the 'guide catheter approach' , or both

Study, year	Infusate (volume)	Infusion rate (duration)	Decrease of brain/ core body temperature (versus baseline)	Time to target Temp (min)	Duration of focal cerebral ischemia (h)	Infarct volume decrease	Time point of cooling and catheter approach
In healthy humans							
Choi et al. [93], 2010	4.0 – 17.0 °C saline (330 mL)	33 mL/min (10 min)	–0.84 °C / –0.15 °C	Not reported	No ischemia	Not reported	No ischemia, ICCI via guide catheter
In ischemic stroke patients with proximal artery occlusion							
Peng et al. [94] , 2016	4.0 °C Ringer solution (500 mL)	50 mL/min (10 min)	Not reported	Not reported	< 6	–50% ‡	Before reperfusion, intra-arterial cold infusion into the middle cerebral artery via microcatheter
Chen et al. [95], 2016 *	4.0 °C saline (350 mL)	10 mL/min (5 min), followed by 30 mL/min (10 min)	–2 °C / –0.3 °C	Not reported	< 8	Not reported	Intra-arterial cold infusion into the middle cerebral artery via microcatheter before reperfusion, followed by ICCI via guide catheter after reperfusion. Intra-arterial cold infusion was interrupted during endovascular reperfusion.
Wu et al. [96], 2018 *	4.0 °C saline (350 mL)	10 mL/min (5 min), followed by 30 mL/min (10 min)	Not reported	Not reported	< 6	–19.1 mL ‡‡	Intra-arterial cold infusion into the middle cerebral artery via microcatheter before reperfusion, followed by ICCI via a large-bore distal-access catheter after reperfusion. Intra-arterial cold infusion was interrupted during endovascular reperfusion.

* Pre- and post-reperfusion cold infusion was interrupted due to thrombectomy. MCA, middle cerebral artery

‡ Volume at 7 days after treatment versus volume on baseline MRI

‡‡ Volume comparison (versus standard thrombectomy) after baseline factor adjusting at three to seven days after treatment

In acute ischemic stroke, the earlier an occluded vessel is recanalized, the higher reperfusion rate and more favorable prognosis could be obtained [120-122]. A similar time dependency is assumed in the case of therapeutic hypothermia mediated neuroprotection. Hypothermia that is established before recanalization may protect the ischemic-hypoxic brain tissue more effectively by early inhibition of the progressive pathophysiological cascades and alleviating reperfusion damage [74, 123].

Obviously, when using the 'microcatheter approach' as described above and conducted in the three clinical studies [94-96], administration of cold infusion either before or after vessel recanalization has critical disadvantages: the occupation of the small lumen of the microcatheter by the cold infusion or the mechanical thrombectomy devices inevitably delays reperfusion of the ischemic brain tissue or the initiation of therapeutic hypothermia, respectively (**see Figure 2A, 2B, 2C**). Furthermore, due to the interruption of the cold infusion during the endovascular mechanical thrombectomy procedure when the catheter is occupied by the thrombectomy device (**see Figure 2B**), the targeted brain territory that had been cooled by cold infusion would immediately rewarm at the moment of recanalization when the warm cerebral blood flow is restored. Re-induction of hypothermia in that brain tissue after reperfusion not only causes a further fluctuation of brain temperature but also requires an additional volume of cold infusion potentially leading to fluid overload.

Continuous pre- to post-reperfusion intra-carotid artery cold infusion

To overcome these disadvantages, ICCI via the large-lumen guide catheter seems to be an optimal alternative.

Firstly, in clinical routine, guide catheters are usually continuously flushed with saline which is conventionally heparinized during most endovascular procedures in order to prevent backflow of the blood into the catheter and related clot formation [124, 125]. Conventional guide catheters may thus be easily used for continuous cold infusion.

Secondly, cold infusion could be initiated much earlier during the endovascular mechanical thrombectomy procedure (**Figure 2D**). During the diagnostic and therapeutic cerebrovascular procedures in cerebrovascular diseases, in general, guide catheter is required and placed into the carotid artery at the very beginning of the procedure and represents the first path that is established for the purpose of a cerebral angiography and facilitating the delivery

of other devices required for subsequent interventions such as microwire, microcatheter, stent retriever and/or a clot suction device that are used for revascularization in cerebral artery stenosis or occlusion [126, 127].

Thirdly, when cold infusion would be administered using the large-lumen guide catheter, the microcatheter would still be available for all kinds of thrombectomy devices throughout the endovascular procedure (**Figure 2D**). The endovascular mechanical thrombectomy workflow would thus not be affected and ICCI could be initiated before reperfusion without causing any delay of the critically time dependent recanalization of the occluded cerebral artery. Moreover, hypothermia could be established without potentially marked fluctuations of brain tissue temperature as the delivery of cold infusion would not or only briefly require an interruption during the endovascular mechanical thrombectomy intervention. Only during the short phase of clot retrieval, it would be recommendable to reduce or stop orthograde flow with proximal balloon guide catheter in order to avoid dislocation of thrombus particles into the distal circulation [128, 129].

Additionally, conventional guide catheters have obviously larger size in contrast to microcatheters, which are respectively around 6 to 8 French (2.0 to 2.67 mm in outer diameter) and smaller than 3 French (1.0 mm in outer diameter) [130, 131] . This size advantage of guide catheter enables catheter modification for achieving better practicability aiming at ICCI, as existing examples of catheter modification for heat isolation [119], closed loop circuit [90, 132] .

The neuroprotective effects of continuous pre- to post-reperfusion ICCI has been only conducted in a single middle cerebral artery occlusion model in canines [119]. In this study's experimental setup, cold saline was delivered into the carotid artery using the microcatheter rather than via the guide catheter. Notably, the guide catheter used in this study was modified with enhanced heat insulation properties, primarily to minimize rewarming of the pre-chilled saline as it was infused through the microcatheter. However, due to the occupation of the guide catheter during cold saline delivery, this method - if translated into the real-world clinical setting - would inevitably disrupt the workflow of endovascular mechanical thrombectomy in stroke patients. In this canine study, a lowest brain temperature of 23.8 °C and average cooling rates of more than 2 °C/minute were observed with 4 °C ICCI at infusion rates between 20 and 40 mL/minute [119]. Furthermore, a dramatic reduction of infarct volume as well as excellent neurological outcomes were also found in this study including only 3 animals and using

historical data as the control group. Additionally, the duration of middle cerebral artery occlusion and thus focal cerebral ischemia was limited to 45 minutes [119], which is relatively short compared to real-world acute ischemic stroke caused by proximal vessel occlusion where the endovascular mechanical thrombectomy procedure alone may take this amount of time [133, 134]. The benefits of ICCI in this study cannot, therefore, be extrapolated to cases of severe ischemic stroke and related complications, such as hemorrhagic transformation [135, 136].

To summarize, ICCI administered using the 'guide catheter approach' appears to be the most practical strategy for realizing effective continuous selective brain cooling from before to after reperfusion in the setting of endovascular mechanical thrombectomy. However, the many treatment variables of ICCI including different infusate temperatures, composition, infusion rates and/or the overall hypothermia duration, and their effects on vital and blood parameters should be better elucidated to prevent another failure of such a promising treatment during the process of translation [49, 56]. Despite the clear advantages of large animal studies with canines or primates, whose gyrated brains are more similar to the human brain with regard to size and structure compared to the lissencephalic brains of rodents, major ethical concerns and high costs render large animal studies less optimal for the repeated experiments that will be required to address the multiple open questions on how to optimally deliver ICCI before designing a randomized clinical trial in the future.

To the best of our knowledge, no small animal model has been established so far that would allow the evaluation of intra-arterial cold infusion continuously administered from before to after reperfusion.

Therefore, the main objectives of our study were:

(1) to develop a novel infusion system that allows for an uninterrupted infusion of fluids into the carotid artery from before to after reperfusion in a reproducible small animal stroke model.

(2) to establish a cold infusion protocol that permits induction and maintenance of mild local brain hypothermia around 35°C before reperfusion and moderate hypothermia of around 32 °C after reperfusion.

(3) to evaluate the neuroprotective effects of ICCI that is continuously administered using present experimental setup from before to after reperfusion, at both the structural and functional levels.

(4) to investigate the impact of continuous pre- to post-reperfusion ICCI on hemorrhagic infarct transformation, systemic physiological parameters, the cerebral blood flow and blood parameters including blood gases.

Materials and Methods

Continuous pre- to post-reperfusion intra-carotid artery cold infusion

This is a prospective randomized-controlled open-label interventional preclinical study in rats with blinded endpoint assessment (PROBE) and consists of three parts:

Part I: developing a novel infusion system that allows for continuous pre- to post-reperfusion ICCI in a filament middle cerebral artery occlusion rat model and investigating the infusion rate dependent cooling efficacy of ICCI (with saline at temperatures of 0 °C to 1 °C).

Part II, investigating the neuroprotective effects as well as side effects of ICCI when administered to achieve brain-selective moderate hypothermia of around 32 °C in a rat model of severe focal cerebral ischemia over 100 minutes of middle cerebral artery occlusion.

Part III, MRI based dynamic in-vivo evaluation of infarct growth as well as neurofunction in a rat model of moderate focal cerebral ischemia over 60 minutes during long-term survival over 2 weeks.

The study protocol was approved by the competent authority, the Regierungspräsidium Tübingen, Germany (animal test protocol no. N3/13). Animal handling and surgical operations were performed in accordance with the guideline provided by the animal welfare care committee of Tübingen University.

Animals, treatments and groups

Adult male Sprague-Dawley rats (Charles River, Sulzfeld, Germany) were kept in specific-pathogen-free facilities with 12/12-hours reverse light-dark cycle and food/water access ad libitum at the Hertie Institute for Clinical Brain Research, Tübingen, Germany and the Werner Siemens Image Center, Tübingen, Germany, where parts I + II and part III of the study were respectively conducted. Before any experiments were undertaken (including training for neurofunctional tests), two weeks of acclimation were ensured.

Except for group control, all the other groups received specific infusion treatments. Briefly, in the two cold infusion groups, 0.9% saline at a temperature of 0 °C to 1 °C was delivered either directly into the ischemic hemisphere via the ipsilateral internal carotid artery

(ICCI group) for selective brain cooling or via the right femoral vein (intra-venous cold infusion group) for whole-body cooling. In the warm infusion group, 0.9% saline at 37 °C was infused via the ipsilateral carotid artery (intra-carotid artery warm infusion group). The total volume of saline to be infused was calculated to equal half of the circulating blood volume, i.e. 30 mL per kg body weight [137].

Details on the four experimental groups and treatments in each part of the study are summarized in **Figure 3**.

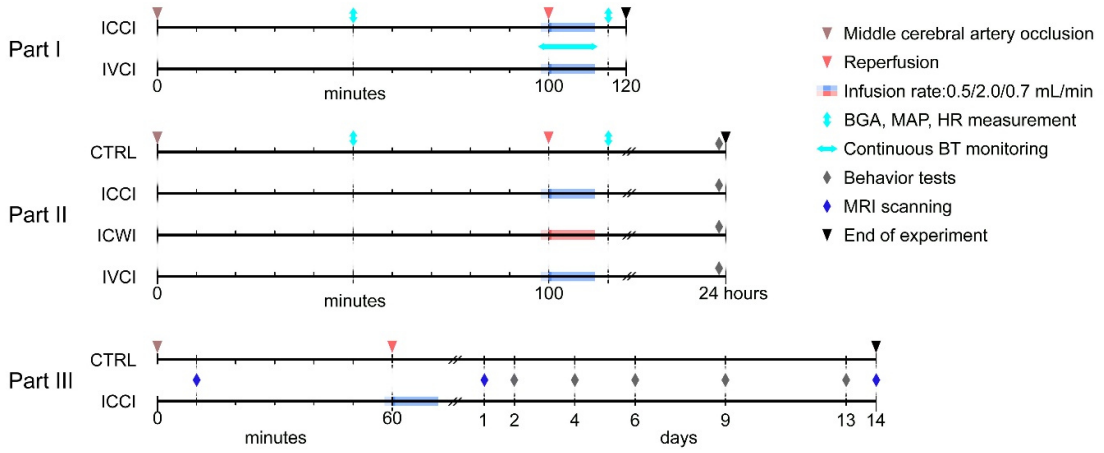

Figure 3 Schematic view of experimental design including timing and duration of ischemia and infusion. In **part I** and **part II** rats were designated to 100 minutes middle cerebral artery occlusion. Blood gas analysis (**BGA**), mean arterial blood pressure (**MAP**) and heart rate (**HR**) measurements were conducted before middle cerebral artery occlusion (not shown on this figure), at around 50 minutes after filament insertion and after treatment/reperfusion. The reproducibility of the final infusion protocol was confirmed with continuous brain temperature (**BT**) monitoring during infusion. In part II, neurofunctional tests including modified neurological severity score (mNSS), cylinder test, beam walking were conducted before taking the brain at around 24 hours after treatment. In **part III**, rats were allowed to survive for 2 weeks after reperfusion. During middle cerebral artery occlusion before treatment, at 24 hours and 2 weeks after treatment, rats were scanned with MRI for dynamic evaluation of infarct growth. Neurofunctional tests including mNSS and cylinder test were conducted before operation, at day 2, day 4, day 6, day 9, day 13 after reperfusion.

Anesthesia and analgesia

Anesthesia of spontaneously breathing rats was induced using 5% isoflurane (CP-Pharma, Burgdorf, Germany) delivered in a mixture of oxygen (at a flow of 0.2 L/minute) and air (at a flow of 1.0 L/minute) to provide an inspiratory oxygen fraction of around 30%. During anesthesia induction, corneal reflex and pain reflex of the rats were regularly checked with a cotton swab and by clipping the paws with a forceps. Following successful anesthesia induction (i.e., loss of corneal reflex and pain reflex), isoflurane concentration was lowered to 1.5% to 2% for maintenance of anesthesia.

For analgesia, Carprofen (5 mg/kg; Pfizer Deutschland, Berlin, Germany) and lidocaine (AstraZeneca, Wedel, Germany) were injected into the abdominal subcutaneous tissue and around incisions, respectively. Atropine (0.1 mg/kg; B. Braun, Melsungen, Germany) was also injected into the abdominal subcutaneous tissue for improving the airway and cardiocirculatory condition of anesthetized rats.

Implantation of probes for thermal assessment and laser Doppler flowmetry

Throughout the experiments in **part I**, regional cerebral blood flow in the ischemic core as well as temperature in the striatum and cortex of both hemispheres were continuously monitored with laser Doppler flowmetry (PeriFlux 5000, Perimed, Järfälla, Sweden) and with thermocouple probes (diameter, 0.4 mm; AD instruments, Dunedin, New Zealand), respectively.

The location of the laser Doppler flowmetry probe for cerebral blood flow monitoring was 1 mm posterior to the bregma, 6 mm lateral to the midline and about 3 mm below the horizontal parietal plane (**Figure 4A**). To monitor cortical and deep (striatal) brain temperature in both hemispheres, 4 thermocouple probes were implanted. In order to simplify the experimental procedures meanwhile minimizing the traumatic injury incurred by unnecessary additional insertion of the probes into the brain parenchyma, two thermocouple probes designated for brain temperature measurements within the same hemisphere were bundled together with a piece of catheter (diameter: 1.1 mm, length: 33 mm), which was obtained from a 20G peripheral intra-venous cannula (B. Braun, Melsungen, Germany) (**Figure 4B**).

In about 2 mm distance from the catheter tip, i.e., the location of the temperature sensor for deep brain temperature monitoring, a side hole was made on catheter wall under a

stereomicroscope (Leica, Wetzlar, Germany), where the second temperature sensor was fixed, for reducing the potential thermal insulation effect of the catheter sheath outside the cortical temperature sensor (**Figure 4B**). The catheter was inserted about 5 mm beneath the cortical surface at a location of 1 mm posterior to the bregma and 3 mm lateral to the midline. Symmetrically to the midline the other catheter sheath with two thermocouple probes was implanted at the same depth (**Figure 4B**).

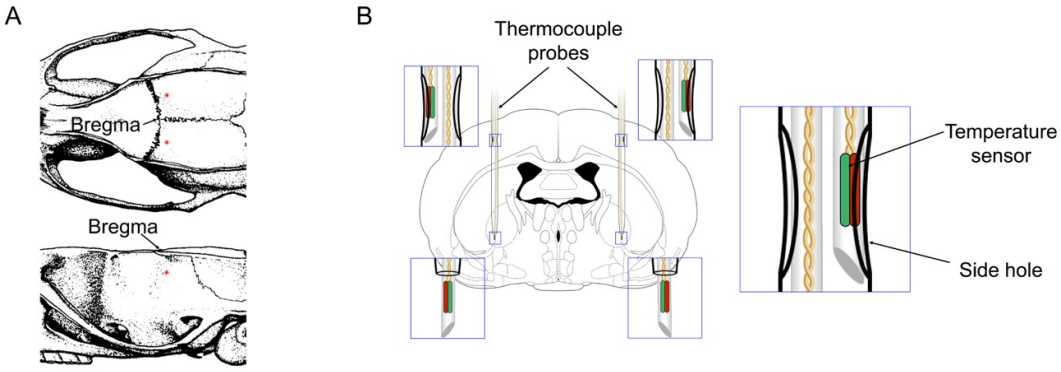

Figure 4 Illustration showing the location of the thermocouple probes (**A, upper**), the laser Doppler probe (**A, lower**), and the two thermocouple probes in each hemisphere, bundled with a catheter sheath (**B**). Modified figure of rat skull, brain sketch were taken from the study [138] and brain atlas [139] by Paxinos George et al..

The cranial bone was exposed by making a midline incision between lines of bilateral auricles and bilateral eyes. At aforementioned coordinates, a laser Doppler flowmetry probe holder (Perimed, Järfälla, Sweden) was attached with glue (Drechseln, weiden, Germany). Then rats were transferred to and fixed on a stereotaxic frame (Stoelting, Dublin, Ireland). Burr holes were carefully made with a microdrill (drill tip diameter 0.8 mm; CellPoint Scientific, Gaithersburg, USA) at the location where thermocouple probes would be implanted. Through the hole, a needle was vertically inserted for about 2 mm in order to pierce the meninges. After exclusion of bleeding, the needle was replaced with the cannula bundling two thermocouple probes and inserted slowly into the designated depth.

Femoral artery canalization

In supine position, a 1 cm long incision was made on the right groin. Femoral artery was then carefully isolated with blunt dissection techniques. Two knots were made around the femoral artery with a 4 - 0 suture while the proximal (directed towards the heart) was left untightened. As proximally as possible, the femoral artery was then temporarily clipped. During clipping a hole was made on the femoral artery between the two knots, through which a piece of polyethylene - 50 tubing (inner diameter 0.58 mm, outer diameter 0.96 mm; HSE-Harvard Apparatus GmbH, March-Hugstetten, Germany), pre-filled with heparinized 0.9% saline (10 units/mL), was introduced and fixed with the untightened suture.

Arterial blood pressure and heart rate were measured at 20 minutes before middle cerebral artery occlusion (i.e., immediately after the operation of laser Doppler probe implantation and successful femoral artery canalization), again at around 50 minutes after middle cerebral artery occlusion (during middle cerebral artery occlusion), and immediately after completion of the infusion in the three infusion groups (i.e., the ICCI group, the intra-carotid artery warm infusion group, and the intra-venous cold infusion group). In the control group, these measurements were conducted at equivalent time points.

Additionally, a subset of rats from each study group underwent continuous monitoring of arterial blood pressure and heart rate, which was initiated a few minutes before start of infusion in the treatment groups and at equivalent time points in the control group until wound closure.

Blood gases as well as hemoglobin, glucose, and serum electrolytes were analyzed with CG8+ cartridges on the i-STAT point-of-care system (both Abbott, North Chicago, IL, USA) after each session of intermittent arterial blood pressure and heart rate measurements or at the equivalent time points in rats that received continuous blood pressure and heart rate monitoring and in rats of the control group.

Middle cerebral artery occlusion

Middle cerebral artery occlusion was established with the filament method. Briefly, in supine position, a midline neck incision of about 1.5 cm length was made. After having exposed the carotid artery sheath with two cotton swabs, the right common carotid artery, the external carotid artery, and the internal carotid artery were carefully dissected without injuring

surrounding nerves. The external carotid artery was then ligated with a segment of 4 - 0 suture as distally as possible. Following temporary clipping of the common and the internal carotid artery, the external carotid artery was cut proximal of the ligation. A silicone coated 4 - 0 filament (coating diameter/length: 0.41 – 0.43 / 3 – 4 mm; Doccol, Sharon, MA, USA) was then inserted retrogradely into the external carotid artery. Another knot was made around the stump of the external carotid artery with a 4 - 0 suture to fix the filament and close the opening. After removal of the clip from the internal carotid artery, the filament was further advanced into the internal carotid artery and gently pushed forward until successful blocking of the middle cerebral artery opening. Correct positioning was confirmed by a sudden drop of cerebral blood flow on laser Doppler flowmetry. The inserted filament was then fixed and secured with a clip around the internal carotid artery.

In laser Doppler flowmetry monitoring controlled groups, rats with initial residual cerebral blood flow lower than 30% and mean residual cerebral blood flow during ischemia lower than 40% of baseline value were considered to have a successful middle cerebral artery occlusion. Rats with unsuccessful middle cerebral artery occlusion were excluded from further randomization for treatment and euthanized immediately.

Cooling System Setup

To simulate the integration of ICCI into acute ischemic stroke care in a rat model, i.e., with the start of cold infusion as soon as the guide catheter would have been introduced into the internal carotid artery, we developed a new infusion port. In brief, a 21G Safety-Multifly® cannula (Sarstedt, Nuembrecht, Germany) was bent and its sharp pinpoint was removed using hemostatic forceps. Under a stereo microscope, the cannula outlet was blunted, and a hole was made on the cannula wall with a microdrill (drill tip diameter 0.6 mm; CellPoint Scientific, Gaithersburg, USA).

To avoid vessel wall damage as well as fluid leakage (bleeding) during infusion via potential residual spaces between the tubing wall and the vessel wall created by the filament thread (**Figure 5, left**), the front part of the cannula was coated with elastic silicone (**Figure 5, middle and right**). To further ensure the seamless connection of the infusion port to the external carotid artery, a longitudinal concavity was molded by imprinting the filament thread into the elastic silicone on the convex surface of the front part of the cannula (**Figure 5, middle and right**).

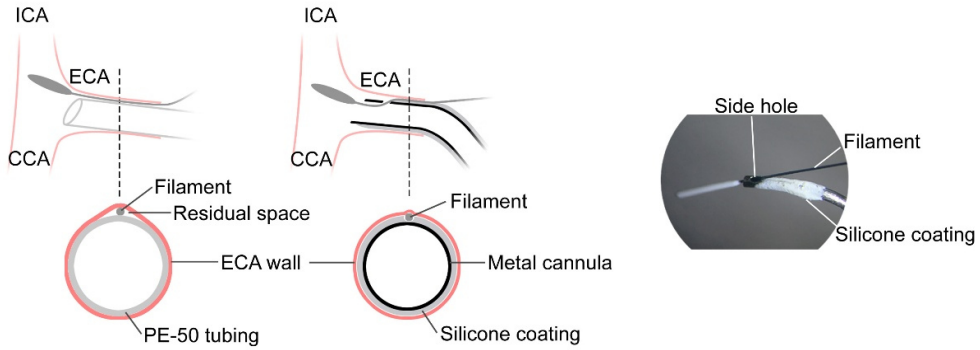

Figure 5 Sketch of a conventional polyethylene-50 infusion tubing (**left**) used for intra-carotid artery fluid delivery compared to the newly developed elastic silicone coated infusion port (**middle and right**) that was used in this study. Sagittal (**upper row**) planes are sketched together with corresponding coronal planes (**lower row**). CCA, common carotid artery; ECA, external carotid artery; ICA, internal carotid artery; PE, polyethylene.

A programmable automatic syringe pump (Pump 11 Elite; Harvard Apparatus, Holliston, MA, USA) was used for controlled saline infusion. To obtain cold and warm saline for infusion, a temperature control system with a dual in-line SC-20 heater/cooler (Warne Instruments, CT, USA) was implemented. To avoid potential rewarming of the chilled saline while flowing through the interposition polyethylene-50 infusion tubing especially at low flow rates due to its exposure to the surrounding air at room temperature before entering the carotid artery, we added a secondary closed-loop cooling circuit around the tubing. This additional cooling system was placed between the dual in-line SC-20 heater/cooler and the infusion port outlet (**Figure 6**) and was connected to a refrigerated bath circulator, Phoenix II/P2-C25P (Thermo Fisher Scientific, Karlsruhe, Germany).

Target temperature of the dual in-line SC-20 heater/cooler was set to 0 °C for ICCI and intra-venous cold infusion and to 37 °C for intra-carotid artery warm infusion. Depending on the real-time saline temperature at the infusion port outlet, cooling performance parameters of the secondary cooling system were adjusted. In our experiments, target temperature of the Phoenix II/P2-C25P was set to –20 °C or 37 °C, respectively, and with a medium coolant circulation speed.

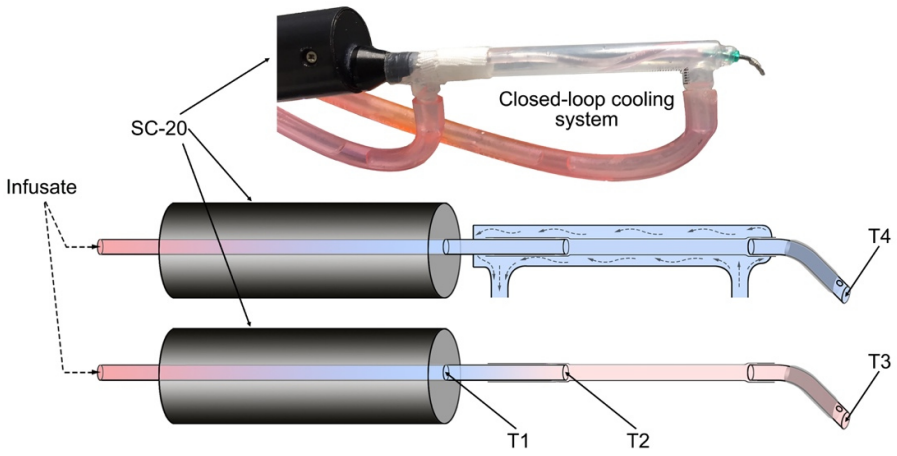

Figure 6 Photo (**upper)** and sketch (**middle**) of the closed-loop cooling system developed in our study and sketch illustration of the cooling systems before modification (**lower**). Black cylinders represent the commercially available dual in-line SC-20 heater/cooler from Warne Instruments (CT, USA). The lowest target temperature 0 °C was set for intra-carotid artery cold infusion (ICCI) group and intra-venous cold infusion group. A target temperature of 37 °C was set for group intra-carotid artery warm infusion. In groups with cold infusion, an additional closed-loop cold water circulating cooling system was integrated, which was powered by Phoenix II/P2-C25P circulator. The temperature of circulating water was set to −20 °C in cold infusion groups or 37 °C in intra-carotid artery warm infusion group, to minimize the temperature change (especially re-warming of the cold saline) affected by ambient environment before entering rats' carotid artery. **T1** to **T4** represent the locations where infusate temperature was measured without (**T1** to **T3**) and with (T4) the additional closed-loop cooling system (see results in **Table 5**). A polyvinylchloride interposition tube of 4 cm length (inner diameter: 1.3 mm; Sarstedt, Germany) allowed visual control during the microsurgical insertion of the infusion port into the external carotid artery. **(***Figure was modified from Figure 3, Wang Yi, et al. Transl Stroke Res. 2021 Aug;12(4):676-687)*

Continuous intra-carotid artery infusion

10 minutes before reperfusion, the suture around the external carotid artery was loosened. The thread end of the filament was then inserted into the side hole of the infusion port. The infusion port was then introduced into the re-opened external carotid artery and pushed further until reaching the carotid bifurcation (**Figure 7A, 7B**). To reduce the risk of a potential shift of the enlarged filament tip at the middle cerebral artery occlusion site and, thus, unintentional reperfusion, the stretching of the filament end was strictly avoided.

The infusion pump was switched on for a few seconds until all bubbles were discharged from the tubing. Then the infusion port was fixed with a piece of 4 - 0 suture around the external carotid artery (**Figure 7C**).

Pre-reperfusion infusion was initiated by starting the automatic infusion pump and simultaneously removing the clip from the internal carotid artery (**Figure 7D**). During ICCI or intra-carotid artery warm infusion, reperfusion was established by simply retracting the filament and right after, removing the clip around common carotid artery (**Figure 7E**).

During the experiments all rats were placed on an external heating pad that was connected to a rectal temperature-feedback-controlled T-1000 homeothermic system (CWE, CA, USA) to maintain the rats' core body temperatures at around 37.5 °C except in the whole-body hypothermia intra-venous cold infusion group.

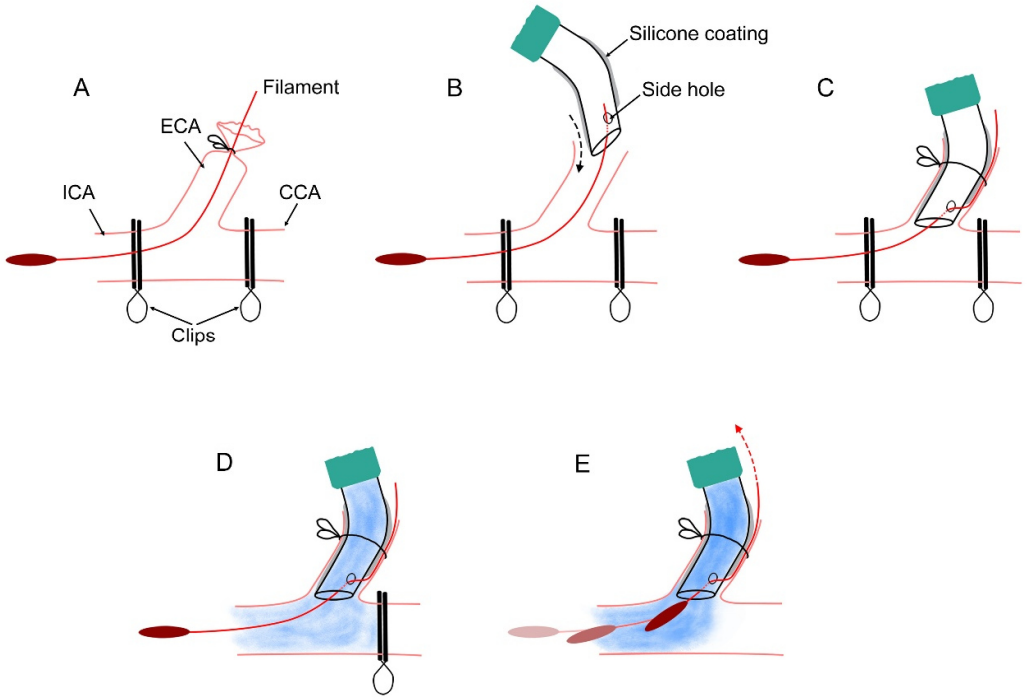

Figure 7 Illustrative steps of connecting the intra-carotid artery infusion port for uninterrupted pre- to post-reperfusion cold (0 – 1 °C saline) and warm (37 °C saline) intra-carotid artery infusion. (**A**) shows the filament-induced middle cerebral artery occlusion. (**B**) illustrates the insertion of our newly developed elastic silicone-coated infusion port with a side hole into the external carotid artery during ischemia, and (**C**) the infusion port in its final position. (**D**) shows pre-reperfusion intra-carotid artery cold or warm infusion before the filament is retracted, followed by (**E**) which shows intra- and post-reperfusion intra-carotid artery cold or warm infusion during and after filament retraction (recanalization). CCA, common carotid artery; ECA, external carotid artery; ICA, internal carotid artery. *(Figure was modified from Figure 2, Wang Yi, et al. Transl Stroke Res. 2021 Aug;12(4):676-687)*

Intra-venous cold infusion

In order to compare brain cooling efficacy of ICCI as well as its potential neuroprotective effects with that of whole-body cooling, the same infusion system (and protocol) was applied in intra-venous cold infusion via the right femoral vein. In order not to counteract the induction of whole-body hypothermia, the external heating pad was turned off during infusion of cold saline intra-venously.

Post-surgery care

Rats from experiment part II and part III were temporally kept in an infrared lamp (IR 812, Efbe-Schott, Bad Blankenburg, Germany) warmed transfer cage after wounds closure. They were sent back to home cages after regaining consciousness and activity. Pellet crumbs moistened with drinking water were provided ad libitum in a petri dish. Carprofen (5 mg/kg) was injected subcutaneously for analgesia every 12 hours after the operation. In the long-term survival groups (i.e. 2 weeks) of part III, this analgesic process was extended for another two days. In addition, wound healing, body weight and pain severity of rats were controlled at 1, 2, 4, 6, 9, 13, 14 days after the surgery. Rats were euthanized in case prespecified criteria indicating suffering were met (i.e., weight loss of more than 20% of baseline body weight and/or rated pain score **(see Table 5)** of more than 3 points).

Table 5 Pain score

Score (point)	**0**	**1**	**2**
Fur	Normal	Moderate scruffy	Scruffy
Movement	Active	Moderate active	No movement
Body posture	Normal	Moderate kyphosis	Severe kyphosis

TTC staining

In part II, after the last session of neurofunctional assessment at 24 hours post-reperfusion, rats were deeply anesthetized with isoflurane 5% (in room air). Cardiac flushing was performed with 20 mL cold (4 °C) isotonic saline. Following decapitation, forebrains were collected and cut coronally into slices with a thickness of 2 mm in a chilled rat brain matrix (Leica, Wetzlar, Germany). Brain slices were visually assessed for hemorrhage and stained with 2% 2, 3, 5 - triphenyltetrazolium chloride (TTC, Sigma-Aldrich, Steinheim, Germany) at room temperature for 15 minutes. The stained brain slices were rinsed with saline twice and then immersed in 4% paraformaldehyde (Sigma-Aldrich, Steinheim, Germany) at 4 °C for 24 hours. The obtained brain slices were photographed together with a ruler as a reference measuring scale.

MRI scanning

All animals in Part III were scanned with a 7 Tesla ClinScan small animal scanner equipped with a rat whole body transmitter coil and a 4-channel rat brain surface receiving coil (Bruker BioSpin, Germany). Scanning was conducted in the period between middle cerebral artery occlusion was established and before study treatment, at 24 hours and at 2 weeks after reperfusion. In the scanning before treatment, imaging protocol consisted of T2 weighted, perfusion weighted and diffusion weighted acquisitions, the time points of which were separately at about 8, 18, and 39 minutes after middle cerebral artery occlusion. The same scanning protocol was applied in the latter two sessions. Apparent diffusion coefficient (ADC) maps were calculated from the diffusion weighted images.

Infarct volume and brain edema measurement in short-term survival groups

Regions of interests, i.e., the whole brain, the right hemisphere, and the infarct areas on images of TTC stained slices were semi-automatically contoured with Photoshop CC 2018 (version 19.1.6, Adobe, San Jose, California, USA) (**Figure 8A**). Briefly, after opening the original picture with Photoshop, the quick selection tool was applied for creating selection of the whole brain section on each slice (**Figure 8A, upper left, yellow contour**), which was then manually adjusted using the lasso tool (**Figure 8A, upper middle, red contour**). Final selections were then filled with red color (RGB 255, 0, 0) on a new layer and named as “R”. The red mask layer was then indicated invisible. By referring to the anatomical midline on each brain slice, the left region of each selection was subtracted using the lasso tool, and the

remaining selection (**Figure 8A, middle, green contour**) was filled with green color (RGB 0, 255, 0) on a new layer named as "G". This layer was then indicated invisible.

Regions of lesion areas (edema + infarction) were preliminarily contoured with Color Range Command and manually adjusted by referring to the staining of the contralateral brain structure in the left hemisphere (**Figure 8A, lower, yellow contour**). A blue mask of the affected area was created on a new layer named as "B" (RGB 0, 0, 255). Layers named as R, G and B were toggled visible and respectively exported as JPEG images and saved in a file folder for further measurements. (**Figure 8A, right**)

The areas of all the exported masks were measured automatically using the ImageJ software (version 1.52a, National Institutes of Health, Bethesda, USA) (**Figure 8B**). The macro (**see Appendix for the macro code**) was created by recording the steps of commands that were implemented in one trial measurement. The obtained value of areas in pixels was converted into square millimeters (mm^2) by referring to the reference measuring scale (photographed ruler).

The volume of the whole brain, the right hemisphere and the injured brain territory (mixture of infarct volume and brain edema) were calculated by multiplying the corresponding surface areas with 2 (mm). Volume was expressed in mm^3.

Volume of the adjusted infarct volumes were calculated with the simplified formula: volume of whole brain – 2 × volume of right hemisphere + volume of injured brain territory (i.e. mixture of brain edema and infarct). The extent of brain edema [140] was calculated according to: (volume of right hemisphere / (volume of whole brain – volume of right hemisphere) – 1) × 100%.

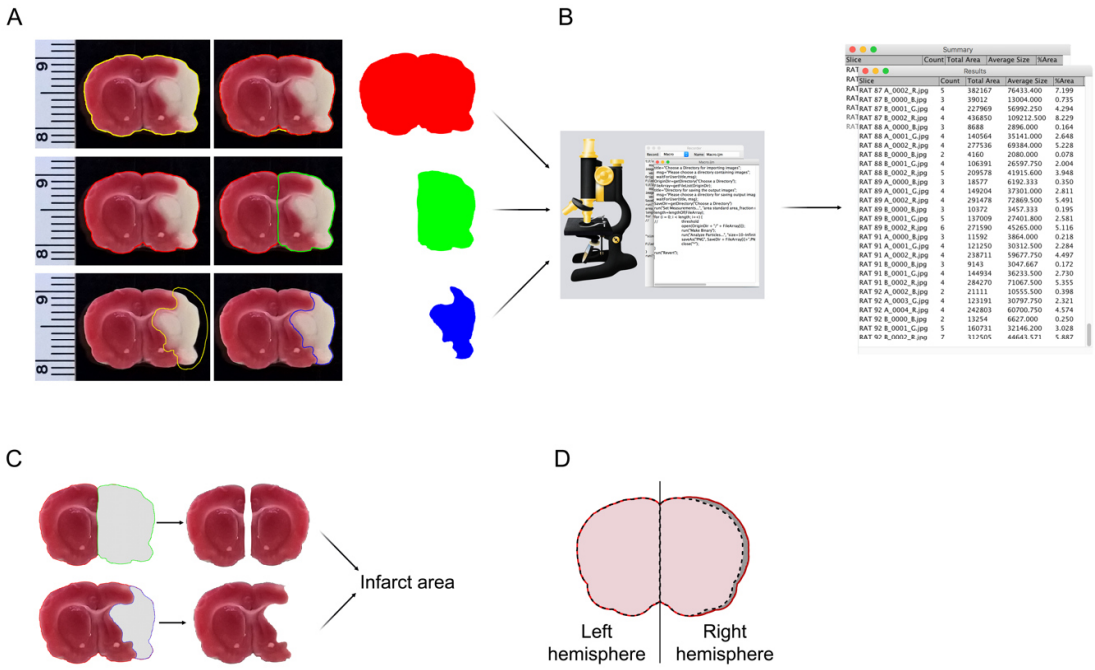

Figure 8 Exemplary software assisted contouring of regions of interest (ROIs) on TTC stained brain slices (**A**), batch measuring of generated ROI masks (**B**), infarct volume correction (**C**) and extent of brain edema calculation (**D**). The whole brain was automatically contoured with the quick selection tool of Photoshop CC 2018 (A, upper left, yellow region), the selection was then manually modified with subtractive/additive lasso tool for removing or adding regions mis-included/excluded regions (**A, upper row, red contour**). Mask of whole brain was generated by filling the final selection with red color (RGB:255, 0, 0) (**A, upper row, red mask**). By referring to the anatomical midline, the right infarcted hemisphere was contoured by excluding the contralateral hemisphere on the whole brain selection with subtractive lasso tool, which was then masked with green color (RGB:0, 255, 0) (**A, middle row, right**). Infarcted region was automatically selected with color range selection function, generated selection was then modified with lasso tool (**A, lower row, blue contour**). On new working path, this region was filled with blue color (RGB: 0, 0, 255). Region that beyond brain tissue area was deleted by applying selection generated with the whole brain mask. Areas of all the masks were then automatically measured in ImageJ software (version 1.52a, National Institutes of Health, Bethesda, USA) with its bunch function (**B**). By referring to the calibrating ruler on brain slices, the area (in pixels) was converted to square millimeters.

Measured infarct area was adjusted by excluding edema, i.e. volume of retained water. Area of healthy brain before ischemia was estimated by doubling the area of contralateral hemisphere (**C, upper right**) and residual healthy brain area was calculated by subtracting the area of injured brain territory (mixture of infarcted brain tissue and retained water) from measured whole brain after infarction (**C, lower right**). The area difference between estimated health brain and residual healthy brain equals to the area of brain tissue developed into infarction. Infarct volume was calculated by multiplying slice thickness (2 mm). Extent of edema represents the degree of brain expansion (see gray region, **D**) that results from edema. Which could be calculated by (volume of right hemisphere – volume of left hemisphere)/volume of left hemisphere. Volume of left hemisphere in our study was calculated by volume of whole brain – volume of right hemisphere.

Infarct volume and brain edema evaluation in long-term survival groups

In long-term survival groups of part III, MRI of each rat obtained at different time points were co-registered with the Image Registration & Fusion Tool (PFUS). Regions of interest were contoured and measured with the Image processing & VOI analysis tool (PBAS). Both tools are used with PMOD software (PMOD Technologies LLC, Zurich, Switzerland). Rats without acute ischemia on both baseline diffusion and perfusion MRI were excluded from further Image processing and analysis.

MRI co-registration and brain territory segmentation

In the co-registration process, firstly, raw T2-MRI in DICOM format (Digital Imaging and Communications in Medicine) of all rats that were obtained before treatment / reperfusion (baseline T2-MRI) were co-registered with an established rat brain template (provided by Werner Siemens imaging center, Tübingen, Germany) and saved as saved as NIfTI format (Neuroimaging Informatics Technology Initiative). Then each adjusted baseline T2-MRI was used as the reference for the later on registrations of subsequent MRI sequences that were obtained at the respective prespecified time points, i.e., (a) ADC maps and perfusion MRI before treatment (i.e., baseline), (b) ADC maps and T2-MRI at 24 hours after reperfusion, and (c) T2-MRI at 2 weeks after reperfusion.

To avoid the observer bias in contouring the regions of interest, we applied a semi-automatic contouring method. Firstly, regions of interest including the whole brain, the left and the right hemisphere, the striatum and the cortex of both hemispheres, were contoured by referring to corresponding anatomical structures on baseline T2-MRI. Structures outside the regions of interest were masked out.

The contoured regions of interest were then further imported into the baseline ADC maps, 24-hour ADC maps and 24-hour T2-MRI, and 2-week T2-MRI. Manual modifications of contours were performed when there were shifts of middle line or cortex as a result of brain swelling at the 24-hour or brain shrinkage at the 2-week time points. Hypo-diffused regions on 24-hour ADC maps, high-intensity regions on 24-hour and 2-week T2-MRI were manually contoured by referring to the normal signal intensity within the same brain region on the contralateral healthy hemisphere.

Lesion volume and extent of edema at 24 hours

On 24-hour ADC maps and 24-hour T2-MRI post-reperfusion, volume of manually contoured brain territories with apparent hypo-diffusion coefficient and with high-intensity respectively were automatically obtained with PMOD software. However, these volumes could overestimate the infarct volume, as a result of water retention (edema) at 24 hours after middle cerebral artery occlusion.

To obtain more accurate infarct volume measurements, the PMOD-measured infarct volume was corrected as described above using the infarct volume correction method for TTC stained slices (see **Figure 8D**). Specifically, the infarct volume equals to the difference between volume of healthy (left) hemisphere and the volume of residual healthy brain tissue of ischemia attacked hemisphere. The former could be directly obtained from PMOD, since the left hemisphere has to be contoured, and the latter was calculated by subtracting the measured injured volume (mixture of infarct and edema) from the volume of right hemisphere. The same correction method was applied in striatal and cortical infarction. Infarct volume on 2 weeks T2-MRI was directly measured without correction.

Extent of edema was calculated with the formula [140]: (volume of right hemisphere – volume of left hemisphere) / volume of left hemisphere.

Thresholds determination for infarct volume prediction on baseline ADC maps

The normal ADC value of target regions including the whole hemisphere, cortex, striatum of the left (healthy) hemisphere was measured separately on each slice of baseline ADC maps (**Figure 9, step 1, green contours**). In the control group, the ADC values of each target area on all the slides were then respectively multiplied by a series of thresholds ranging from 60% to 90%. Within the corresponding target areas (**Figure 9, step 1, blue contours**) on each slice of the infarcted hemisphere, obtained calculated ADC values were applied for automatic contouring of hypo-diffused areas with the thresholding function of PMOD software (**Figure 9, step 2, left and middle column**).

Volumes of generated whole hypo-diffused brain territories, hypo-diffused cortex, and hypo-diffused striatum were then respectively compared with actually measured whole, cortical and striatal lesion volumes on 24-hour ADC maps and infarct volume on 2-week T2-MRI in control group (see exemplary analysis of whole lesion and infarcted area on 24-hour

ADC maps and 2-week T2-MRI, **Figure 9, step 2 right**). Together with the results of correlation analysis between generated hypo-diffusion volumes and measured infarct volumes, thresholds that result in minimal lesion or infarct volume difference between generated and measured volumes, with highest correlation were decided as the optimal thresholds for predicting infarct volume at 2 weeks post-reperfusion on T2-MRI as well as the lesion volume at 24 hours post-reperfusion on ADC maps (see **Figure 9, step 3, optimal threshold I, II**).

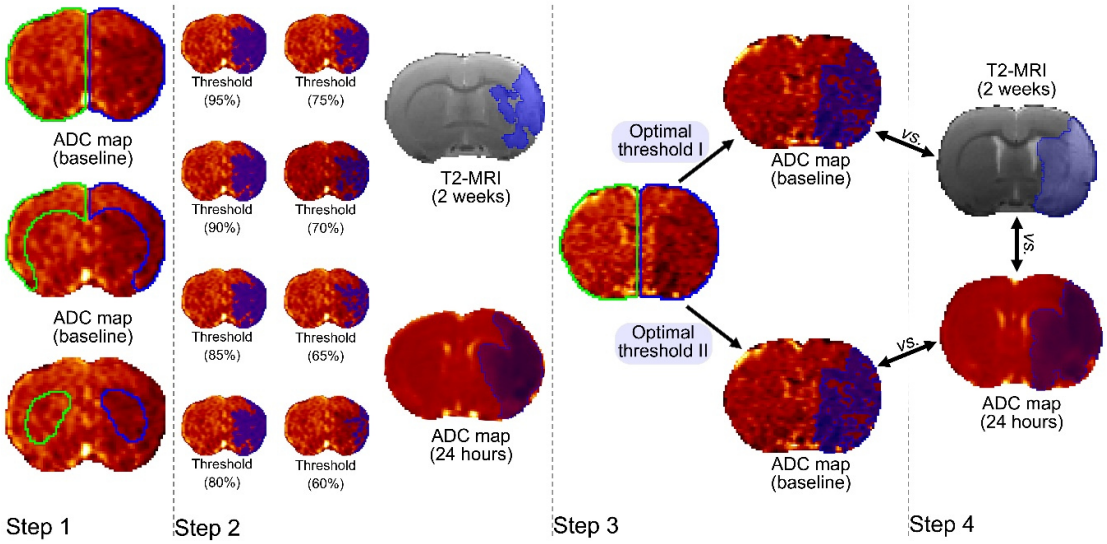

Figure 9 Workflow of threshold-based relative comparison of whole infarct volume (here, the analysis of whole lesion/infarct was taken as an example of the overall analysis workflow), cortical infarct volume and striatal infarct volume. On each slice of baseline apparent diffusion coefficient (**ADC**) maps of control animals, ADC of left (healthy) hemisphere was measured and multiplied by a range of thresholds (60% – 95%) (**Step 1**). With the calculated new ADC values, hypo-diffused areas were automatically generated on the right hemisphere. The volume of each threshold derived hypo-diffused brain region was calculated with PMOD software (**step 2**). By comparing with the manually measured infarct volume on 2-week T2-MRI and whole lesion volume on 24-hour ADC maps, the optimal thresholds I and II that could best predict the measured infarct volumes on 2-week T2-MRI and lesion volume on 24-hour ADC maps, respectively, were determined. In the intra-carotid artery cold infusion (ICCI) group, measured ADC on each slice of left hemisphere was multiplied by the optimal thresholds I and II, respectively (**Step 3**). The calculated ADC values of each slice were further applied for generating hypo-diffused regions on the right hemisphere on baseline ADC map (**Step 3**). The two volumes of generated hypo-diffused brain regions were respectively compared with infarct volume on 2-week T2-MRI and lesion volume on 24-hour ADC maps. Infarct volumes measured on 2-week T2-MRI and lesion volume on 24-hour ADC were also compared.

Evaluation of intra-carotid artery cold infusion effects on brain lesion, edema at 24 hours and final infarction at 2 weeks post-reperfusion

In group ICCI (**Figure 9, step 3 – 4**), firstly, the ADC of the whole hemisphere, cortex and striatum on each slice of left (healthy) side was measured with PMOD. The Obtained values were multiplied with the optimal thresholds determined in step 2 (**Figure 9**). On baseline ADC maps, these calculated values were then applied for generating hypo-diffused brain region on corresponding slide within whole right hemisphere, cortex and striatum respectively. Volumes of each hypo-diffused brain territory were exported and compared with the lesion and infarct volumes respectively measured on 24-hour ADC maps and on 2-week T2-MRI. In addition, the latter two volumes were also compared with each other.

Neurofunctional testing

For neurofunctional assessment, the modified neurological severity score (mNSS), cylinder test and beam walking test were performed in part II of the study until 24 hours after reperfusion. In part III of the study, modified neurological severity score (mNSS) and cylinder test were performed until 2 weeks after reperfusion. In both two parts, baseline neurofunction was evaluated at 1 hour before surgery. Follow-up assessments were conducted at 24 hours after reperfusion in part II of the study, and at day 2, 4, 6, 9, and 13 after reperfusions in part III of the study.

The mNSS is a comprehensive method for evaluating the overall neurofunction in rodents. By referring to the evaluation criteria reported by [141], deficits of motor, sensory, reflex, and balance were assessed by two independent raters who were blinded to the treatments. In case of different scores assigned by the two raters, the mean value of both assessments was calculated. The total mNSS of ranges between 0 and 18 points, with higher scores indicating more severe neurological deficits.

The cylinder test for evaluation of asymmetrical forelimb use [142] was conducted over 5 and 10 minutes at baseline and each follow-up assessment, respectively. The setup of the cylinder (diameter / height: 20 / 30 cm) was performed according to [143]; before each session, the cylinder and the transparent board were cleaned with a 70% ethanol solution. Results of the cylinder test are expressed as percentage of right forelimb touches (ipsilateral to the infarcted hemisphere) in relation to the total number of cylinder wall touches with the left or right forelimb.

The beam walking task (length / width: 60 / 3 cm) required five training sessions per day on three consecutive days before surgery. The beam was placed at a height of 45 cm and connected with the rats' home cages. Foot slips of the rats' affected left fore- and hind limbs were recorded. Performance in the beam walking task was expressed as the percentage of left fore- or hind limb slips in relation to the total number of steps.

Vital parameter Acquisition

LabChart 8 software and PowerLab (both AD Instruments, Dunedin, New Zealand) were used to record regional cerebral blood flow (laser Doppler flowmetry), arterial blood pressure, as well as brain and rectal temperature curves. Mean arterial pressure and heart rate were obtained using the blood pressure module for LabChart 8 (AD instruments). Prism 8 (GraphPad, San Diego, CA, USA) was used for plotting graphs and statistical analyses. Artwork was created with Photoshop CC 2018 (Adobe, San Jose, California, USA).

Data analysis

Data were analyzed and graphs were generated with GraphPad Prism version 8.4.2 (GraphPad Software, Massachusetts, USA). When not specifically noted, normally distributed data sets are reported as mean ± standard deviation. Ordinary one-way ANOVA with Bonferroni's correction for post-hoc multiple comparisons was applied for inter-group comparisons. Non-normally distributed data are reported as median [25% percentile, 75% percentile]. Non-parametric one-way variance analysis (Kruskal-Wallis test) with uncorrected Dunn's test was taken for post-hoc multiple comparisons. Artwork were created with Photoshop CC 2018 version 19.1.6 (Adobe, San Jose, California, USA)

Results

General outcome

In total, 137 rats were included in this study (**Figure 10**).

In part I of the study, 18 rats (age: 11 to 12 weeks, weight: 360 to 470 g) were used. In the first step, four rats received sequential ICCI treatment at different infusion rates ranging from 0.2 to 2.0 mL/minute to evaluate their respective brain cooling efficacy. Nine other rats were used for determining the potential final continuous infusion protocol based on the results from step 1. Applying the final sequence of different infusion rates, another four rats received the full continuous pre- to post-reperfusion ICCI and one more rat underwent intra-venous cold infusion using the same infusion protocol. In part I of the study, one ICCI-treated rat died from subarachnoid hemorrhage at the time of filament retraction, which was confirmed in autopsy.

In part II of the study, 92 rats (23 rats per study group) were used. Of these, 35 rats needed to be excluded prior to randomization; 34 of which were excluded due to an unstable or too high residual regional cerebral blood flow as determined by laser Doppler flowmetry and one rat died soon after ischemia induction. Three other rats died after randomization but prior to treatment due to surgical failure during the attempt to insert the infusion port into the internal carotid artery (two rats in the ICCI group and one rat in the intra-carotid artery warm infusion group). Consequently, 54 rats were available for pre-post-treatment analyses of vital parameters and blood gases (grey shaded boxes in **Figure 10**).

The mean body weight of the 54 rats in part II was 403 ± 13 g and was similar in the four study groups ($F(3, 50) = 0.71$, $p = 0.5519$). In the three infusion groups (ICCI, intra-carotid artery warm infusion, and intra-venous cold infusion), 12.1 ± 0.4 mL of saline were infused over a period of 16.5 ± 0.6 minutes. Infusion volumes ($F(2, 37) = 0.45$, $p = 0.6392$) and durations ($F(2, 37) = 0.42$, $p = 0.6622$) were similar among the three treatment groups. Four rats died before follow-up assessment at 24 hours after reperfusion (one rat in the ICCI group, two rats in the intra-carotid artery warm infusion group, and one rat in the intra-venous cold infusion group). Exclusion rate until successful reperfusion was comparable between the three infusion groups ($\chi^2(2) = 1.9045$, $p = 0.5925$), and between the control group and the infusion groups ($\chi^2(1) = 1.5120$, $p = 0.2188$). Autopsy revealed subarachnoid hemorrhage in

all deceased rats. The remaining 50 rats entered infarct / edema volume and neurofunctional outcome analyses.

In part III of the study, 26 rats were randomized 1:1 to receiving either ICCI or no infusion (control group). Two rats (one rat in the control group and one in the ICCI group) died of autopsy-confirmed subarachnoid hemorrhage immediately after reperfusion / infusion treatment and another two rats (one rat in the control group and one in the ICCI group) were excluded from further analysis because of unsuccessful middle cerebral artery occlusion which was retrospectively confirmed on baseline MRI images (i.e., before treatment). The remaining 22 rats (eleven per group) were included for further assessment of treatment effects.

The mean body weight of the 22 rats in part III of the study was 412 ± 23 g with no statistically significant inter-group difference (unpaired t-test, $p = 0.08$). In the ICCI group, 12.0 ± 0.6 mL of cold saline were infused over a period of 16.5 ± 0.8 minutes. One rat in the control group died between 36 and 48 hours post-reperfusion because of massive hemispheric cerebral infarction. One rat in the ICCI group lacked baseline ADC maps due to technical issues.

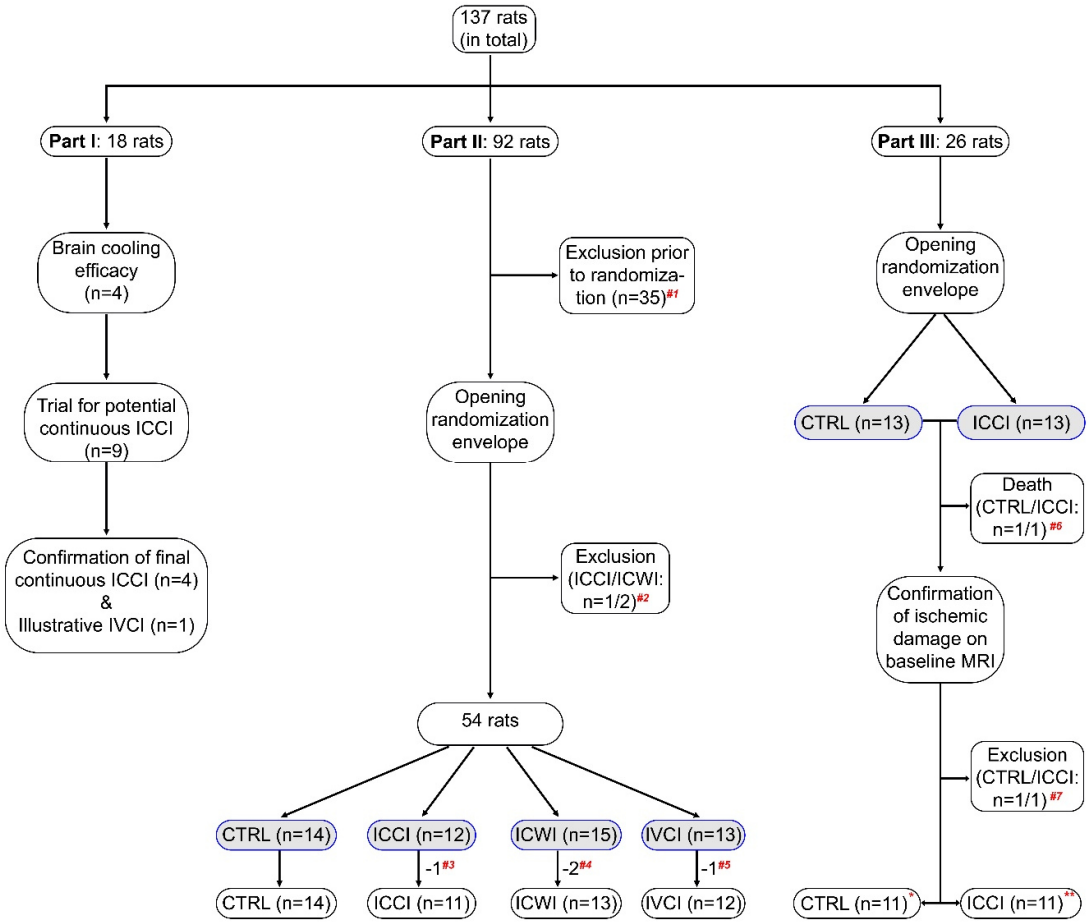

Figure 10 Flow diagram of animal usage in **part I**, **II**, and **III**. CTRL = control group, ICCI = intra-carotid artery cold infusion group, ICWI = intra-carotid artery warm infusion group, IVCI = intra-venous cold infusion group, [#1] including 34 rats with unstable laser Doppler curves and one rat that died soon after filament insertion; [#2] excluded due to surgical failure during connection of the infusion tube: one rat from ICCI group and two rats from ICWI group. [#3, #4, #5] four rats (1 / 2 / 1 rat from ICCI / ICWI / IVCI group respectively) died before 24 hours after reperfusion. [#6] two rats (1 / 1 rat from CTRL / ICCI group) died immediately after reperfusion with autopsy-confirmed subarachnoid hemorrhage. [#7] two rats (1 / 1 rat from CTRL / ICCI group) were excluded for unsuccessful middle cerebral artery occlusion. [*] including the one rat that died between 36 and 48 hours post-reperfusion because of massive hemispheric cerebral infarction. [**] including the one rat that lacked baseline apparent diffusion coefficient (ADC) maps due to technical issues.

Part I: Continuous pre- to post-reperfusion ICCI in rats

Cooling system performance assessment

Room temperature saline could be successfully cooled down to the target temperature around 0 °C after passing through the dual in-line SC-20 heater / cooler (**Table 6**) at measure point T1 which is illustrated in **Figure 6**. However, temperature of the saline rapidly increased to 3 °C to 9 °C on its way to the outlet (measure point T2; 2.5 cm distance from T1) of the dual in-line SC-20 heater / cooler (**Table 6 and Figure 6**). At the connection point of the infusion port with the external carotid artery (measure point T3; 4 cm distance from T2), fluid temperature further increased to about 5 °C at the highest infusion flow rate of 2.0 mL/minute and up to 19 °C at the lowest infusion flow rate of 0.2 mL/minute (see **Table 6 and Figure 6**).

With the additional custom-made closed-loop cooling system (**Figure 6**) that was developed to prevent the re-warming of cooled saline before entering the rats' circulation, fluid temperature could be successfully maintained around 0 °C up to the outlet of the cooling system at measure point T4 (**Table 6 and Figure 6**)

Table 6 Temperature of the infusate before entering the rat circulation

Infusion rate (mL/min)	0.2	0.5	0.7	1.0	1.5	2.0
T1 (°C)	0.1 ± 0.4	–0.4 ± 0.2	−0.5 ± 0.1	−0.6 ± 0.1	−0.6 ± 0.1	−0.3 ± 0.1
T2 (°C)	8.9 ± 0.7	5.0 ± 0.4	4.5 ± 0.4	3.9 ± 0.1	3.2 ± 0.3	3.0 ± 0.3
T3 (°C)	18.5 ± 0.2	11.0 ± 0.2	9.3 ± 0.3	7.4 ± 0.1	5.6 ± 0.2	4.6 ± 0.1
T4 (°C)	2.8 ± 0.4	0.2 ± 0.2	−0.3 ± 0.3	−0.3 ± 0.3	−0.1 ± 0.3	0.3 ± 0.3

Saline temperature immediately after cooling with the SC-20 cooler (T1), at cooler's outlet (T2), and at the tip of the infusion port without (T3) and with (T4) the additional custom-made closed-loop cooling system **(Figure 6)**. Infusion rates ranged from 0.2 to 2.0 mL/min. Temperature data are reported as mean ± standard deviation of 30 seconds of stable measurement. (*Table was modified from Table 1, Wang Yi, et al. Transl Stroke Res. 2021 Aug;12(4):676-687*)

Flow rate dependent brain cooling efficacy during ischemia and after reperfusion

Different patterns of brain temperature drop during 30 seconds of ICCI treatment before reperfusion and after reestablishment of cerebral blood flow were observed (**Figure 11**).

Before reperfusion, when blood supply from the internal carotid artery and the middle cerebral artery was blocked, only the ipsilateral striatum rather than the ipsilateral cortex was cooled. Little to no cooling efficacy was observed at the lowest infusion rate of pre-reperfusion ICCI of 0.2 mL/minute. The cooling rate of pre-reperfusion ICCI plateaued at an infusion rate of 0.5 mL/minute and could not be further increased by increasing the infusion rate.

In contrast, when ICCI was administered after reperfusion (post-reperfusion), i.e., after the ipsilateral internal carotid artery blood flow was re-established by removing the temporary clip around the common carotid artery and the filament, both striatum and cortex ipsilateral to the treated hemisphere could be effectively cooled. Furthermore, speed and extent of brain temperature decrease within both cortex and striatum were infusion rate dependent.

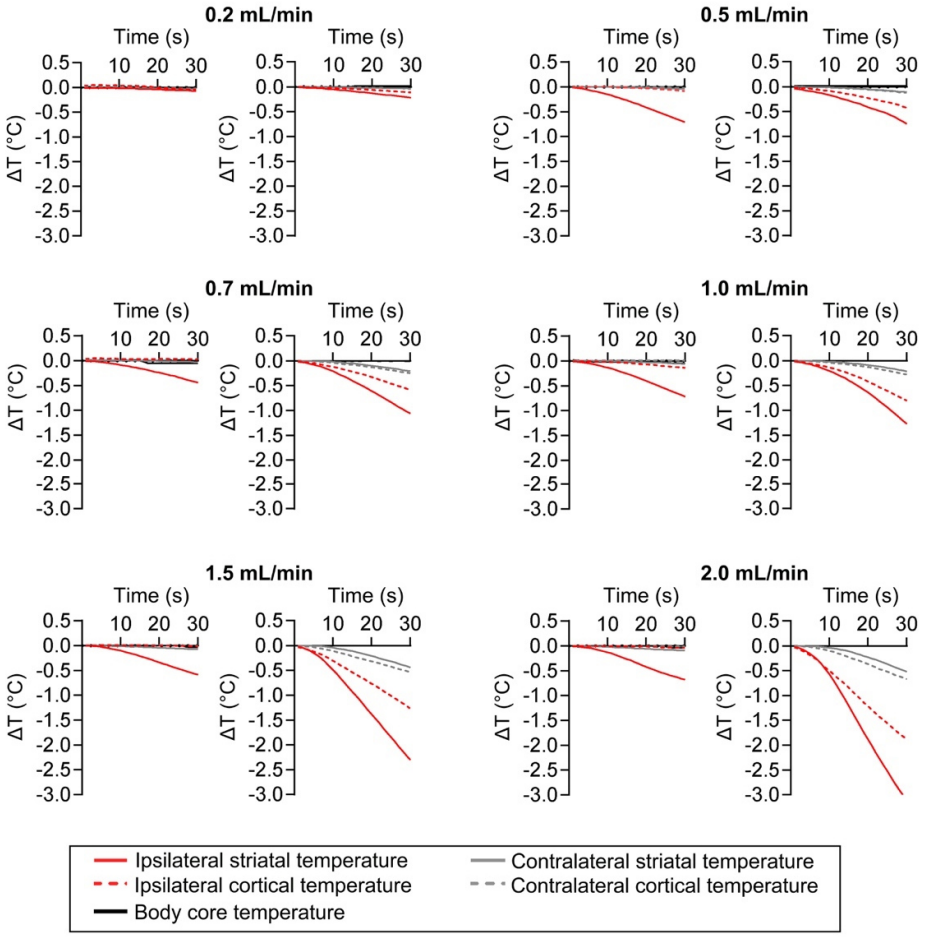

Figure 11 Brain cooling efficacy of intra-carotid artery cold infusion (ICCI). Decrease of core body temperature and mean brain temperature drop (Δ**T**) within ipsilateral and contralateral striatum and cortex during 30 s of pre-reperfusion ICCI (**left**) and post-reperfusion ICCI (**right**) at each infusion rate. ICCI infusion rates ranged from 0.2 to 2.0 mL/min. Infusion rates were sequentially tested in each animal and each trial lasted for 30 seconds. Brain temperature was required to return to normal range (36.5 °C to 37.5 °C) before starting a new trial. (*Figure was modified from Figure 4, Wang Yi, et al. Transl Stroke Res. 2021 Aug;12(4):676-687)*

Continuous pre- to post-reperfusion infusion protocol

To establish a continuous pre- to post-reperfusion infusion protocol that could simulate the application of ICCI during the clinical workflow of the endovascular mechanical thrombectomy procedure and aiming at inducing moderate brain hypothermia as quickly as possible and at maintaining hypothermia for as long as possible using a fixed maximal fluid volume that corresponded to half of the rats' circulating blood volume (i.e., 30 mL per kg of body weight), a sequence of different volumes and flow rates was generated for each treatment phase, i.e., before, during and after reperfusion. The lowest effective infusion rate of 0.5 mL/minute was chosen for the pre-reperfusion ICCI treatment. After 2 minutes of pre-reperfusion ICCI at 0.5 mL/minute, temperature of ischemic striatum was decreased by 2.3 ± 0.3 °C (**Figure 12**).

Since there was infusion rate dependent cooling efficacy during post-reperfusion ICCI (**Figure 11**), the maximal infusion rate (2.0 mL/minute) was chosen during filament retraction and reperfusion in order to rapidly reach moderate brain hypothermia of around 32 °C in the ischemic brain tissue. Over a duration of 42 seconds ICCI treatment at 2.0 mL/minute after reperfusion, ipsilateral striatal temperature was decreased on average by 5.3 ± 1.8 °C compared with baseline (**Figure 12**).

During the post-reperfusion phase, ICCI at 0.7 mL/minute could maintain ipsilateral hypothermia at 32.1 ± 0.3 °C for 14.6 ± 0.84 minutes (**Figure 12**). The mean total saline volume for continuous pre- to post-reperfusion ICCI was 12.6 ± 0.6 mL and the mean overall infusion duration was 17.3 ± 0.8 minutes.

Using the same sequential infusion protocol, intra-venous cold infusion mediated whole-body cooling exhibited obviously much slower and less effective brain cooling. The lowest brain temperature occurred at the end of infusion. Compare with baseline, brain temperature decreased by about 1.5 °C. Patterns of temperature curves of all the monitored brain regions and rectal temperature were similar during intra-venous cold infusion (**Figure 12**).

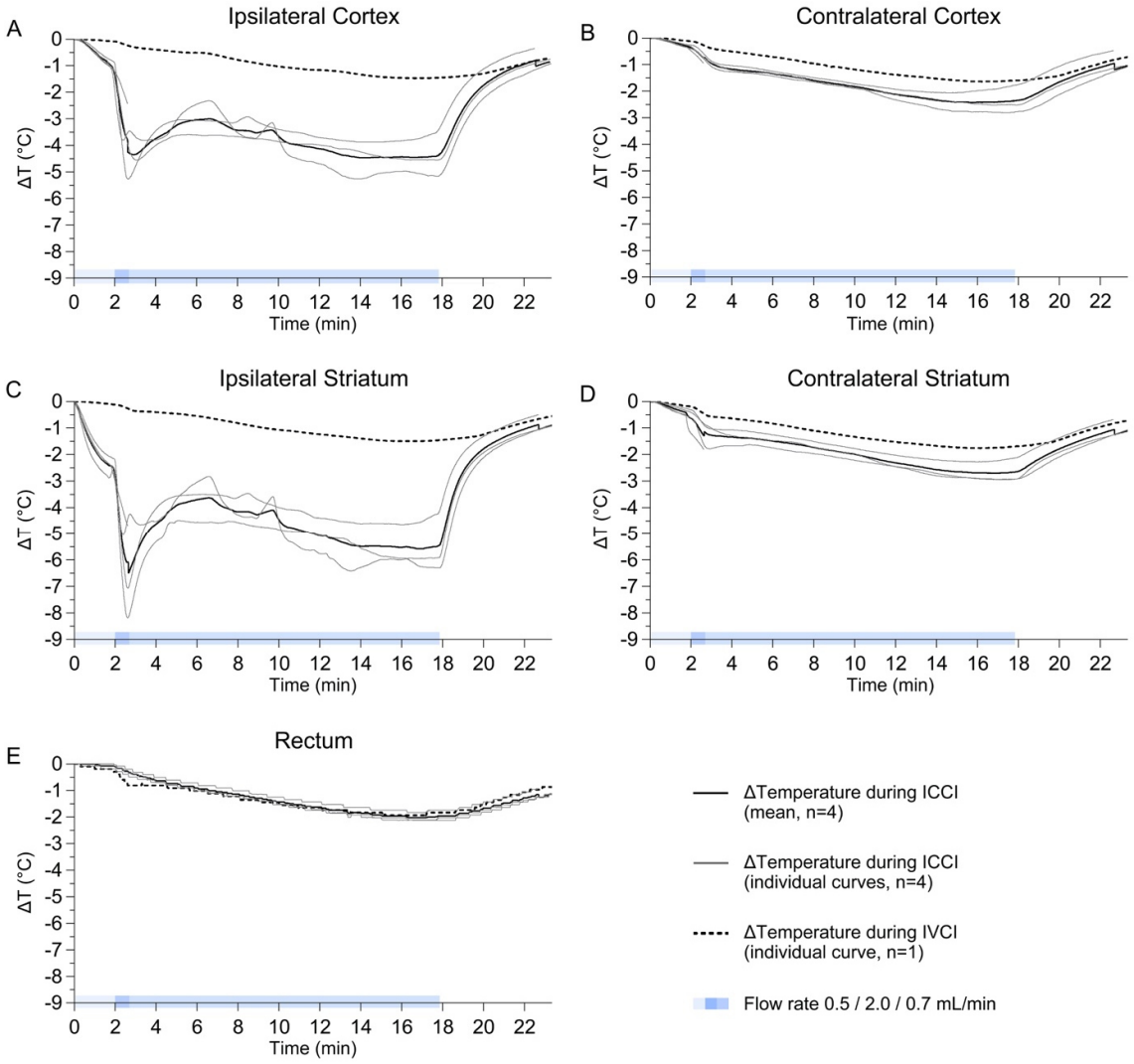

Figure 12 Relative brain and core body temperature during continuous pre- to post-reperfusion intra-carotid (ICCI) and intra-venous cold infusion (IVCI). Individual and mean temperature decrease (**ΔT**, relative to baseline temperature) in the ipsilateral (**A**) and contralateral (**B**) cortex, the ipsilateral (**C**) and contralateral (**D**) striatum, as well as individual and mean decrease of core body temperature (**E**) during continuous pre- to post-reperfusion ICCI (n = 4) and intra-venous cold infusion (n = 1). (*Figure was modified from Figure 5, Wang Yi, et al. Transl Stroke Res. 2021 Aug;12(4):676-687)*

Part II: neuroprotection assessment in rats undergoing 100 minutes middle cerebral artery occlusion

Infarct volume and brain edema at 24 hours

Mean infarct volumes at 24 hours were 138.5 mm^3 (interquartile range, 81.8 to 215.9) in the control group (n = 14), 148.1 mm^3 (interquartile range, 45.1 to 289.6) in the intra-carotid artery cold infusion (ICCI) group (n = 11), 102.6 mm^3 (interquartile range, 68.6 to 226) in the intra-carotid warm infusion group (n = 13), and 135.2 mm^3 (interquartile range, 61.1 to 226.5) in the intra-venous cold infusion group (n = 12). No significant difference was found between groups (H (3) = 5.27, p = 0.15).

Corresponding relative extent of brain edema at 24 hours was 6.4% (interquartile range, 3.9 to 9.4), 7.6% (interquartile range, 3.6 to 8.5), 3.5% (interquartile range, 2.6 to 7.6), and 8.8% (interquartile range, 4.4 to 10.7), respectively. No significant differences between groups were found (H (3) = 0.46, p = 0.93) (**Figure 13**).

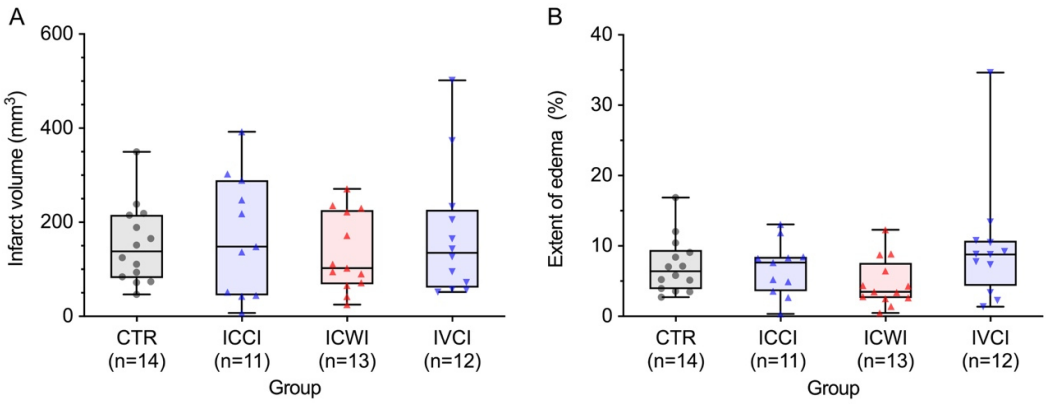

Figure 13 Infarct volume (**A**) and extent of brain edema (**B**) at 24 hours after reperfusion. CTRL = control group (n = 14), ICCI = intra-carotid artery cold infusion group (n = 11), ICWI = intra-carotid artery warm infusion group (n = 13), IVCI = intra-venous cold infusion group (n = 12). Data were presented as median, lower (25%) and upper (75%) quartiles, range of minimum to maximum.

Functional outcomes at 24 hours

All the rats exhibited neurofunctional integrity before surgery without inter-group differences (**Figure 14**). At 24 hours after reperfusion, all rats presented with impaired neurofunction, i.e., an increased modified neurological severity score, a higher preference of ipsilateral forepaw usage in the cylinder test, and a higher rate of missteps during the beam walking test. No significant inter-group difference was detected at 24 hours after reperfusion in mNSS ($H(3) = 3.15$, $p = 0.37$), cylinder test ($H(3) = 3.69$, $p = 0.297$), beam walking test ($H(3) = 3.73$, $p = 0.29$) (**Figure 14, Table 7**).

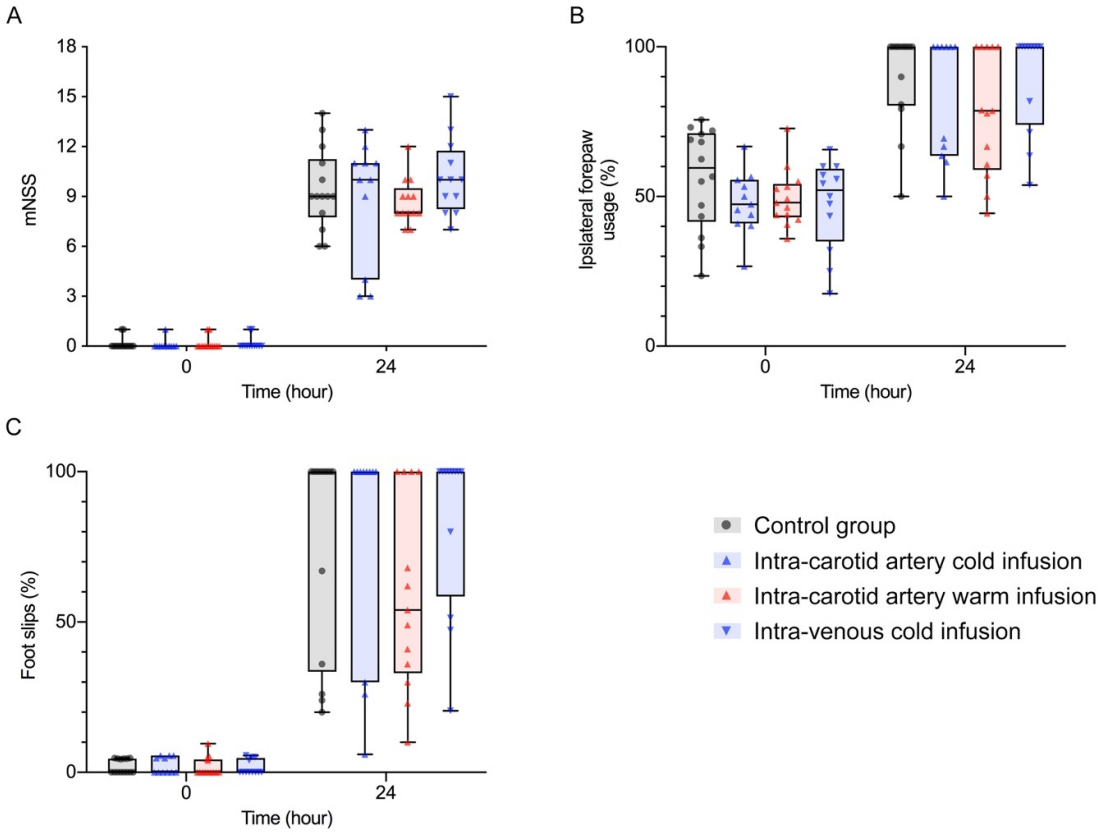

Figure 14 Neurofunctional assessment one hour before surgery and 24 hours after reperfusion. Modified neurological severity score (**A**), ipsilateral forelimb usage in cylinder test (**B**), and contralateral foot slips during beam walking (**C**). Control group (CTRL, number of animals: n = 14), Intra-carotid artery cold infusion group (ICCI, number of animals: n = 11), Intra-carotid artery warm infusion group (ICWI, number of animals: n = 13), Intra-venous cold infusion group (IVCI, number of animals, n = 12). Data were presented as median, lower (25%) and upper (75%) quartiles, range of minimum to maximum.

Table 7 Neurofunctional outcomes

	CTRL (n = 14)	ICCI (n = 11)	ICWI (n = 13)	IVCI (n = 12)
mNSS (points)				
Baseline	0 (0 – 0)	0 (0 – 0)	0 (0 – 0)	0 (0 – 0)
Follow-up	9.0 (7.8 – 11.3)	10.0 (4.0 – 11.0)	8.0 (8.0 – 9.5)	10.0 (8.3 – 11.8)
Percentage of ipsilateral forelimb usage (%)				
Baseline	59.6 (41.5 – 71.1)	47.4 (41.0 – 55.6)	48.0 (43.1 – 54.2)	52.2 (35.0 – 59.3)
Follow-up	100 (80.4 – 100)	100 (63.6 – 100)	78.7 (58.9 – 100)	100 (74.0 – 100)
Incidence of contralateral foot slips (%)				
Baseline	0 (0 – 4.5)	0 (0 – 5.6)	0 (0 – 4.3)	0 (0 – 4.8)
Follow-up	100 (33.5 – 100)	100 (30.0 – 100)	54.0 (33.0 – 100)	100 (58.5 – 100)

Baseline was assessed one hour before surgery, and follow-up evaluations were performed 24 hours after reperfusion. Values are provided in median and interquartile range. CTRL = control group, ICCI = intra-carotid artery cold infusion group, ICWI = intra-carotid artery warm infusion group, IVCI = intra-venous cold infusion group.

Mean residual regional cerebral blood flow during ischemia and its correlation with infarct and edema volumes

We analyzed the correlation between mean residual regional cerebral blood flow measured by laser Doppler flowmetry during middle cerebral artery occlusion and lesion volume at 24 hours post-reperfusion. The latter represents the sum of infarct volume and retained water volume.

In the control group, a negative linear correlation between lesion volume and mean residual regional cerebral blood flow values during middle cerebral artery occlusion was observed (**Figure 15**). (Person r = –0.73, P = 0.003, n = 14).

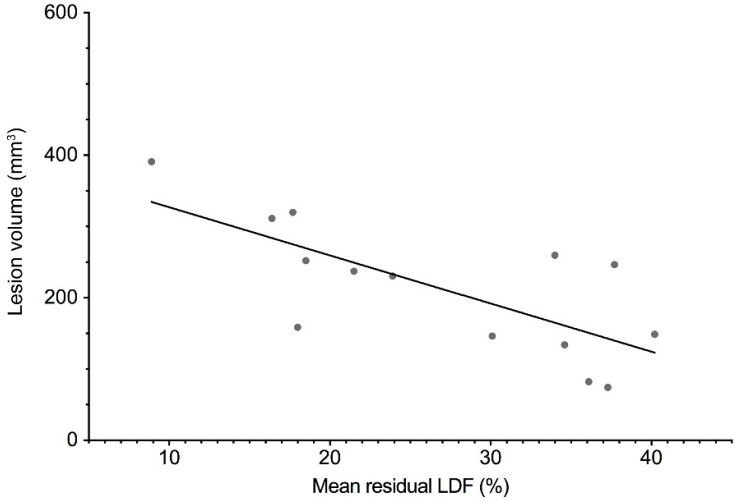

Figure 15 Correlation between mean residual laser Doppler flow (LDF) values during middle cerebral artery occlusion and lesion volume of ischemic brain tissue (the mixture of infarction and edema) at 24 hours post-reperfusion in the control group (n = 14).

Infarct volume and brain edema in post-hoc defined subgroups according to the rats' residual regional cerebral blood flow

In the following post-hoc analysis, rats in each group were allocated into two subgroups depending on their mean residual regional cerebral blood flow on laser Doppler flowmetry during middle cerebral artery occlusion. Rats with a mean residual regional cerebral blood flow lower than 25% of baseline cerebral blood flow were allocated to the severe ischemia group, resulting in 7, 7, 5, and 6 rats of the control group, the ICCI group, the intra-carotid artery warm infusion group and the intra-venous cold infusion group, respectively.

Rats with a mean residual regional cerebral blood flow between 25% and 40% of baseline cerebral blood flow were allocated to the moderate ischemia group, resulting in 7, 4, 8, and 6 rats of the control group, the ICCI group, the intra-carotid artery warm infusion group, and the intra-venous cold infusion group, respectively.

In each treatment group, the median infarct volume of severe ischemia rats was larger than that of rats with moderate ischemia. This difference reached statistical significance in the control group ($p = 0.048$) and the ICCI group ($p = 0.039$) (unpaired t-test, **Figure 16, Table 8**). Same as for the total cohort analysis, no significant treatment dependent differences were found in neither subgroup of rats with severe nor moderate ischemia.

More extensive brain edema was observed in severe ischemia rats as compared with moderate ischemia rats, but, likewise to infarct volumes, statistical significance was only reached in the control group ($p = 0.041$) and the ICCI group ($p = 0.039$) (**Figure 16, Table 8**). No significant treatment dependent differences were found in either subgroup of rats with severe or moderate ischemia (**Figure 16, Table 8**).

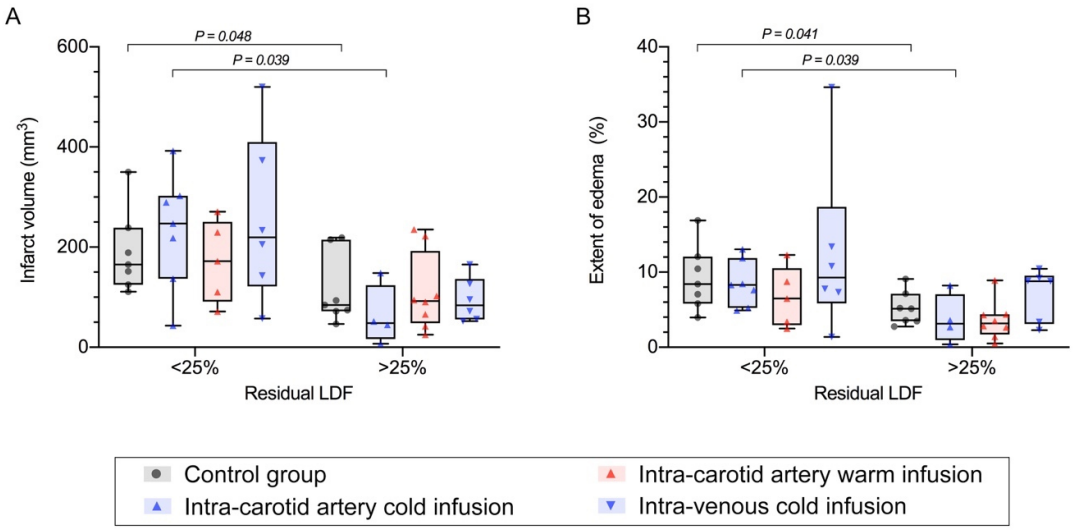

Figure 16 Infarct volume (**A**) and brain edema (**B**) in the subgroups of rats with severe focal cerebral ischemia (defined as a residual regional cerebral blood flow on laser Doppler flowmetry of less than 25% compared to baseline (< 25%)) and rats with moderate focal cerebral ischemia (defined as a mean residual regional cerebral blood flow of 25% to 40% of baseline (> 25%)).

Table 8 Infarct volume and extent of brain edema in subgroups

	rLDF < 25%	rLDF > 25% to < 40%	
Infarct volume (mm^3)			
CTRL (n = 7 / 7)	165.6 (125.1 – 238.8)	84.3 (71.8 – 214.9)	p = 0.048
ICCI (n = 7 / 4)	247.4 (137.0 – 302.8)	48.5 (16.8 – 124.0)	p = 0.039
ICWI (n = 5 / 8)	171.8 (91.1 – 250.3)	92.6 (48.1 – 192.3)	p = 0.135
IVCI (n = 6 / 6)	219.4 (121.9 – 410.0)	83.7 (55.4 – 136.5)	p = 0.298
Extent of edema (%)			
CTRL (n = 7 / 7)	8.4 (5.8 – 12.1)	5.1 (3.5 – 7.1)	p = 0.041
ICCI (n = 7 / 4)	8.3 (5.2 – 11.9)	3.2 (1.0 – 7.1)	p = 0.039
ICWI (n = 5 / 8)	6.5 (3.0 – 10.5)	3.2 (1.7 – 4.4)	p = 0.135
IVCI (n = 6 / 6)	9.3 (5.8 – 18.7)	8.8 (3.1 – 9.5)	p = 0.298

Values are provided in median and interquartile range. CTRL = control group, ICCI = intra-carotid artery cold infusion group, ICWI = intra-carotid artery warm infusion group, IVCI = intra-venous cold infusion group; Comparisons of infarct volume and extent of edema in rats with severe ischemia (i.e., residual laser Doppler flow (rLDF) < 25% of baseline) and moderate ischemia (i.e., rLDF > 25% to < 40% of baseline) were performed with unpaired t-test after log transformation.

Neurofunctional performance in the post-hoc defined subgroups with severe and moderate ischemia

The baseline neurofunctional performance in the mNSS, the cylinder test and the beam walking test obtained for the severe ischemia rats was comparable to that of the rats with moderate ischemia with no significant difference between the two subgroups within each treatment group ($p > 0.05$, unpaired t-test) and also with no significant differences between treatment groups within each subgroup.

At 24 hours, control group rats with severe ischemia had higher rate of foot slips in the beam walking test compared to rats with moderate ischemia (unpaired t-test, $P = 0.004$).

mNSS trended to be also lower in control rats with moderate ischemia, but statistical significance could not be reached (unpaired t-test, $P = 0.07$).

Rate of ipsilateral forepaw preference of severely ischemic rats in the cylinder test was comparable with moderately ischemic rats in group control (unpaired t-test, $P = 0.387$).

No statistically significant differences were found when comparing severe to moderate ischemia rats in the three infusion groups.

While no significant differences between treatment groups was found within the severe ischemia subgroup at the 24-hour timepoint, mNSS was lower in the subgroup of moderate ischemia rats in the ICCI group compared to moderate ischemia rats in the control group ($p = 0.0013$) and the two other infusion groups, intra-carotid artery warm infusion group ($p = 0.0015$) and intra-venous cold infusion group ($p = 0.0006$) (**Figure 17, Table 9**). No significant inter-treatment group differences were detected in the cylinder and the beam walking test in the subgroup of moderate ischemia rats.

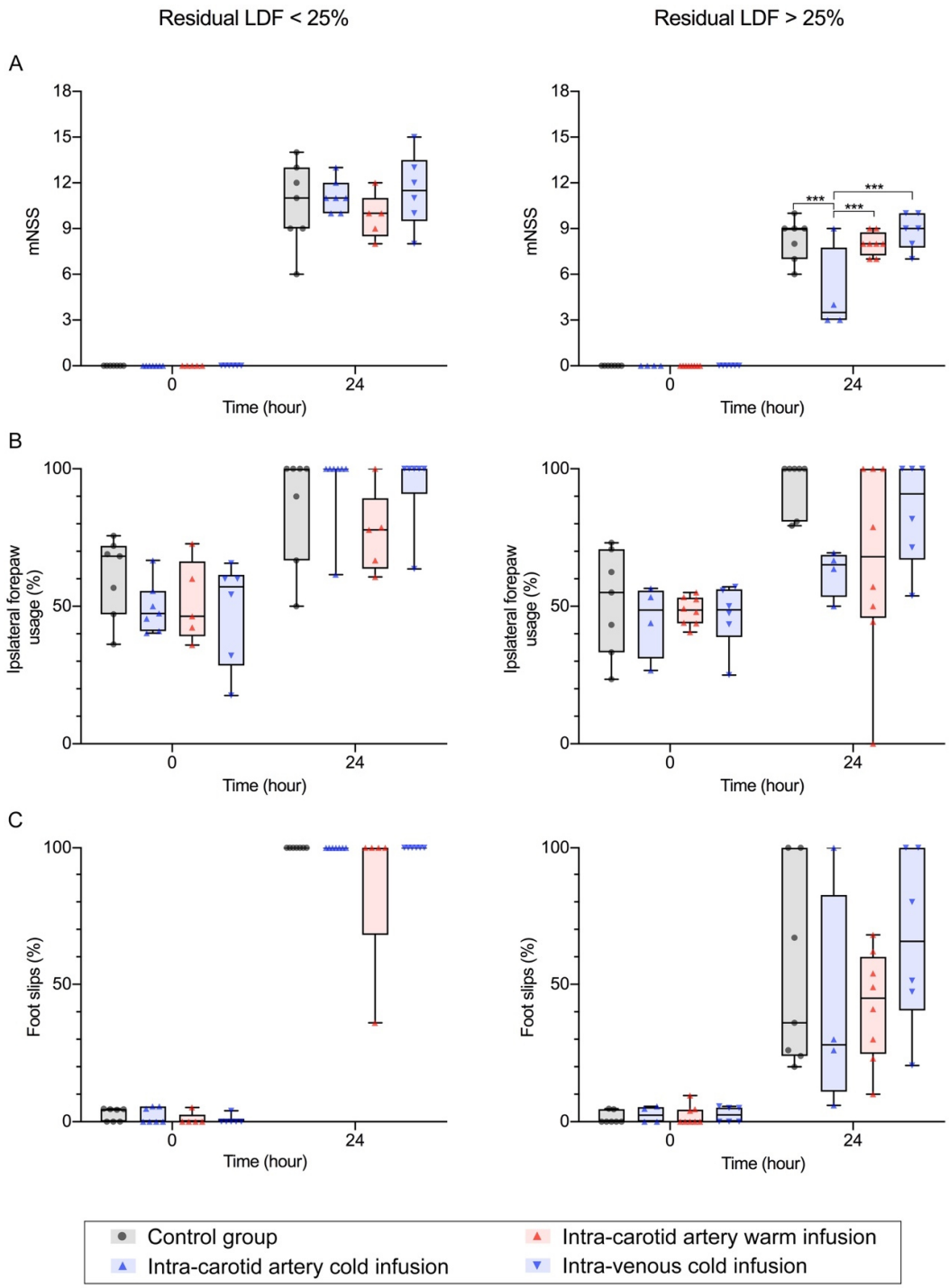

Figure 17 Neurofunctional assessments at 1 hour before surgery and at 24 hours after middle cerebral artery occlusion in the two subgroups. Severe ischemia, with a residual regional cerebral blood flow on laser Doppler (LDF) of < 25% of baseline (CTRL: control group, n = 7; ICCI: intra-carotid artery cold infusion group, n = 7; ICWI: intra-carotid artery warm infusion group, n = 5; IVCI: intra-venous cold infusion group, n = 6), and moderate ischemia, with a residual LDF of 25% to 40% of baseline (CTRL: n = 7; ICCI: n = 4; ICWI: n = 8; IVCI: n = 6). (**A**) Modified neurological severity score (mNSS), (**B**) percentage of ipsilateral (to infarcted hemisphere) forelimb usage in cylinder test, (**C**) incidence of contralateral foot slips during beam walking.

Table 9 Neurofunctional assessments at 1 hour before surgery (baseline) and at 24 hours after middle cerebral artery occlusion in subgroups

	Time point	mNSS (points)	Ipsilateral forelimb usage (%)	Foot slips (%)
rLDF < 25%				
CTRL (n = 7)	baseline	0 (0 – 0)	68.2 (47.1 – 72.0)	4.4 (0 – 4.6)
	24-hour follow-up	11.0 (9.0 –13.0)	100 (66.7 – 100)	100 (100 –100)
ICCI (n = 7)	baseline	0 (0 – 0)	47.4 (41.0 – 55.6)	0 (0 – 5.6)
	24-hour follow-up	11.0 (10.0 –12.0)	100 (100 – 100)	100 (100 – 100)
ICWI (n = 5)	baseline	0 (0 – 0)	46.4 (39.1 – 66.4)	0 (0 – 2.6)
	24-hour follow-up	10.0 (8.5 –11.0)	77.8 (63.7 – 89.4)	100 (68 –100)
IVCI (n = 6)	baseline	0 (0 – 0)	57.2 (28.5 – 61.4)	0 (0 – 1.0)
	24-hour follow-up	11.5 (9.5 –13.5)	100.0 (90.9 – 100)	100 (100 –100)
rLDF > 25%				
CTRL (n = 7)	baseline	0 (0 – 0)	55.0 (33.3 – 70.8)	0 (0 – 4.6)
	24-hour follow-up	9.0 (7.0 – 9.0)	100 (80.8 – 100)	36.0 (24.0 – 100)
ICCI (n = 4)	baseline	0 (0 – 0)	48.6 (31.0 – 55.7)	2.4 (0 – 5.6)
	24-hour follow-up	3.5 (3.0 – 7.7) *** ### §§§	65.2 (53.4 – 68.7)	28.0 (11.0 – 82.5)
ICWI (n = 8)	baseline	0 (0 – 0)	48.6 (43.9 – 53.1)	0 (0 – 4.4)
	24-hour follow-up	8.0 (7.3 – 8.7)	68.0 (45.8 – 100)	45.0 (24.8 – 60.0)
IVCI (n = 6)	baseline	0 (0 – 0)	48.8 (38.9 – 56.1)	2.5 (0 – 5.1)
	24-hour follow-up	9.0 (7.8 – 10.0)	90.9 (67.0 – 100)	65.7 (40.6 – 100)

Values are provided in median and interquartile range. CTRL = control group, ICCI = intra-carotid artery cold infusion group, ICWI = intra-carotid artery warm infusion group, IVCI = intra-venous cold infusion group, n = number of animals, *** p = 0.0013, versus CTRL (at 24-hour follow-up in subgroup with moderate ischemia, i.e., a residual regional cerebral blood flow on laser Doppler (rLDF) of 25 to 40% of baseline ; ### p = 0.0015, versus ICWI (at 24-hour follow-up in the subgroup of moderate ischemia); §§§ p = 0.0006, versus IVCI (at 24-hour follow-up in the subgroup of moderate ischemia).

Vital parameters, blood gases and regional cerebral blood flow analysis

Rectal temperature

Rectal temperature was comparable in all four study groups before middle cerebral artery occlusion (measured at –2 minute before filament insertion), during ischemia (from 2 to 94 minutes, and at 96 minutes, i.e., just before infusion in the intervention groups) (**Table 10**). Change of rectal temperature was significantly influenced by treatments ($F(9, 150) = 15.88$, $p < 0.0001$, **Table 10**): intra-venous cold infusion lowered rectal temperature faster, deeper, and longer compared to intra-carotid artery cold infusion ($p < 0.05$ for intra-venous cold infusion versus all other groups from pre-reperfusion infusion until after treatment, and for intra-carotid artery cold infusion versus all other groups only during post-reperfusion infusion) (**Table 10**)

Regional cerebral blood flow

At filament insertion, regional cerebral blood flow dropped to below 40% of baseline in all 54 included rats. Regional cerebral blood flow (range) in control group, the ICCI group, the intra-carotid warm infusion group and the intra-venous cold infusion group were 21% ± 7 (14 to 36), 18% ± 4 (12 to 26), 18% ± 6 (9 to 30), and 20% ± 4 (12 to 25), respectively, with a similar decrease across groups ($F(3, 50) = 0.61$, $p = 0.6089$).

Mean regional cerebral blood flow during middle cerebral artery occlusion (from 2 to 94 minutes after filament insertion, and at 96 minutes, i.e., just before the start of infusion in the intervention groups) was comparable between groups (**Table 10**). After reperfusion, regional cerebral blood flow increased to above 80% of baseline values (before filament occlusion of the middle cerebral artery), and treatment effects were no longer detectable (**Table 10**).

Mean arterial pressure and heart rate

All 54 rats underwent intermittent arterial pressure and heart rate assessment. Mean arterial pressure and heart rate were comparable between groups before (at –20 minute) and during middle cerebral artery occlusion (at 50 minutes) (**Table 10**).

From during middle cerebral artery occlusion (at 50 minutes) to values at 120 minutes (i.e., after infusion in the intervention groups), mean arterial pressure decreased in all groups, which were –7 ± 8 mmHg in the control group, –11 ± 10 mmHg in the ICCI group, –12 ± 9 mmHg in the intra-carotid artery warm infusion group, and –15 ± 10 mmHg in intra-venous cold infusion group. Heart rate also decreased in all groups (–41 ± 37 bpm in the control group, –58 ± 32 bpm in the ICCI group, –36 ± 34 bpm in the intra-carotid artery warm infusion group, and –80 ± 28 bpm in the intra-venous cold infusion group).

No interaction of treatments could be detected for mean arterial pressure ($F(3, 47) = 1.59$, $p = 0.2044$), treatments significantly influenced heart rate ($F(3, 47) = 4.72$, $p = 0.0058$). Decrease of heart rate was most pronounced after intra-venous cold infusion group ($p < 0.05$, versus the control group and the intra-carotid warm infusion group)

Table 10 Vital parameters, regional cerebral blood flow before, during, and after operation

Time point	Minutes from MCA occlusion	CTRL	ICCI	ICWI	IVCI
Rectal temperature (°C)					
before MCA occlusion	0	37.2 ± 0.6	37.3 ± 0.5	37.5 ± 0.4	37.4 ± 0.5
during MCA occlusion	2 to 94	37.4 ± 0.3	37.3 ± 0.2	37.5 ± 0.3	37.4 ± 0.3
before treatment	96	37.6 ± 0.7	37.2 ± 0.6	37.4 ± 0.4	37.3 ± 0.4
pre-reperfusion infusion	99	37.6 ± 0.7	37.1 ± 0.5	37.4 ± 0.5	37.0 ± 0.5
post-reperfusion flushing	100.5	37.6 ± 0.7	37.0 ± 0.5	37.4 ± 0.4	36.3 ± 0.9
post-reperfusion infusion	110	37.4 ± 0.6	36.3 ± 0.6	37.2 ± 0.4	35.6 ± 0.6
after treatment	120	37.3 ± 0.5	36.4 ± 0.8	37.1 ± 0.4	34.8 ± 0.7
rCBF (%)					
before MCA occlusion	–2	101 ± 2	100 ± 4	98 ± 8	100 ± 3
during MCA occlusion	2 to 94	27 ± 10	23 ± 10	28 ± 8	26 ± 9
before treatment	96	30 ± 15	21 ± 12	31 ± 13	25 ± 11
pre-reperfusion infusion	99	29 ± 15	17 ± 9	24 ± 13	27 ± 11
post-reperfusion flushing	100.5	101 ± 29	79 ± 24	110 ± 33	109 ± 43
post-reperfusion infusion	110	126 ± 27	105 ± 19	126 ± 47	129 ± 29
after treatment	120	128 ± 25	108 ± 32	115 ± 51	132 ± 35
MAP (mmHg)					
before MCA occlusion	–20	90 ± 9	89 ± 9	92 ± 9	85 ± 12
during MCA occlusion	50	85 ± 9	85 ± 10	89 ± 8	82 ± 10
before treatment	96	85 ± 4 (n = 4)	87 ± 9 (n = 8)	88 ± 7 (n = 9)	79 ± 9 (n = 8)
pre-reperfusion infusion	99	85 ± 4 (n = 4)	79 ± 13 (n = 8)	79 ± 15 (n = 9)	84 ± 7 (n = 8)
post-reperfusion flushing	100.5	83 ± 1 (n = 4)	76 ± 17 (n = 8)	70 ± 16 (n = 9)	81 ± 8 (n = 8)
post-reperfusion infusion	110	78 ± 5 (n = 9)	76 ± 9 (n = 9)	85 ± 8 (n = 11)	71 ± 10 (n = 9)
after treatment	120	78 ± 6 (n = 11)	74 ± 12	77 ± 7	67 ± 8
Heart rate (bpm)					
before MCA occlusion	–20	381 ± 51	352 ± 39	364 ± 36	353 ± 39
during MCA occlusion	50	377 ± 63	378 ± 41	371 ± 59	376 ± 53
before treatment	96	356 ± 44 (n = 4)	377 ± 43 (n = 8)	369 ± 48 (n = 9)	369 ± 50 (n = 8)
pre-reperfusion infusion	99	354 ± 46 (n = 4)	372 ± 42 (n = 8)	370 ± 47 (n = 9)	366 ± 50 (n = 8)
post-reperfusion flushing	100.5	343 ± 40 (n = 5)	360 ± 42 (n = 8)	365 ± 44 (n = 9)	363 ± 48 (n = 8)
post-reperfusion infusion	110	325 ± 28 (n = 9)	330 ± 31 (n = 10)	344 ± 39 (n = 11)	335 ± 39 (n = 9)
after treatment	120	338 ± 56 (n = 11)	321 ± 33	334 ± 36	296 ± 40

Values are provided in mean ± standard deviation; number of animals (n) was 14 in the control group (CTRL), 12 in the intra-carotid artery cold infusion group (ICCI), 15 in the intra-carotid warm infusion group (ICWI) and 13 in intra-venous cold infusion group (IVCI). Numbers (n) of animals included for individual analyses are reported if less than total number of each group; MCA = middle cerebral artery, rCBF = regional cerebral blood flow assessed by laser Doppler flowmetry. MAP = mean arterial pressure, bpm = beats per minute

Continuous vital parameter monitoring

Change of regional cerebral blood flow was significantly influenced by treatments ($F(9, 150) = 15.88$, $p < 0.0001$): a slight but significant decrease of regional cerebral blood flow was observed during pre-reperfusion in rats treated with intra-carotid infusion (cold and warm) but not during pre-reperfusion of intra-venous cold infusion, and not in control rats (**Table 11**; $p < 0.05$ for the ICCI group versus the intra-venous cold infusion group, and for the intra-carotid artery warm infusion group versus both, the control group and the intra-venous cold infusion group).

In the subset of rats that received additional continuous arterial pressure and heart rate monitoring (which were n = 4 / 7 / 7 / 7 in the control group, the ICCI group, the intra-carotid artery warm infusion group, and the intra-venous cold infusion group, respectively), we observed a transient decrease of mean arterial pressure in most rats during the pre-reperfusion phase of cold and warm intra-carotid artery infusion, but not during pre-reperfusion phase of intra-venous cold infusion and not in rats of the control group (**Figure 18C, Table 11**). No such effects were found on heart rate.

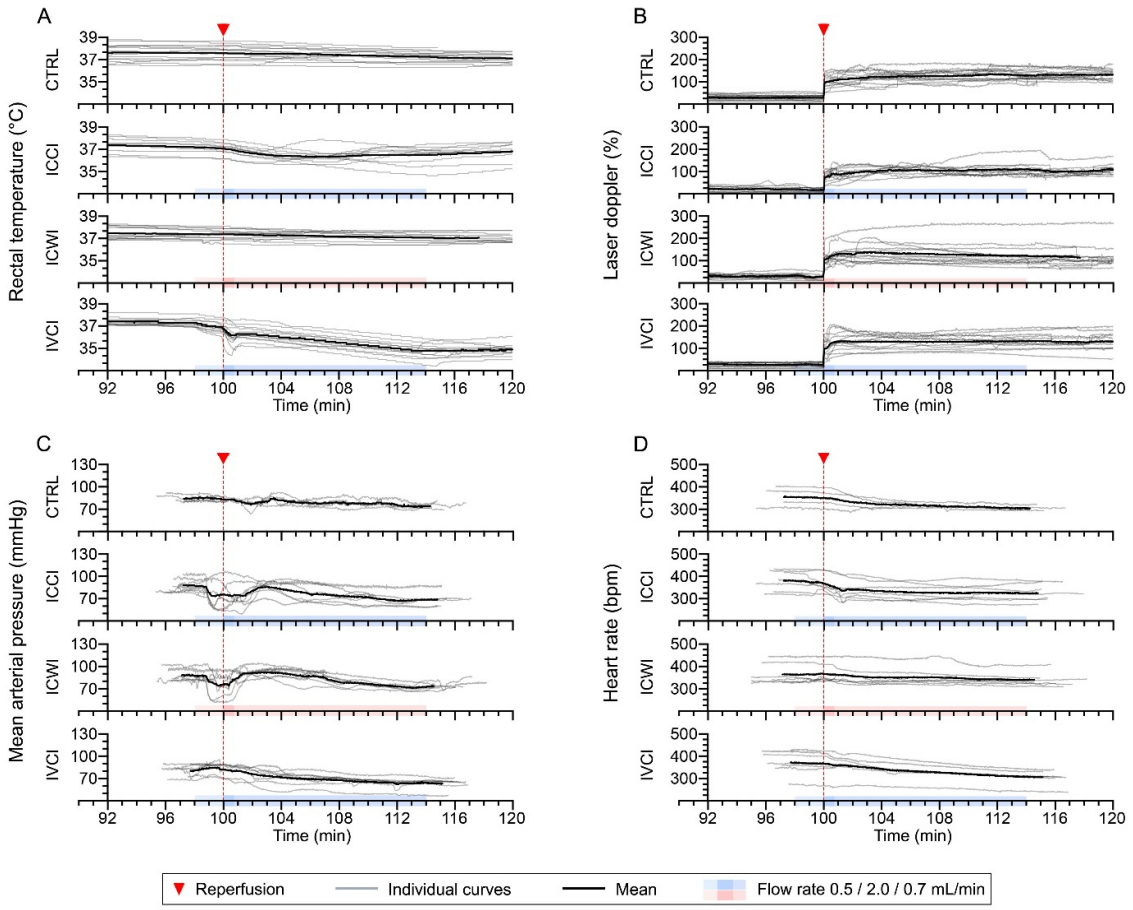

Figure 18 Curves of core body temperature (**A**), regional cerebral blood flow reflected by laser Doppler (**B**), mean arterial pressure (**C**) and heart rate (**D**) during infusion or corresponding time points in the control group. All rats received continuous monitoring of core body temperature and regional cerebral blood flow. Number of animals was respectively 14 / 11 / 13 / 12 in the control group (CTRL), the intra-carotid artery cold infusion group (ICCI), the intra-carotid artery warm infusion group (ICWI), and the intra-venous cold infusion group (IVCI). Part of the rats (number of animals = 4 / 7 / 7 / 7, respectively) also underwent additional continuous mean arterial pressure and heart rate monitoring.

Table 11 Relative change of vital parameters during infusions or corresponding time points in the control group

	CTRL	ICCI	ICWI	IVCI	
Rectal Temperature (°C)					
pre-reperfusion infusion	–0.0 ± 0.1	–0.1 ± 0.1	–0.0 ± 0.1	–0.3 ± 0.2	F (3, 50) = 23.89, p < 0.0001 *
post-reperfusion flushing	–0.0 ± 0.1	–0.2 ± 0.1	–0.0 ± 0.1	–1.0 ± 0.6	F (3, 50) = 26.28, p < 0.0001 *
post-reperfusion infusion	–0.1 ± 0.5	–0.8 ± 0.7	–0.2 ± 0.3	–1.7 ± 0.4	F (3, 50) = 30.20, p < 0.0001 *
after treatment	–0.3 ± 0.6	–0.7 ± 1.0	–0.3 ± 0.5	–2.5 ± 0.5	F (3, 50) = 31.75, p < 0.0001 *
rCBF (%)					
pre-reperfusion infusion	0 ± 2	–4 ± 6	–6 ± 5	+2 ± 3	F (3, 50) = 9.51, p < 0.0001 *
post-reperfusion flushing	+71 ± 20	+57 ± 22	+79 ± 25	+84 ± 37	F (3, 50) = 2.39, p = 0.0802
post-reperfusion infusion	+96 ± 32	+83 ± 28	+95 ± 40	+104 ± 28	F (3, 50) = 0.82, p = 0.4885
after treatment	+99 ± 32	+86 ± 40	+84 ± 43	+107 ± 36	F (3, 50) = 1.07, p = 0.3722
MAP (mmHg)					
pre-reperfusion infusion	0 ± 0	–8 ± 14	–6 ± 9	+5 ± 6	F (3, 24) = 3.07, p = 0.0470 *
post-reperfusion flushing	–2 ± 4	–11 ± 20	–18 ± 16	+2 ± 7	F (3, 24) = 2.63, p = 0.0735
post-reperfusion infusion	–6 ± 7	–12 ± 10	–2 ± 9	–10 ± 5	F (3, 24) = 2.26, p = 0.1071
after treatment	–11 ± 4	–16 ± 12	–11 ± 10	–14 ± 9	F (3, 24) = 0.30, p = 0.8254
HR (bpm)					
pre-reperfusion infusion	–2 ± 2	–5 ± 9	+1 ± 9	–3 ± 3	F (3, 24) = 1.03, p = 0.3952
post-reperfusion flushing	–7 ± 2	–17 ± 23	–3 ± 12	–6 ± 5	F (3, 24) = 1.77, p = 0.1796
post-reperfusion infusion	–39 ± 38	–51 ± 29	–16 ± 20	–41 ± 21	F (3, 24) = 2.36, p = 0.0970
after treatment	–52 ± 43	–56 ± 33	–25 ± 25	–65 ± 26	F (3, 24) = 2.20, p = 0.1143

Baseline value obtained immediately before treatment was taken as the reference for calculation of vital parameter changes. rCBF = regional cerebral blood flow reflected by laser Doppler, MAP = mean arterial pressure, HR = heart rate, bpm = beats per minute), CTRL = control group (n = 4), ICCI = intra-carotid artery cold infusion group (n = 7), ICWI = intra-carotid artery warm infusion group (n = 7), IVCI = intra-venous cold infusion group (n = 7)

Arterial blood tests

Blood gases, electrolytes, glucose, hematocrit, and hemoglobin were comparable between groups before (at –20 minutes) and during middle cerebral artery occlusion (at 50 minutes). Treatments significantly interacted with all parameters (**Table 12, Table 13**).

The decrease of pH ($p < 0.05$, versus all other groups), arterial partial pressure of oxygen ($p < 0.05$ versus intra-carotid warm infusion), oxygen saturation ($p < 0.05$ versus all other groups), and the increase of arterial partial pressure of carbon dioxide ($p < 0.05$, versus intra-carotid warm infusion) were most pronounced in rats that were treated with intra-venous cold infusion group (**Table 12**)

After any type of infusion, hemoglobin, hematocrit, glucose, and base excess decreased, and sodium increased ($p < 0.05$, all infusion groups versus the control group) (**Table 13**).

Table 12 Blood gases

Time point	Minutes from MCA occlusion	CTRL	n	ICCI (n = 12)	ICWI	n	IVCI	n	
pH									
before MCA occlusion	–20	7.38 ± 0.04	13	7.38 ± 0.03	7.37 ± 0.03	15	7.39 ± 0.04	13	F (3, 49) = 0.61, p = 0.6086
during MCA occlusion	50	7.36 ± 0.04	13	7.36 ± 0.02	7.37 ± 0.03	13	7.36 ± 0.06	12	F (3, 46) = 0.13, p = 0.9419
after treatment	120	7.32 ± 0.03	11	7.28 ± 0.04	7.29 ± 0.03	15	7.22 ± 0.05	11	
	Delta (120 – 50)	–0.04 ± 0.03	11	–0.08 ± 0.04	–0.07 ± 0.03	13	–0.14 ± 0.05	10	F (3, 42) = 11.17, p < 0.0001 *
pCO2 [mmHg]									
before MCA occlusion	–20	50 ± 5	13	48 ± 4	48 ± 3	15	47 ± 7	13	F (3, 49) = 0.78, p = 0.5103
during MCA occlusion	50	52 ± 6	13	50 ± 6	49 ± 5	13	49 ± 10	12	F (3, 46) = 0.55, p = 0.6539
after treatment	120	57 ± 6	11	56 ± 7	55 ± 7	15	68 ± 14	11	
	Delta (120 – 50)	+5 ± 5	11	+5 ± 8	+5 ± 4	13	+16 ± 7	10	F (3, 42) = 9.07, p < 0.0001 #
pO2 [mmHg]									
before MCA occlusion	–20	100 ± 13	13	94 ± 17	99 ± 10	15	97 ± 16	13	F (3, 49) = 0.36, p = 0.7831
during MCA occlusion	50	89 ± 7	13	93 ± 7	96 ± 7	13	93 ± 13	12	F (3, 46) = 1.04, p = 0.3856
after treatment	120	83 ± 12	11	85 ± 10	89 ± 8	15	72 ± 12	11	
	Delta (120 – 50)	–8 ± 17	11	–8 ± 9	–5 ± 9	13	–22 ± 17	10	F (3, 42) = 3.32, p = 0.0288 #
Base excess [mmol/L]									
before MCA occlusion	–20	3.8 ± 1.4	13	3.3 ± 1.9	3.3 ± 1.0	15	3.0 ± 1.4	13	F (3, 49) = 0.68, p = 0.5688
during MCA occlusion	50	3.8 ± 1.8	13	3.3 ± 2.1	2.8 ± 1.2	13	2.1 ± 1.5	12	F (3, 46) = 2.37, p = 0.0829
after treatment	120	3.6 ± 1.5	11	–0.7 ± 1.6	–0.2 ± 1.5	15	–0.4 ± 1.6	11	
	Delta (120 – 50)	–0.3 ± 1.3	11	–4.0 ± 1.2	–2.9 ± 1.4	13	–2.6 ± 1.2	10	F (3, 42) = 17.42, p < 0.0001 *
HCO_3^- [mmol/L]									
before MCA occlusion	–20	29 ± 2	13	28 ± 2	28 ± 1	15	28 ± 2	13	F (3, 49) = 1.06, p = 0.3727
during MCA occlusion	50	29 ± 2	13	29 ± 2	28 ± 1	13	28 ± 2	12	F (3, 46) = 1.74, p = 0.1722
after treatment	120	29 ± 2	11	26 ± 1	26 ± 2	15	27 ± 2	11	
	Delta (120 – 50)	+0 ± 1	11	–3 ± 1	–2 ± 1	13	–1 ± 1	10	F (3, 42) = 11.62, p < 0.0001 *
sO2 [%]									
before MCA occlusion	–20	97 ± 1	13	96 ± 2	97 ± 1	15	97 ± 2	13	F (3, 49) = 0.86, p = 0.4658
during MCA occlusion	50	96 ± 1	13	97 ± 1	97 ± 1	13	96 ± 2	12	F (3, 46) = 1.12, p = 0.3501
after treatment	120	94 ± 3	11	94 ± 3	95 ± 2	15	89 ± 5	11	
	Delta (120 – 50)	–2 ± 3	11	–3 ± 3	–1 ± 1	13	–7 ± 5	10	F (3, 42) = 7.89, p = 0.0003 *

Blood gases before / during middle cerebral artery (MCA) occlusion, immediately after treatment in infusion groups or equivalent time points in control group (CTRL, number of animals as noted). ICCI, intra-carotid artery cold infusion (number of animals = 12), ICWI = intra-carotid artery warm infusion (number of animals as noted), IVCI = intra-venous cold infusion (number of animals as noted). pCO2 = partial pressure of carbon dioxide, pO2 = arterial partial pressure of oxygen, HCO_3^- = Hydrogencarbonate, sO2 = oxygen saturation. Delta (120 – 50) represents the relative change of blood gases after treatment in contrast to during MCA occlusion. Data are presented as mean values ± standard deviation. * intra-venous cold infusion versus all other groups, # intra-venous cold infusion versus intra-carotid artery warm infusion

Table 13 Serum electrolytes, glucose, hematocrit and hemoglobin

Time point	Minutes from MCA occlusion	CTRL	n	ICCI (n = 12)	ICWI	n	IVCI	n	
Na^+ [mmol/L]									
before MCA occlusion	–20	138 ± 1	13	137 ± 2	138 ± 1	15	137 ± 1	13	F (3, 49) = 0.81, p = 0.4922
during MCA occlusion	50	136 ± 2	13	137 ± 1	136 ± 1	13	136 ± 2	12	F (3, 46) = 0.16, p = 0.9196
after treatment	120	138 ± 2	11	140 ± 2	140 ± 2	15	139 ± 1	11	
	Delta (120 – 50)	+1 ± 2	11	+3 ± 1	+3 ± 1	13	+3 ± 1	10	F (3, 42) = 7.01, p = 0.0006 *
K^+ [mmol/L]									
before MCA occlusion	–20	4.7 ± 0.3	13	4.7 ± 0.6	4.6 ± 0.2	15	4.8 ± 0.4	13	F (3, 49) = 0.51, p = 0.6783
during MCA occlusion	50	5.2 ± 0.3	13	5.1 ± 0.5	4.9 ± 0.5	13	5.0 ± 0.5	12	F (3, 46) = 1.06, p = 0.3765
after treatment	120	5.1 ± 0.5	11	4.6 ± 0.4	4.5 ± 0.5	15	4.9 ± 0.6	11	
	Delta (120 – 50)	–0.1 ± 0.4	11	–0.5 ± 0.4	–0.4 ± 0.4	13	–0.1 ± 0.4	10	F (3, 42) = 3.90, p = 0.0151 *
Glucose [mg/dL]									
before MCA occlusion	–20	231 ± 23	13	249 ± 48	223 ± 24	15	226 ± 35	13	F (3, 49) = 1.52, p = 0.2212
during MCA occlusion	50	221 ± 26	13	233 ± 35	217 ± 26	13	228 ± 31	12	F (3, 46) = 0.72, p = 0.5432
after treatment	120	219 ± 22	11	208 ± 39	191 ± 20	15	205 ± 20	11	
	Delta (120 – 50)	+2 ± 16	11	–25 ± 19	–25 ± 24	13	–20 ± 18	10	F (3, 42) = 4.92, p = 0.0051 *
Hematocrit [%]									
before MCA occlusion	–20	39 ± 1	13	40 ± 2	41 ± 2	15	40 ± 2	13	F (3, 49) = 2.12, p = 0.1093
during MCA occlusion	50	39 ± 2	13	41 ± 2	41 ± 2	13	40 ± 2	12	F (3, 46) = 1.38, p = 0.2617
after treatment	120	38 ± 1	11	35 ± 2	36 ± 1	15	35 ± 2	11	
	Delta (120 – 50)	–1 ± 1	11	–6 ± 1	–5 ± 2	13	–5 ± 1	10	F (3, 42) = 26.60, p < 0.0001 *
Hemoglobin [g/dL]									
before MCA occlusion	–20	13.2 ± 0.5	13	13.8 ± 0.8	13.9 ± 0.7	15	13.6 ± 0.7	13	F (3, 49) = 2.3, p = 0.0885
during MCA occlusion	50	13.4 ± 0.5	13	13.8 ± 0.8	13.8 ± 0.5	13	13.7 ± 0.5	12	F (3, 46) = 1.35, p = 0.2713
after treatment	120	13.0 ± 0.4	11	11.8 ± 0.9	12.1 ± 0.4	15	11.9 ± 0.6	11	
	Delta (120 – 50)	–0.4 ± 0.4	11	–2.0 ± 0.4	–1.7 ± 0.6	13	–1.8 ± 0.4	10	F (3, 42) = 27.71, p < 0.0001 *

Sodium (Na^+), potassium (K^+), glucose, hematocrit and hemoglobin before / during middle cerebral artery (MCA) occlusion, immediately after treatments in infusion groups or equivalent time points in control group (CTRL, number of animals as noted). ICCI = intra-carotid artery cold infusion (number of animals = 12), ICWI = intra-carotid artery warm infusion (number of animals as noted), IVCI = intra-venous cold infusion (number of animals as noted). Delta (120 – 50) represents the relative change after treatment in contrast to during middle cerebral artery occlusion. Data are presented as mean values ± standard deviation. * control group versus all other groups

Part III: Neuroprotection assessment with MRI in rats undergoing 60 minutes of middle cerebral artery occlusion

Mean and median ADC in the contralateral healthy hemisphere

Baseline ADC maps were available in all 11 rats of the control group and in 10 out of 11 rats of the ICCI group. Baseline ADC maps were obtained 39 minutes after filament insertion and middle cerebral artery occlusion and before treatment in intra-carotid artery cold infusion group. On baseline ADC maps mean and median ADC could be directly measured.

Pooled (n = 21) mean ADC in the whole healthy contralateral hemisphere was 616 (interquartile range, 603 to 640) × 10^{-6} mm^2/second. Pooled mean ADC in the healthy contralateral cortex was 642 (interquartile range, 617 to 660) × 10^{-6} mm^2/second. It was higher than that in the healthy contralateral striatum, 606 (interquartile range, 590 to 627) × 10^{-6} mm^2/second ($p = 0.0033$).

Pooled median ADC in the whole healthy contralateral hemisphere, cortex and striatum were 628 (interquartile range, 614 to 644) × 10^{-6} mm^2/second, 648 (interquartile range, 633 to 669) × 10^{-6} mm^2/second, and 603 (interquartile range, 589 to 626) × 10^{-6} mm^2/second, respectively. Pooled median ADC of the whole healthy contralateral hemisphere and cortex were higher than that in the striatum ($p = 0.028$ and $p < 0.0001$ respectively), and the pooled median ADC in the healthy contralateral hemisphere was lower than in the cortex ($p = 0.015$) (**Figure 19A**).

There were no significant intergroup differences (control group, n = 11 versus intra-carotid artery cold infusion group, n = 10) in mean or median ADC between the same brain regions (i.e., healthy contralateral hemisphere, cortex and striatum). In accordance with the pooled analyses, cortex had the highest mean and median ADC values in the individual study groups (**Figure 19B, 19C**).

In pooled analysis, the mean ADC values of the whole contralateral (healthy) hemisphere and cortex for each individual rat were not normally distributed. However, the median ADC values of the cortex and striatum for each rat were normally distributed, and the median ADC values of the whole healthy hemisphere was close to a normal distribution. (**Figure 19A**). Because median ADC values tended to be more homogeneous compared to mean ADC values

in both the pooled analysis and the intra-group analysis (**Figure 19**), we took the median ADC value of each brain region (contralateral hemisphere, cortex, and striatum) as the reference for calculating the thresholds for the predictions of lesion volume on 24-hour ADC maps and final infarct volume on 2-week T2-MRI.

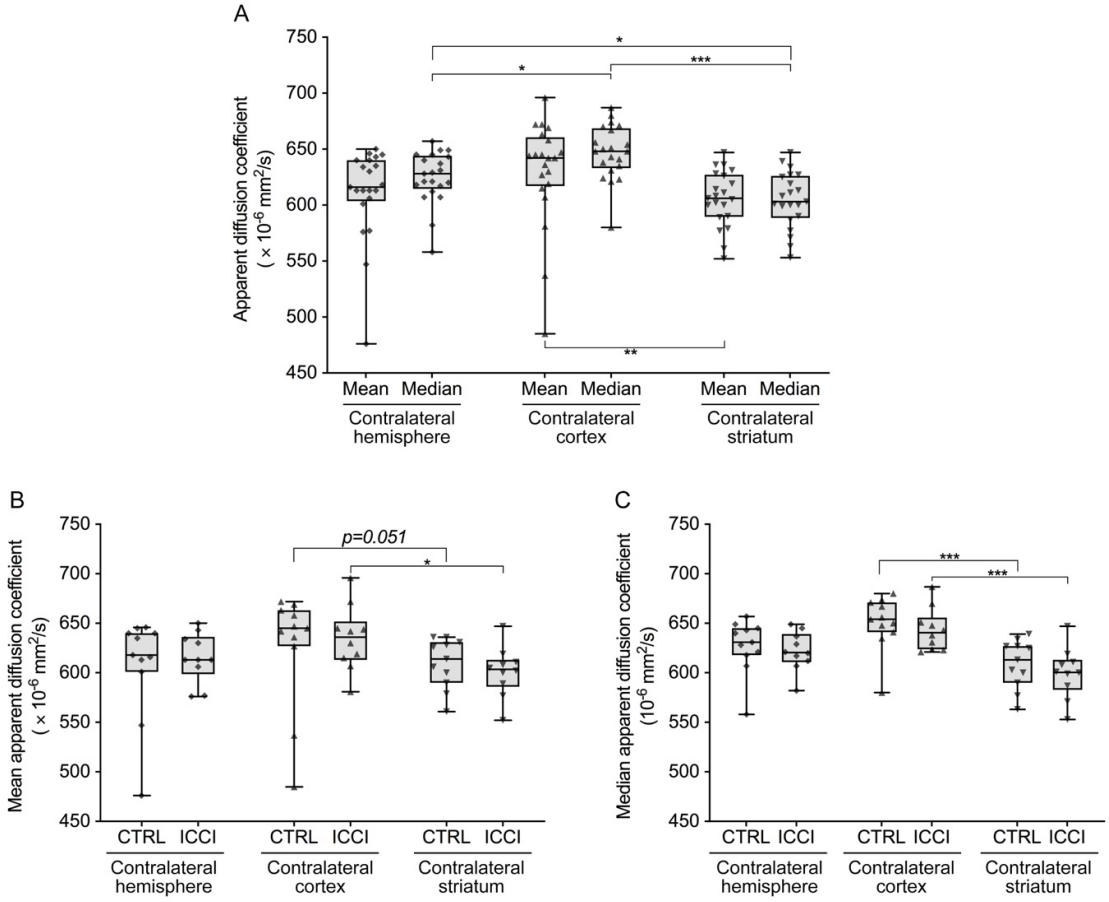

Figure 19 Mean and median apparent diffusion coefficient (ADC) at baseline in the healthy contralateral hemisphere, cortex, and striatum. Pooled analyses (**A**) included all rats with available ADC maps at baseline (number of animals, n = 21). Mean (**B**) and median (**C**) baseline ADC of healthy contralateral whole hemisphere, cortex, and striatum between control group (CTRL, n = 11) and intra-carotid artery cold infusion group (ICCI, n = 10). Data were presented as median, lower (25%) and upper (75%) quartiles, range of minimum to maximum.

Determination of ADC thresholds for predicting lesion volume on 24-hour ADC maps and infarct volume on 2-week T2-MRI

On baseline ADC maps of control animals, volumes of automatically generated hypo-diffused region with thresholds ranging between 60% and 90% of median ADC within the whole ischemic hemisphere, cortex and striatum were listed in **Table 14**.

With thresholds of 70%, 80% and 75%, volumes of generated whole, cortical, striatal hypo-diffused regions on baseline ADC maps are comparable to manually measured lesion volume within each target brain territory on 24-hour ADC maps ($p > 0.05$ in each comparison, paired t-test) (**Figure 20, Table 14**).

Spearman correlation analysis further showed that there is significant correlation between generated whole hypo-diffused volume on baseline ADC maps and measured whole lesion volume on 24-hour ADC maps ($r = 0.95$, $p < 0.001$), between generated hypo-diffused volume with cortical threshold 80% and lesion volume of cortex on 24-hour ADC maps ($r = 0.85$, $p = 0.025$) (**Table 14**). The correlation between generated baseline hypo-diffused volume with striatal ADC threshold 75% and measure striatum lesion on 24-hour ADC maps is poor ($r = 0.33$, $p = 0.428$) (**Table 14**).

Volumes of generated hypo-diffused territory within the whole ischemic hemisphere, cortex on baseline ADC maps with thresholds 70%, 80% respectively were close to and correlated with corresponding directly measured infarct volume on 2-week T2-MRI ($r = 0.95$, $p < 0.001$ and $r = 0.89$, $p = 0.033$ respectively, see **Figure 20**, **Table 14**). With striatal ADC threshold (70%), the predicted volume and final striatal infarct volume are comparable, but the correlation between them are not significant ($r = 0.46$, $p = 0.302$).

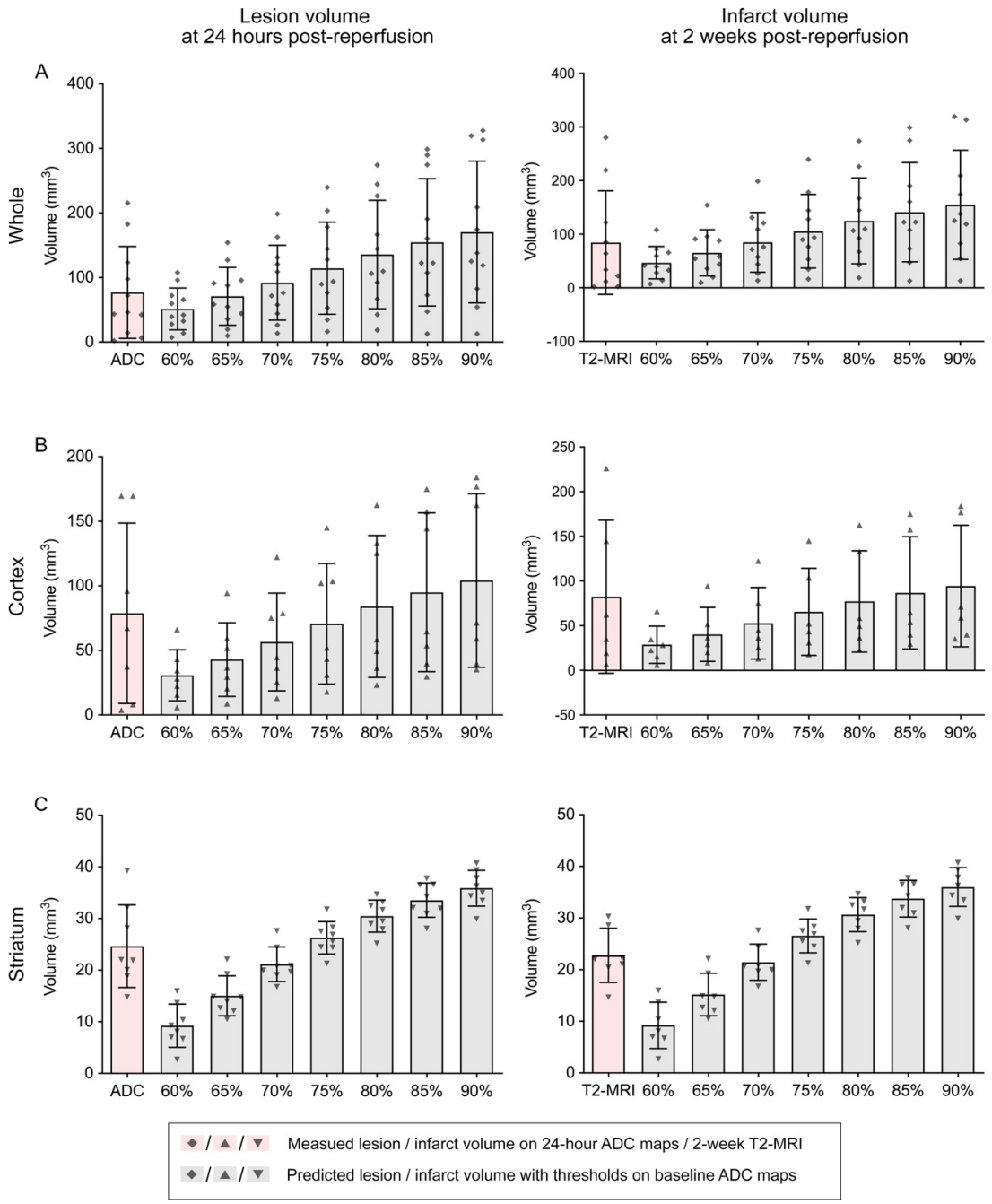

Figure 20 Comparison of thresholds predicted (**grey**) hypo-diffused volumes within ischemia attacked whole hemisphere (**A**), cortex (**B**) and striatum (**C**) on baseline ADC maps with measured (**pink**) lesion volume on 24-hour ADC maps (**left column**) and infarct volume on 2-week T2-MRI weighted images (**right column**) in control group.

Table 14 Spearman coefficient analysis between measured lesion volume on 24-hour ADC maps, final infarct volume on 2-week T2-MRI and volume of hypo-diffused region generated with thresholds on baseline ADC map in control group.

Measured volume (mm^3)		Generated hypo-diffused volume with thresholds on baseline ADC maps (mm^3)						
		60%	65%	70%	75%	80%	85%	90%
on 24-hour ADC								
Whole (n = 11)	77.0 ± 71.2	51.4 ± 32.3	70.9 ± 44.9	92.1 ± 57.9	114.4 ± 71.4	135.8 ± 84.2	154.7 ± 98.7	170.6 ± 110.0
		r = 0.89	r = 0.92	r = 0.95	r = 0.95	r = 0.95	r = 0.95	r = 0.95
		p < 0.001	p < 0.001	p < 0.001	p < 0.001	p < 0.001	p < 0.001	p < 0.001
Cortex (n = 7)	78.9 ± 69.9	30.9 ± 19.8	43.0 ± 28.6	56.6 ± 37.8	70.8 ± 46.7	84.1 ± 54.9	95.0 ± 61.5	104.2 ± 67.2
		r = 0.85	r = 0.85	r = 0.85	r = 0.85	r = 0.85	r = 0.85	r = 0.85
		p = 0.025	p = 0.025	p = 0.025	p = 0.025	p = 0.025	p = 0.025	p = 0.025
Striatum (n = 8)	24.7 ± 8.0	9.2 ± 4.2	15.1 ± 3.9	21.2 ± 3.4	26.3 ± 3.1	30.5 ± 3.1	33.6 ± 3.3	35.9 ± 3.5
		r = –0.33	r = –0.40	r = 0.05	r = 0.33	r = 0.57	r = 0.57	r = 0.57
		p = 0.428	p = 0.327	p = 0.935	p = 0.428	p = 0.151	p = 0.151	p = 0.151
On 2-week T2-MRI								
Whole (n = 10)	84.3 ± 96.5	46.8 ± 30.2	65.3 ± 43.0	85.0 ± 55.8	105.5 ± 68.5	124.9 ± 80.1	141.1 ± 92.7	154.9 ± 102.0
		r = 0.92	r = 0.95	r = 0.95	r = 0.95	r = 0.95	r = 0.95	r = 0.96
		p < 0.001	p < 0.001	p < 0.001	p < 0.001	p < 0.001	p < 0.001	p < 0.001
Cortex (n = 6)	82.5 ± 85.8	28.8 ± 20.8	40.3 ± 30.3	52.9 ± 40.0	65.5 ± 48.8	77.2 ± 56.8	86.8 ± 63.0	94.4 ± 68.0
		r = 0.89	r = 0.89	r = 0.89	r = 0.89	r = 0.89	r = 0.89	r = 0.89
		p = 0.033	p = 0.033	p = 0.033	p = 0.033	p = 0.033	p = 0.033	p = 0.033
Striatum (n = 7)	22.8 ± 5.2	9.2 ± 4.5	15.2 ± 4.1	21.5 ± 3.5	26.6 ± 3.3	30.7 ± 3.3	33.8 ± 3.5	36.0 ± 3.7
		r = 0.07	r = 0.04	r = 0.46	r = 0.54	r = 0.25	r = 0.11	r = 0.11
		p = 0.906	p = 0.964	p = 0.302	p = 0.236	p = 0.595	p = 0.840	p = 0.840

Actual ADC lesion volumes at 24 hours and final infarct volumes at 2 weeks

The actual lesion volumes on 24-hour ADC maps in the ICCI group were similar to those observed in the control group: 73.3 ± 38.2 mm^3 versus 77.0 ± 71.2 mm^3 in the ischemic hemisphere (p = 0.887), 47.1 ± 37.7 mm^3 versus 78.9 ± 69.9 mm^3 in the cortex (p = 0.284), and 20.7 ± 9.3 mm^3 versus 24.7 ± 8.0 mm^3 in the striatum (p = 0.353).

Although the final infarct volumes on T2-MRI at two weeks tended to be smaller in all examined brain regions of the ischemic hemisphere in the ICCI group compared to those in the control group, statistical significance was only reached in the striatum: 69.0 ± 54.9 mm^3 versus 84.3 ± 96.5 mm^3 in the ischemic hemisphere (p = 0.667), 51.6 ± 45.6 mm^3 versus 82.5 ± 85.8 mm^3 in the cortex (p = 0.399), and 15.0 ± 7.6 mm^3 versus 22.8 ± 7.6 mm^3 in the striatum (p = 0.034).

Comparison of predicted and measured volume

Applying the optimal thresholds that were determined using control group data (see **Table 14**) to the baseline ADC maps in the ICCI group, the predicted lesion and infarct volumes for the whole ischemic hemisphere (95.9 ± 42.0 mm^3) and the ischemic cortex (71.0 ± 40.1 mm^3) were larger than the actually measured lesion volumes on 24-hour ADC maps (p = 0.011 and p = 0.007, respectively) and final infarct volumes on 2-week T2-MRI (p = 0.025 and p = 0.013, respectively) (**Figure 21A, 21B, Figure 22**).

In contrast, predicted lesion (18.9 ± 8.8 mm^3) and infarct volumes (15. 0 ± 8.1 mm^3) within striatum in the ICCI group were comparable to actual ADC lesion volumes at 24 hours (p > 0.999) and final infarct volumes at 2 weeks respectively (p = 0.966) (**Figure 21C**).

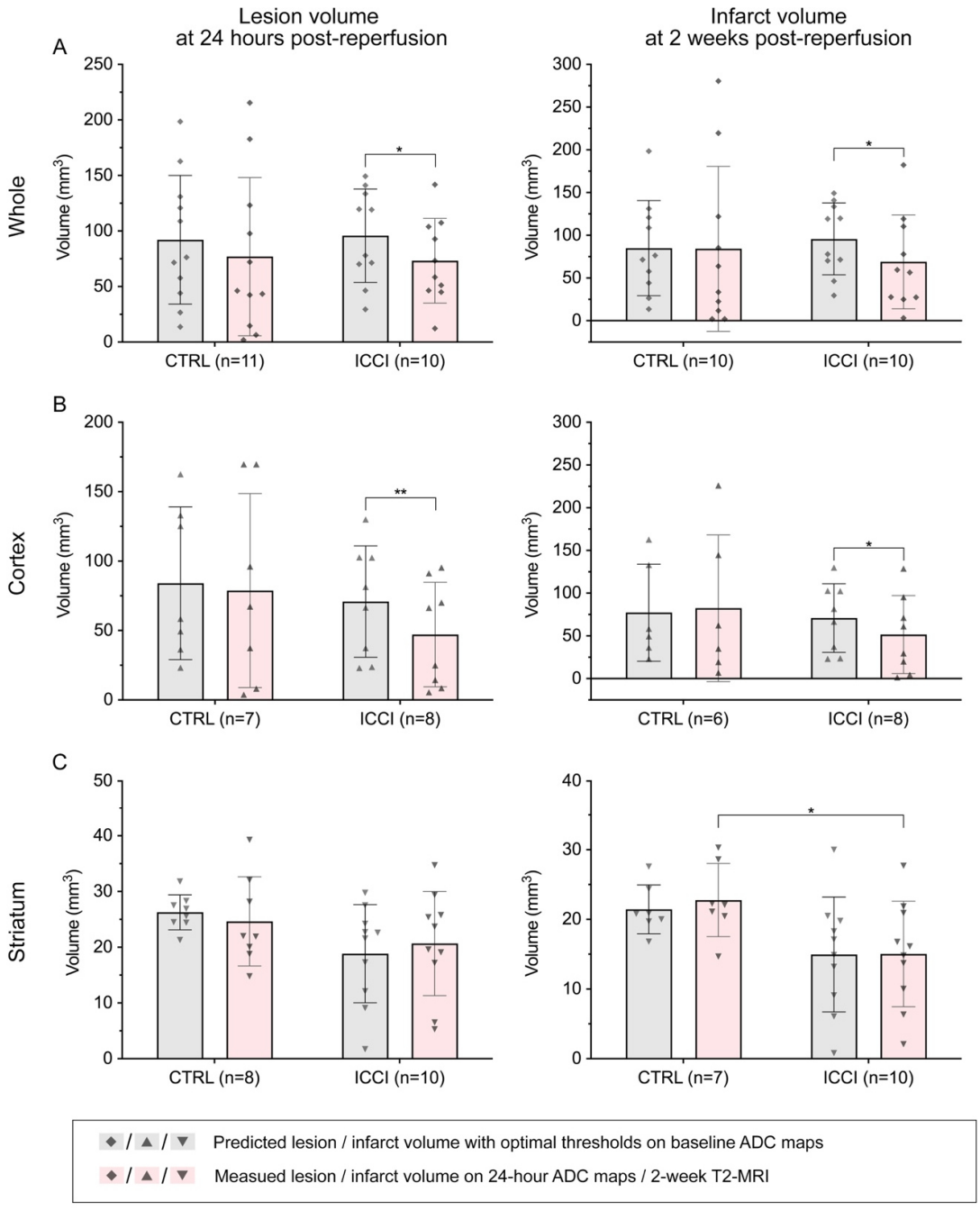

Figure 21 ADC (baseline)-threshold-based predicted lesion / infarct volume (grey shadowed) compared to actually measured (pink shadowed) lesion volume on 24-hour ADC maps (left), and infarct volume on 2-week T2-MRI (right) within whole ischemic hemisphere (**A**), cortex (**B**) and striatum (**C**) in control group (**CTRL**) and intra-carotid artery cold infusion group (**ICCI**). n = number of animals. Inter-group comparisons were conducted with unpaired t-test; volume comparisons between timepoints within the same treatment group, paired t-test was applied. * $p < 0.05$, ** $p < 0.01$

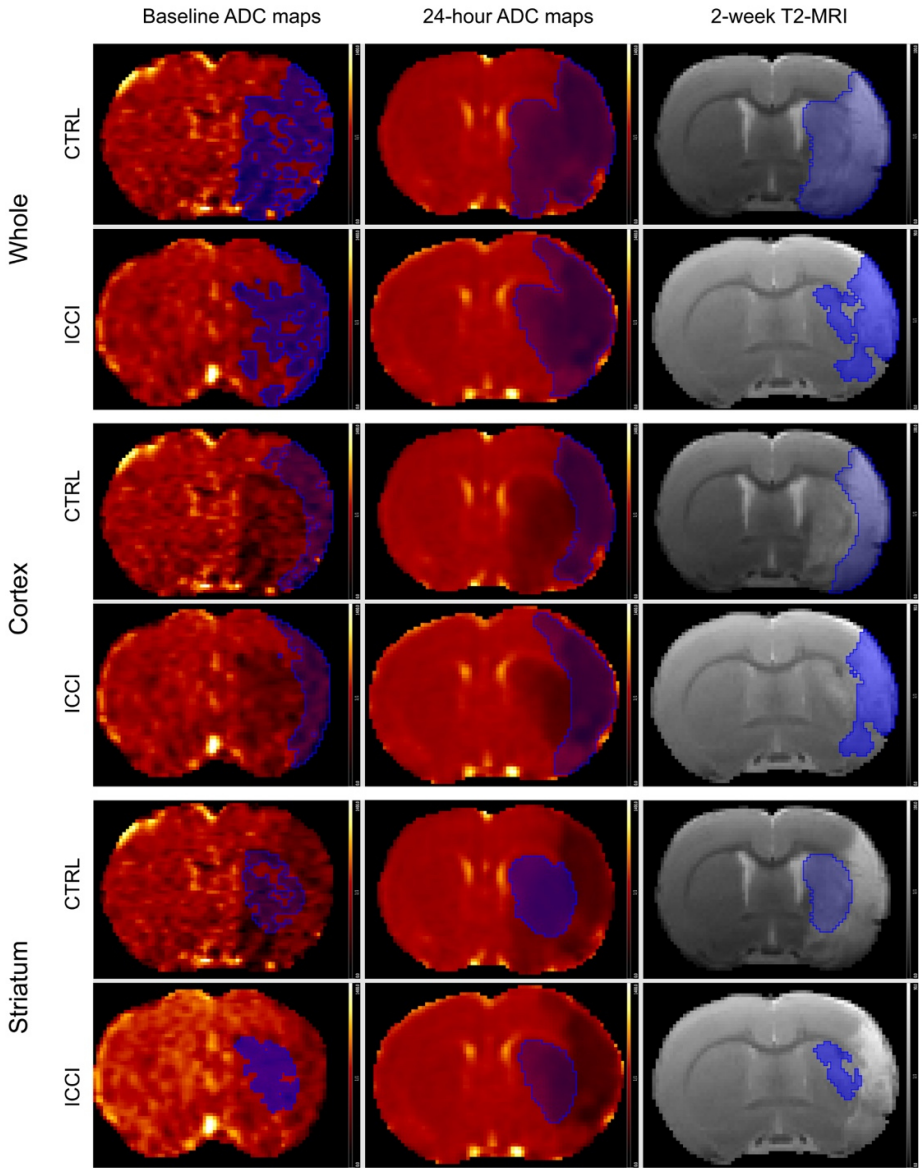

Figure 22 Exemplary predicted lesion on baseline apparent diffusion coefficient (ADC) maps in the whole ischemic hemisphere (threshold: 70% of the median ADC measured in the contralateral healthy hemisphere), in the cortex (threshold: 80% of the median ADC measured in the contralateral healthy cortex), and in the striatum (threshold: 75% of the median ADC measured in the contralateral healthy striatum) (**left column**); lesion areas measured on 24-hour ADC maps, and final infarct volumes on 2-week T2-MRI (**middle and right columns**) in the control group (CTRL) and the intra-carotid artery cold infusion group (ICCI). While the actual (measured) and predicted lesion/infarct volumes were similar in the control group, the actual (measured) lesion/infarct volumes were smaller than the predicted lesion volume in the ICCI group, potentially indicating neuroprotection.

Extent of brain edema at 24 hours

Relative extent of edema on T2-MRI at 24 hours in the ICCI group tended to be lower in all examined brain regions of the ischemic hemisphere in the ICCI group compared to those in the control group, statistical significance was only reached in the striatum (**Figure 23**): 10.7 ± 8.1% versus 6.5 ± 5.4% in the ischemic hemisphere ($p > 0.999$), 15.6 ± 12.3% versus 7.2 ± 5.6% in the cortex ($p = 0.396$), and 41.8 ± 15.9% versus 27.6 ± 14.5% in the striatum ($p = 0.021$).

In both treatment groups, relative extent of edema in the striatum was more pronounced compared to the extent of edema in the whole hemisphere and the cortex (all $p < 0.001$).

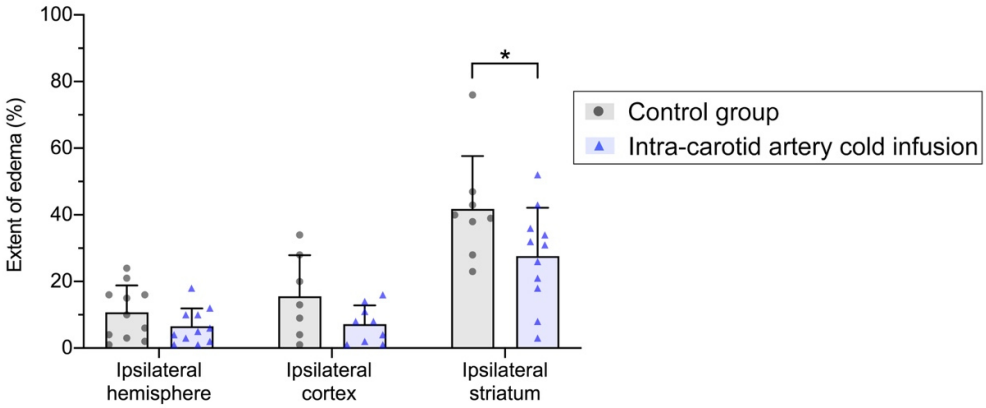

Figure 23 Extent of edema on T2-MRI at 24 hours. All rats (11 rats in the control group, CTRL and 11 rats in the intra-carotid artery cold infusion group, ICCI) were included into the analysis. Cortical lesions were present in 7 out of the 11 rats in the CTRL group and 9 / 11 rats in the ICCI group. Striatal lesions were observed in 8 / 11 rats in the CTRL group and 11 / 11 rats in the ICCI group. (* $p = 0.021$, two-way ANOVA analysis of variance with Bonferroni's correction for multiple comparison)

Neurofunctional testing

Results of neurofunctional testing at baseline (before ischemia and treatment) and on day 2, 4, 6, 9, and 13 after reperfusion and treatment are displayed in **Figure 24**. The highest modified neurological severity scores (mNSS; higher scores indicate more severe neurofunctional deficits) were found during the first evaluation (day 2) after ischemia. mNSS decreased in both study groups over time. Compared to the mNSS on day 2, this decrease became first significant on day 4 after reperfusion in the ICCI group ($p < 0.001$), and on day 6 in the control group ($p = 0.006$). mNSS remained significantly lower at subsequent assessments until day 13 in both groups (all $p < 0.0001$). mNSS was significantly lower in the ICCI group than in the control group at day 9 ($p = 0.0002$) and day 13 ($p = 0.004$).

In the cylinder test, rats of the ICCI group and the control group showed no preference of ipsilateral forepaw usage at baseline (53.91 ± 7.0% versus 48.4 ± 8.2%, respectively). From day 2 after reperfusion until last assessment on day 13, all rats presented ipsilateral forepaw preference in rearing activities. Neither amelioration over time nor difference between treatment groups was observed.

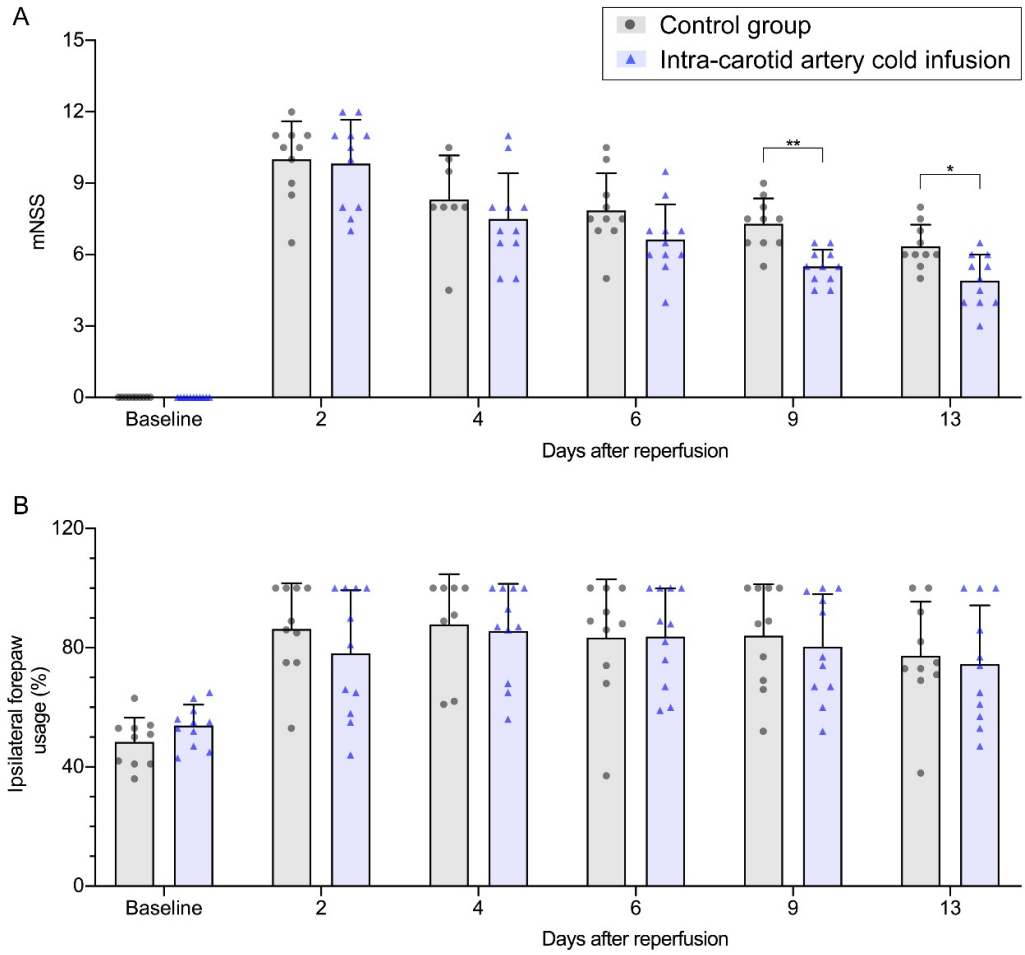

Figure 24 Modified neurological severity score (mNSS, **A**) and ipsilateral forelimb preference tested in the cylinder test (**B**) at baseline before middle cerebral artery occlusion, and on day 2, 4, 6, 9, and 13 after reperfusion and treatment. CTRL = control group, ICCI = intra-carotid artery cold infusion group. Comparisons between time points were conducted using two-way ANOVA analysis of variance with Bonferroni's correction for multiple comparisons. Unpaired t-tests were used for inter-group comparison. ** $p < 0.001$ (0.0002), * $p < 0.01$ (0.004).

Hemorrhagic transformation

No hemorrhagic transformation was observed on T2-MRI at 24 hours after reperfusion. At 2 weeks after reperfusion however, petechial microbleeds in the striatum were observed in 2 out of 10 rats in the control group and in 5 out of 11 rats in the ICCI group (see for example in **Figure 25**).

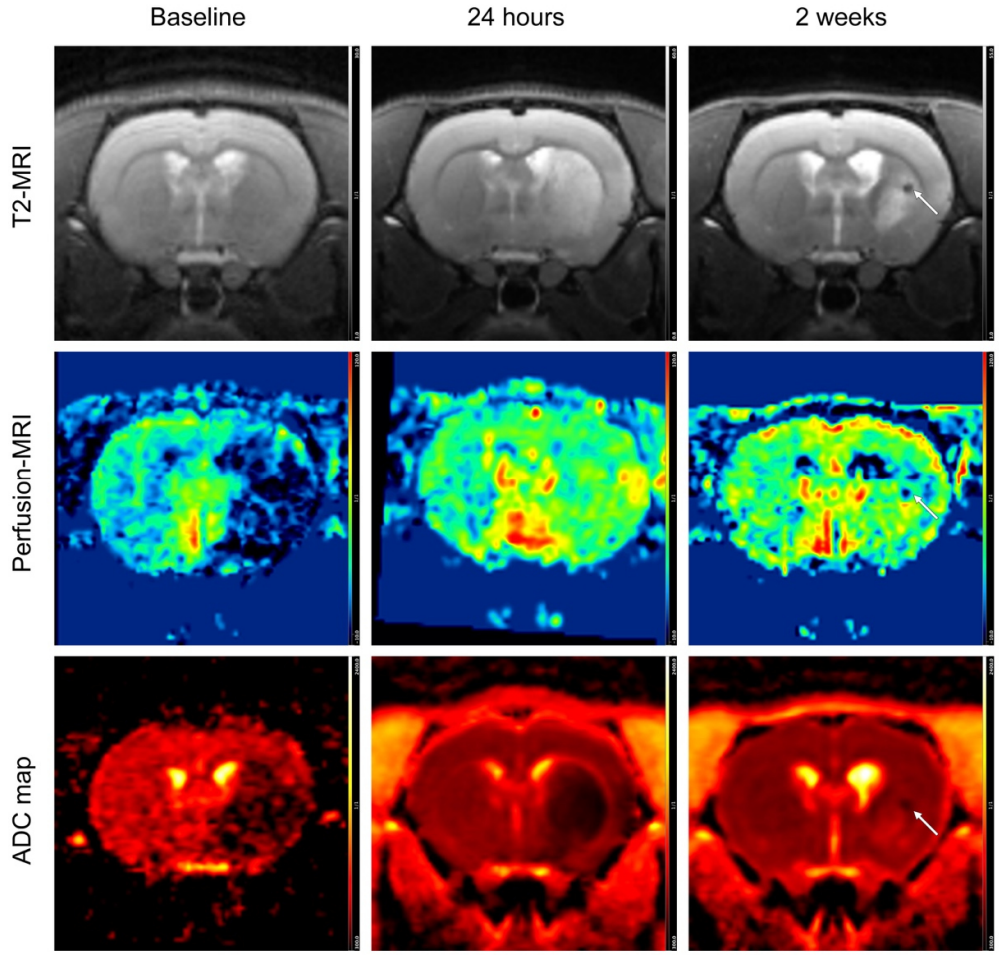

Figure 25 Example of hemorrhagic transformation at two weeks after reperfusion (**white arrow**). MRI scans including T2-MRI, perfusion-MRI, and apparent diffusion coefficient (ADC) map were performed during middle cerebral artery occlusion (baseline), at 24 hours and 2 weeks after reperfusion.

Discussion

Project overview

The present study was composed of three parts.

In part I, we developed a cooling system setup for effective selective brain cooling. Our custom-made infusion port is the first to allow for continuous pre- to post-reperfusion ICCI in rats and potentially applicable to other small animals in future studies involving intra-carotid artery infusion. With this experimental setup, we successfully simulated in a filament middle cerebral artery occlusion rat model the implementation of ICCI into the clinic scenario of endovascular mechanical thrombectomy during which cold fluid could be delivered via the guide catheter as soon as it was introduced into the internal carotid artery and continuously infused until after reperfusion without interfering with the recanalization procedure (see **Figure 1D and Figure 2D**).

In part II of this study, we evaluated the potential neuroprotective effects of continuous pre- to post-reperfusion ICCI in rats undergoing 100 minutes of middle cerebral artery occlusion. Although ICCI-mediated neuroprotection could not be concluded from our primary analysis, post-hoc analyses suggest a potential neuroprotective effect of ICCI in rats with only moderate but not severe cerebral ischemia.

In part III of the study, rats were therefore subjected to only 60 minutes of middle cerebral artery occlusion to obtain larger volumes of potentially salvageable penumbra. In this part, serial MRI was applied for dynamic evaluation of infarct growth by referring to each individual rat's baseline ischemic core volume. Our results suggest potential neuroprotection by ICCI in the better collateralized cortex (penumbra) but not in the densely ischemic striatum (core).

Comparison with previous experimental setups

The current study shows that, with our experimental setup, selective brain hypothermia using ICCI could be induced already before recanalization of the occluded middle cerebral artery (**Figure 1D**). In contrast, in almost all previous preclinical small animal studies, start of intra-arterial cold infusion, and thereby selective brain cooling, was strictly limited to the post-reperfusion phase only (see **Table 1 – 2**).

Ding and colleagues successfully established a rodent stroke model in which cold fluid was directly administered into the middle cerebral artery territory using a modified polyethylene-50 tube. Instead of using the standard filament approach for middle cerebral artery occlusion, this modified polyethylene-50 tube was used instead. In their experimental setup, the tube was introduced into the internal carotid artery for ischemia induction until the its distal tip passed the opening of the middle cerebral artery. In this position, the opening of the middle cerebral artery was blocked by the outer tube wall. When it came to initiate intra-arterial cold infusion, the tube needed to be retracted a few millimeters proximally to the opening of the middle cerebral artery before cold fluid was delivered into the target middle cerebral artery territory.

Although the authors referred to their approach as "pre-reperfusion flushing", retracting the filament by these few millimeters inevitably leads to reperfusion of the middle cerebral artery territory because of the crossflow from the right anterior circulation via the anterior communicating artery (**Figure 1A**) [107].

An additional drawback of the experimental setup used in the study by Ding and colleagues could be the use of the polyethylene-50 tube for middle cerebral artery occlusion [107]. During occlusion, this "hollow filament" could pose a risk of clot formation within the tube because of retrogradely entering blood. These clots may then cause secondary embolization during initiation of intra-arterial cold infusion and by that aggravate ischemic brain damage. In our own experience during continuous blood pressure monitoring via the cannulated femoral artery using a polyethylene-50 tube, clot formation at the tube outlet was frequent and led to loss of blood pressure signal although the tube was filled with heparinized saline. The blood pressure signal could be reestablished only by strong flushing of the tube, which may be regarded as contraindicated in case of the tube being placed into the intracranial circulation.

In other small animal studies (**see Figure 1C, Table 2**), ICCI treatment was even further delayed to many minutes after reperfusion. In these studies, the surgical procedure for connecting and inserting the tube for intra-arterial cold infusion could only be started after the filament for middle cerebral artery occlusion had been removed. In our experimental setup, however, our self-developed infusion port allowed us to insert the infusion tube for later ICCI already during the filament was in its position for middle cerebral artery occlusion and thus to start ICCI before reperfusion without interruption during filament retraction (**Figure 1D**).

Importantly, during our very first experiments, after removal of the clip from common carotid artery for orthograde blood flow restoration (**see Figure 7**), we observed bleeding out of the tiny space caused by the filament thread between the external carotid artery's inner wall and the infusion port's outer wall (**see Figure 5 left**). To prevent this leakage, the tip of the infusion port was coated with elastic silicone, into which a longitudinal concavity was molded with the filament thread. This measure ensured sufficient sealing between the infusion port and the vessel wall also during filament withdrawal (**see Figure 5 middle**).

To provide optimal cooling efficacy of ICCI, preventing the chilled saline from re-warming before entering the rat's circulation is of critical importance. Before conducting any animal experiments, we tested fluid temperature at three positions, i.e., within the commercially available in-line SC-20 cooler, at its outlet and at the tip of infusion port. Extracorporeal re-warming of the chilled infusate flowing through the tube that is exposed to ambient air temperature was significant as observed in our experiment (**see Table 6 and Figure 6**). Especially at low infusion rates (0.2 mL/minute), fluid temperature increased to almost room temperature at the tip of the infusion port which is about 2.5 cm away from measurement point within the cooler. Comparing with previous ICCI studies (**see Table 1, Table 2**) in rats, parameters such as fluid temperature at the tip of the infusion tube before entering the blood stream, tube length (exposure to room temperature) were not reported and remain unknown.

Based on our findings, we needed to integrate an additional external cooling system surrounding the tube in order to maintain the infusate's temperature at below 3 °C before entering the rat's blood stream at an infusion rate of 0.2 mL/minute and around 0 °C when infusion rates were 0.5 mL/minute or higher (**Table 6**). By this measure, we markedly improved ICCI's cooling efficacy in our setup. Doubts about the temperature of the infusate in some previously published preclinical studies arise due to the low infusion rates and the absence of additional measures to ensure its temperature stability [102, 104, 113].

Clinical relevance of the guide catheter approach

Three clinical studies reported the integration of intra-arterial cold infusion into the endovascular mechanical thrombectomy procedure [94-96] . In these studies, the microcatheter was used for cold fluid delivery as soon as it penetrated through the clot occluding the intracranial artery.

At first sight, this strategy may seem very attractive for inducing selective hypothermia of the ischemic brain tissue before reperfusion. However, the main drawback of using the microcatheter for intra-arterial cold infusion is the inevitable delay of arterial recanalization due to the occupation of microcatheter. In these clinical studies, recanalization was delayed for at least five (**see Figure 2A, 2B**) [95, 96] to 10 minutes [94] . To achieve favorable clinical outcomes in patients, delay of recanalization should always be avoided, as timely reperfusion still represents the only proven effective treatment in acute ischemic stroke [28, 144].

Moreover, using the microcatheter for intra-arterial cold infusion would not allow for continuous pre- to post-reperfusion cooling, because cold fluid infusion must be halted during thrombectomy device delivery, as the stent retriever or an aspiration device would fully block the inner lumen of the microcatheter (**see Figure 2A and 2B**). The resulting rapid rewarming of the chilled brain tissue during the break between the pre-reperfusion and post-reperfusion cold infusion may be harmless at best, but could exacerbate brain damage at worst due to the sudden temperature fluctuations.

In order to achieve effective brain cooling as long as possible without causing fluid overload, the fluid's temperature should be maintained as low as possible before entering the circulation [98, 145] . However, the infusate before it enters the target brain's arterial circulation is endangered to be rewarmed if conventional microcatheter is used for delivery.

The total length of the human internal carotid artery is about 15 cm [146] and the outer diameter of the microcatheter is about 3 French (1 mm) or even smaller [130]. Considering the rewarming of the infusate that we could observe in our experimental setup when the polyethylene-50 tube used for ICCI was exposed to air at room temperature over a total length around 6.5 cm, the rewarming of the infusate within a non-insulated standard microcatheter that is exposed to the warmer blood stream over a significantly longer distance could be more relevant. Although brain temperature was not assessed in any of the three clinical studies, cooling efficacy in these studies remains doubtful. Prospectively, to improve the heat insulation property of a microcatheter will remain a challenge as it needs to be flexible and thin for being able to reach distal segments of cerebral arteries.

In contrast, the guide catheter has a much larger lumen compared to the microcatheter and is generally placed in the proximal internal carotid artery. During the routine endovascular

mechanical thrombectomy procedure, the guide catheter is continuously perfused with heparinized saline to avoid retrograde blood flow and thrombi formation within the catheter [147] . Cold infusion could therefore be continuously administered during the whole endovascular mechanical thrombectomy procedure at higher rates without any changes to the catheter itself and the procedure. Since the guide catheter outlet is placed proximal to the vessel occluding clot, cooling of penumbra before reperfusion could be achieved by the inflowing of a mixture of blood and cold fluid via collaterals (see **Figure 1D, Figure 2D**).

Because the guide catheter is larger and does not need to be as flexible as the microcatheter, it could be sufficiently insulated. Up to now, heat-insulated guide catheters for ICCI purpose have been prototyped and successfully tested in healthy pigs [148] and in a canine stroke model [119] .

Brain temperature change during pre- to post-reperfusion ICCI in rats

It was also observed in our study that pre-reperfusion ICCI, i.e., cooling efficacy of ICCI during middle cerebral artery occlusion, could not be further enhanced by increasing the infusion rate of ICCI (see **Figure 11**). This may not be the case in the clinical setting of acute ischemic stroke and pre-reperfusion ICCI. To get more homogenous infarct volume in the filament middle cerebral artery occlusion rat model, the common carotid artery is clipped during ischemia in our study. This is done to prevent the strong blood flow from the common carotid artery from potentially incurring filament shift and resulting in unstable ischemia. In most clinical acute ischemic stroke cases without internal carotid artery occlusion due to stenosis, however, the blood flow from the common carotid artery is not impaired. Blood flowing from the common carotid artery into the internal carotid artery could consequently facilitate cooling via collaterals. Under these circumstances, higher ICCI rates may therefore lead to higher cooling efficacy and earlier reaching of hypothermia in the target tissue, i.e., the ischemic penumbra.

Another phenomenon that we observed during pre-reperfusion ICCI in our study was that the striatum could be more effectively cooled than the cortex in rats (see **Figure 12**). This seems contradictory to the theoretical basis that rodent cortex has better collateral blood supply (i.e., leptomeningeal collaterals [149]) and consequently should be earlier and faster cooled in contrast to striatum during pre-reperfusion cooling phase.

The different paths of cortical and striatal collaterals may be a possible explanation for this finding. Compared to the distance that ICCI must overcome before reaching the cortex via leptomeningeal collaterals originating from the posterior cerebral artery, the distance from the anterior choroidal artery and its branches to deep brain structures adjacent to the striatum is much shorter [150, 151] . Therefore, one can assume that rewarming of ICCI was more significant before reaching the cortex and that ICCI's cooling performance was consequently compromised.

The brain cooling pattern could be different in humans, i.e., cortex could be earlier cooled by cooled blood via leptomeningeal collaterals than severely hypo-perfused striatum cooled by heat transfer, as a result of the increased distance between ischemic core and adjacent cerebral artery main trunk filled with cold blood. But this possibility requires further studies to confirm. In a microcatheter based continuous ICCI study, which was conducted in relatively larger brain (canine), brain temperatures of 4 regions ipsilateral to treated hemisphere during both pre- and post-reperfusion cold infusion were monitored [119]. Unfortunately, coordinates information of implanted thermoprobes was not reported, the potentially different manner of brain temperature change between striatum and cortex in larger brains could therefore not be concluded.

Necessity of ICCI studies in small animals

With regard to translatability of results to the clinical human setting, large animal ICCI studies may be more attractive compared to studies in small animals including rats. ICCI mediated thermodynamic effects on larger gyrencephalic brains for instance, canine, non-human primates could better reflect the real condition when transferred in human. However, high cost and ethical considerations especially for canine and non-human primates, clearly limit the application. Pigs have been the most widely accepted species for large animal experiments, but the rete mirabilis poses a major challenge for simulation of endovascular mechanical thrombectomy in ischemic stroke [152]. To avoid waste of resources, it is critical to determine ICCI related basic treatment variables before proceeding to larger animal studies, such as optimal timing, target temperature, cooling duration, protocol of rewarming and composition of cold infusion etc. By applying our ICCI setup, all these questions could be easily addressed in small animal studies. Furthermore, the brain temperature curves resembling those reported in the canine study [119], in which a similar infusion protocol was applied (i.e., cold saline delivered into the internal carotid artery via a microcatheter from 5 minutes before

reperfusion and continued for 20 minutes after reperfusion), suggests that rodent studies could be significantly comparable in addressing above-mentioned questions, with reduced ethical concerns and more efficient use of resources.

In part II and III of this study, we aimed to answer a more prerequisite question before future optimization of ICCI variables for better treatment effect. Namely, whether continuous pre- to post-reperfusion ICCI is neuroprotective and how ICCI affects physiological parameters, blood gases and regional hemodynamics. Since there are no previous studies that investigated the optimal duration of ICCI for neuroprotection in focal cerebral ischemia, we aimed at the longest possible duration of hypothermia by using the highest infusion volume that we assumed could be tolerated also by patients, i.e., a volume that corresponds to half of the individual rat's blood volume. The underlying rationale for this decision was based on previous clinical trials investigating intra-venous cold infusion mediated whole body cooling in patients suffering cardiac arrest or stroke. In these trials, patients received comparable volumes of cold fluid which was reported to have been tolerated without serious adverse effects [51] [153] .

The overall duration of local hypothermia that was achieved in the present study was around 14 minutes. This duration was longer than that in all existing small animal intra-arterial cold infusion studies, in which cooling duration ranged from 3 to 10 minutes (see **Table 1**). Longer infusion duration that ranges from 15 to 30 minutes was reported in the majority pre-reperfusion or post-reperfusion ICCI studies by limiting infusion rate to less than 0.4 mL per minute or infusing the fixed small volumes of, for instance 7.5 mL, intermittently over up to 30 min [102] (see also **Table 2**). Only one of those studies applied ice-cold saline as infusate and delivered into internal carotid artery as we did in the present work [104]. In this study, a duration of 30 minutes was achieved with a fluid volume of 6 mL at an infusion rate of 0.2 mL/minute and striatal temperature decreased to below 35 °C. The study's target cortical temperature of 34 °C was reached after 20 minutes of infusion.

The results of part I in our study however indicate that the cooling performance at an infusion rate of only 0.2 mL/minute as used in the latter study is very limited (**Figure 11**) and in our pre-tests aiming to identify the cooling performance of ICCI at different infusion rates, the lowest temperature in the striatum at an infusion rate of 0.2 mL/minute was 36 °C and reached only after 12 minutes of infusion. In addition, our study found that core body temperature continuously decreased throughout the entire infusion period, with the lowest

temperature being measured at the end of the cold infusion (see **Figure 12, Figure 18 Table 10, Table 11**). The lower cortical temperatures reported in the above-mentioned study [104] could, therefore, reflect the combined effect of accidental passive systemic cooling (i.e., heat loss incurred core body temperature decrease during operation) and active selective brain cooling, rather than being solely attributable to local brain cooling.

Confusing findings were also reported in two studies by Ji et al. [102] and Kurisu et al. [101], in which saline at the same temperature (10 °C) was infused at rates of 0.25 mL/minute and 0.32 to 0.41 mL/minute, respectively. Interestingly, the cortical temperature in the former study, which used an only marginally lower infusion rate, was noticeably higher than that of the latter study (36.5 °C versus 34.8 °C). Those conflicting findings further suggest that baseline core body temperature and heat loss during the experimental procedure can be significantly influenced by factors such as ambient temperature and the use of a peripheral heating system, which could be critical factors leading to over- or underrating of the true cooling performance of the selective brain cooling method. In prospective ICCI studies, core body temperature should, therefore, be strictly controlled during the experiment and transparently reported.

Rats have relatively thin cranial structure, which by itself could promote heat loss within the cortex during general anesthesia [154]. The heat loss in the cortex may further be aggravated during surgical preparation of the skull for thermoprobe implantation [155]. This could be another important reason that results in overestimation of the cooling efficacy of intra-arterial cold infusion in majority of previous studies that showed very strong neuroprotective effects of intra-arterial cold infusion. In a study conducted by Chen et al., it was reported that both cortical and striatal temperatures were decreased to around 30 °C within 5 minutes and remained reduced as long as 50 minutes [113]. However, when looking at the core body temperature curve, it recovered back to the normal range within a few minutes. This finding is logically hard to understand if there is no contribution of heat loss incurred brain temperature decrease or impaired rewarming.

Due to the larger size, the thicker cranial structure and the abundant cerebral blood flow, human brains are less affected by ambient temperature, even when surface head cooling devices are applied [78]. In order to avoid passive heat loss during skull surgery and associated decrease of cortical temperature potentially enhancing neuroprotection, and also to avoid traumatic brain damage due to implantation of thermocouple probes, no invasive brain

temperature measurement was conducted in part II and part III of our study, in which we evaluated the neuroprotective efficacy of ICCI.

Intraluminal filament method for middle cerebral artery occlusion in rats

There are various methods have been developed for establishing middle cerebral artery occlusions in rodents. The most straightforward method is to close middle cerebral artery temporally with a micro clip, suture or permanently with prothrombotic measures (photo thrombosis, electrocoagulation). But craniectomy is required and recognized as the main drawback of this category of methods. As the physiological condition such as intracranial pressure, brain temperature could be changed through interruption of skull intact, and the operation itself incurs intracranial inflammation, brain trauma, blood-brain barrier disruption [156-158].

Another category of establishing acute ischemic stroke model in rodents is to block the middle cerebral artery proximally via endovascular approach, i.e., by inserting filament with enlarged tip, modified microtubes, or delivering emboli that could be in vitro prepared autologous blood clots (thromboembolic model) or macrospheres[106, 158]. Notably, the thromboembolic model seems to be more resemble to human acute ischemic stroke, as it responds to thrombolysis therapy [159]. There is also unpredictable partial or complete autolysis during thromboembolism and high variation of infarct volume/location as the situation in clinic [158]. These properties of thromboembolic method could however make it hard for treatment effect evaluation in pre-clinical neuroprotection studies, especially for those studies designed with endovascular mechanical recanalization, and for the labs not equipped with imaging facilities for baseline ischemia control. Thromboembolic middle cerebral artery occlusion model seems more suitable for mechanism investigation and thrombolytic agents development [160, 161].

Middle cerebral artery occlusion of rodents with intraluminal monofilament has been widely used for decades since its first introduction by Koizumi et al. [162] and modification by Longa et al.[163]. In contrast to direct middle cerebral artery clamping after craniectomy, the filament method offers several advantages. It preserves the integrity of the skull and, most importantly, allows for the induction of infarction in deep brain structures by occluding penetrating arteries that originate from the Willis circle, such as the anterior choroidal artery. This closely mimics one of the key features of human middle cerebral artery occlusion with

basal ganglia infarction [164]. Besides, the filament method enables precise control over the timing of occlusion and reperfusion.

Following the isolation of the carotid bifurcation, the filament can be introduced via the external or the common carotid artery, namely the Longa's and Koizumi approaches respectively. Both approaches have been reported to induce comparable total infarct volumes [165, 166]. But one disadvantage of the Koizumi's approach is that the common carotid artery must be permanently ligated after middle cerebral artery occlusion. This common carotid artery occlusion potentially leads to impaired hemodynamics in the ipsilateral hemisphere. Morris et al. reported a significantly impaired reperfusion in mice in which middle cerebral artery occlusion was induced following the Koizumi method [166]. In addition, less severe neuroinflammatory response while higher death rate were found when middle cerebral artery occlusion was conducted with the Koizumi approach in mice [165].

These advantages imply that the filament middle cerebral artery occlusion model established with the Longa's approach might be more practical for resembling clinical stroke. Together with technical considerations with the isolated external carotid artery stump enabling easier manipulations of the infusion port used for ICCI during ischemia as planned in our study, we decided in favor of the Longa's approach for establishing middle cerebral artery occlusion.

As with other methods, the high variability of infarction is a major concern in the filament rodent stroke model, as it increases animal usage and impairs statistical power [167]. Without considering inter-strain variable factors, from a technical perspective, introducing the filament of the right size (diameter and length) is therefore of critical significance for obtaining homogenous ischemia insult. However, a crucial reality is that choosing the "right" filament is more or less empirical, since it relies on the manufacturer's recommendation, which is based on the rat's body weight. The anatomical variability among individual rodents, for example the vessel size of the Willis circle, the location of the openings of middle cerebral artery and deep brain structures supplying penetrating arteries, cannot be evaluated in each rat in order to determine the most suitable filament.

In the control group of part III of our study, out of 11 rats who underwent successful middle cerebral artery occlusion and developed infarcts, 4 had no cortical infarcts, and 3 had no striatal infarcts. Possible reasons for these findings could be that, in rats without cortical

infarct, the middle cerebral artery opening was not completely occluded when using the recommended filament size due to the individual rat's larger vessel diameter of the Willis circle. Alternatively, the recommended filament might not have been long enough to simultaneously block the openings of the middle cerebral artery and the deep brain penetrating arteries that also branch from the Willis circle [150, 151].

Laser Doppler flowmetry is a useful tool for confirming correct placement of the filament for ischemia as well as adequate reperfusion after filament removal in the middle cerebral artery occlusion rodent model. Variability of infarct volumes could be decreased when laser Doppler flowmetry was used during experiments to control the residual cerebral blood flow during induction of focal cerebral ischemia [168].

As soon as the opening of the middle cerebral artery is blocked by the introduced filament, an abrupt decrease of the cerebral blood flow and thus the measured laser Doppler flowmetry curve can be observed in real time. Although the initial decrease of the laser Doppler flow signal has been a primary criterion for exclusion of rats with unsuccessful middle cerebral artery occlusion, laser Doppler flowmetry only covers the regional cerebral blood flow within just 1 mm^3 of brain tissue [169]. The residual laser Doppler flow signal is therefore easily affected by the location of the laser Doppler flowmetry probe and also other blood flow signals that may stem from any arteries located between the brain surface and the probe, mostly small meningeal arteries or remnants within the cranial diploe.

So far there is no consistency in the literature on the threshold, i.e., residual laser Doppler flow value that should be taken for selection of successful middle cerebral artery occlusion in rodents. An initial decrease of the laser Doppler flow signal to a level of below 20% to 50% of the baseline have been reported [170-173]. In order to further minimize the risk of brain lesion variability, some researchers performed secondary subject selection based on the neurofunctional deficits of the rats during ischemia [57] or after reperfusion [57, 101]. The downside of this kind of post-reperfusion selection is, however, that the intactness or the impairment of neurofunction may not be evaluable in rats undergoing hyperacute study treatment that is initiated during middle cerebral artery occlusion as it was the case in our study. In these cases, post-reperfusion neurofunction may be critically influenced by beneficial or adverse effects of the study treatment.

In part II of this project, we conducted continuous regional cerebral blood flow monitoring with laser Doppler flowmetry throughout the whole experiment. Not only could we identify rats with an incomplete middle cerebral artery occlusion at the beginning, i.e., induction of ischemia, but also rats with a partial reperfusion during ischemia due to a displacement of the filament or because of cerebral artery autoregulation. We considered mean residual laser Doppler flow during the whole ischemia period of below 40% of baseline as a successful occlusion of the middle cerebral artery. Rats with a mean laser Doppler flow level above our threshold were excluded from randomization and study treatment.

Correlation between residual laser Doppler flow levels and infarct volume is controversial. There are studies implying that the level of residual laser Doppler flow during middle cerebral artery occlusion is not significantly correlated with the resulting infarct volume in both rats and mice [166, 174, 175]. In our study, strong negative correlation between residual laser Doppler flow levels and infarct volume was observed ($r = -0.73$). Similar finding was reported in a study by Matteo Riva et al. [176]. The laser Doppler flow probe in their study was however placed over the border zone between the anterior and middle cerebral artery territories that reflects the leptomeningeal collateral supply. In contrast, in our study, the laser Doppler probe was attached directly over the lateral middle cerebral artery territory to target the ischemic core.

Rates of successful middle cerebral artery occlusion using silicone coated filament as applied in our study, range from over 60% to 100% depending on the respective literature [177]. Under the relatively stricter criteria in part II of our study, the overall exclusion rate of rats due to insufficient ischemia was around 40%. However, in experimental part III of our study, in which we applied MRI for the exclusion of rats with unsuccessful filament occlusion of the middle cerebral artery, only 2 out of 26 rats were found without acute ischemia on both hyperacute diffusion and perfusion MRI at baseline (i.e., before any study treatment). This great difference (40% versus 8%) implies that the exclusion of rats with "unsuccessful" middle cerebral artery occlusion, as determined by laser Doppler in part II of our study, may have been potentially too extensive.

Drawing the baseline of middle cerebral artery occlusion induced cerebral ischemia before treatment is of critical importance in neuroprotection research. Brain imaging techniques such as MRI or perfusion CT have the great advantage of enabling the quantification of the intensity and the extent of ischemia at baseline and allowing for consecutive evaluation

after treatment. But their drawbacks are also obvious. Firstly, most of the stroke neuroprotection laboratories are not equipped with imaging facilities. Secondly, these imaging techniques only provide a snapshot of ischemia. Fluctuations of cerebral blood flow during ischemia or an accidental reperfusion would not be detected.

Laser Doppler flowmetry seems to continue being the most economic and practical method of detecting ischemia in middle cerebral artery occlusion experiments. But due to its semi-quantitative property and the use of arbitrarily chosen thresholds and probe locations in different neuroprotection laboratories [170-173], so far, a well-defined standard for exclusion of unsuccessful middle cerebral artery occlusion is still absent. In future studies, visually localizing the distal trunk of the middle cerebral artery and direct monitoring of changes in its blood flow after thinning the cranial bone for minimizing the risk of artifacts during measurement could be a promising strategy for standardizing species- and strain-specific laser Doppler flow thresholds.

As to the filament itself, it also needs to be modified in order to obtain more homogeneous ischemia. For example, a widely neglected drawback of the filament is its the stiffness. Insufficient flexibility of the filament's tip may limit its bending to perfectly fit the shape of the Willis circle. Deep brain structures supplying penetrating arteries (like the anterior choroidal artery) that could originate from the inner concave side of the Willis circle may have a higher likelihood to be fully occluded by the enlarged tip of the inserted filament because of better contact with the vessel wall. In contrast, the opening of the middle cerebral artery, when it is located on the outer convex side of the Willis circle, could be less likely to be fully occluded by the filament because of potential residual cavity. Improving the flexibility and softness of presently used filaments to better fit the Willis circle vessel anatomy is of great value for obtaining more uniform middle cerebral artery occlusion results.

The incidence of subarachnoid hemorrhage that results from tear-off of penetrating arteries or perforation of the Willis circle during filament insertion or retraction could be also decreased by using filament with better flexibility. Subarachnoid hemorrhage was a main factor contributing to the rats' death and experimental failure in our study, which could be easily identified on laser Doppler flowmetry curves by the presentation of a sudden severe decrease of regional cerebral blood flow and confirmed with autopsy. The rate of subarachnoid

hemorrhage was 5% (6 of 118 rats) in our study. It is in line with previous studies reporting subarachnoid hemorrhage rates ranging from 0% to 9% [177, 178].

ICCI mediated neuroprotection in middle cerebral artery occlusion rats

Previous studies in which intra-arterial cold infusion was tested achieved moderate selective brain hypothermia for less than 10 minutes [43]. In our study, we could sustain brain temperature at 32 to 33 °C over around 16 minutes when applying our elaborated pre- to post-reperfusion ICCI protocol. However, unlike the consistently reported improvement of functional outcomes and decrease of infarct volumes by 32% [112] to up to 90% [108] in comparison with non-treated rats in the previous studies, in part II of this project, we did not observe significant ICCI mediated neuroprotection at 24 hours post treatment.

Based on the theoretical concept of penumbral salvage in acute ischemic stroke [13] and our post-hoc analysis showing that lesion volumes of control animals negatively correlate with regional cerebral blood flow as assessed by laser Doppler flowmetry, we performed further analyses to evaluate ICCI efficacy within the two subgroups of rats with either moderate focal cerebral ischemia (i.e., 25% to < 40% of the baseline laser Doppler flow levels during ischemia) or severe focal cerebral ischemia (i.e., less than 25% of the baseline laser Doppler flow levels during ischemia). A threshold 25% was chosen because it is close to the median value (27%) of mean residual laser Doppler flow levels in the control group.

While ICCI did not prove any neuroprotective effect in the subgroup of rats with severe ischemia, infarct volumes and the extent of edema tended to be smaller in ICCI-treated rats within the moderate ischemia subgroup. Importantly, this observation was not statistically significant. The previously reported enormous neuroprotective capability of intra-arterial cold infusion in small animal studies could thus not be reproduced in our study (see **Table 1, Table 2**).

The differing results may be attributed to the relatively stricter exclusion criteria. Rats with unstable regional cerebral blood flow (as shown by laser Doppler flowmetry curves) during ischemia were excluded due to concerns about filament displacement during ischemia, which we observed during the experiments where even slight filament movements caused fluctuations in the laser Doppler flowmetry curves. However, changes in regional cerebral blood flow during ischemia could also result from collateral cerebral blood flow. Better

collateral blood flow may allow for greater penetration of ICCI into the ischemic tissue and could indicate a larger potentially salvageable penumbra, which could result in a more pronounced neuroprotective effect upon survival. In a study by Matteo Riva et al., higher variability in regional cerebral blood flow was detected with the laser Doppler probe attached over the border zone between the anterior and middle cerebral artery territories [176]. Another reason for the failure of ICCI as neuroprotectant could be that the neuroprotective efficacy of ICCI is not as strong as anticipated, especially in rats with more severe ischemia. To address this possibility, we conducted another study (part III) aiming to confirm or reject our hypothesis.

In part III of our study, we shortened the duration of middle cerebral artery occlusion to 60 minutes in order to achieve larger volume of potentially salvageable penumbra before treatment. Treatment was once again initiated during middle cerebral artery occlusion, but shortly before reperfusion, to simulate the clinical scenario of endovascular thrombectomy for proximal intracranial arterial occlusion. Additionally, serial MRI scans during ischemia (before treatment), at 24 hours and at two weeks after treatment allowed us to assess infarct development dynamically. Instead of solely comparing the final infarct volumes of the two treatment groups, we took advantage of serial MRI to assess the intra-individual progression of penumbra into infarcted brain tissue, thereby reducing variability.

Perfusion-diffusion mismatch on MRI has been a common practice in the determination of the brain tissue belonging to the irreversibly damaged ischemic core and the potentially salvageable penumbra [179]. Penumbral brain tissue is characterized by critical hypoperfusion on perfusion imaging without signal hyperintensity on diffusion MRI which is commonly regarded as the ischemic core. However, this method may potentially overestimate the penumbra's volume because perfusion thresholds often fail to discriminate the true penumbra from the surrounding less intensely hypo-perfused brain tissue, known as benign oligemia. It varies between subjects and during the course of ischemia due to dynamic changes of blood pressure or cerebral autoregulation [180]. In addition, the hyperintense lesion on diffusion MRI may not necessarily transform into total infarction, which was observed more frequently in acute ischemic stroke patients with small lesion size and successfully treated with thrombolysis or thrombectomy [181] [182].

Delineating salvageable penumbra using the perfusion-diffusion mismatch method for neuroprotection assessment of treatments thus remains a challenge in clinical studies. In

preclinical studies, the situation is less complicated, since ischemia duration and vital parameters could be well controlled. The impact of ischemia severity (collaterals) can be addressed by using standardized stroke models in a single species. By applying research center or even study specific perfusion thresholds that are obtained from control animals the inter-individual variability could be further minimized. Due to the shortened duration of middle cerebral artery occlusion, however, assessing whole brain perfusion MRI was not feasible. In our study, perfusion MRI was limited to 25 slices, which captured a representative but only a small portion of the middle cerebral artery supply territory. Since we were unable to image the entire penumbra, the salvaged volume would remain unclear. We therefore did not apply perfusion-diffusion mismatch-based neuroprotection assessment.

Instead, we evaluated the dynamic impact of ICCI on ischemic brain tissue using hyperacute ADC maps for baseline. In comparison with delineating brain territory on perfusion MRI, ADC maps reflect the combined effect of hypoperfusion severity and duration of cerebral ischemia. The decrease of the ADC occurs within minutes following ischemia onset because of cellular energy failure and consecutive dysfunction of the membrane potential and could be observed earlier than on diffusion MRI [183, 184]. Together with evidence that rapid reperfusion could reverse ADC in both animals and humans [185, 186], it implies that applying ADC with or without other image techniques could be likely to predict the true (reversible) penumbra [187, 188].

Both clinical and animal studies have been conducted to figure out ADC thresholds that could be used for predicting the definite ischemic core. For example, absolute ADC thresholds of 530×10^{-6} mm^2/second were reported in Sprague-Dawley rats [189] and 620×10^{-6} mm^2/second in acute ischemic stroke patients [190]. Considering the potential impact of differences in MR scanner settings, operation program, and of course the animal experimental setup, we determined ADC thresholds specific to this study in our control group. The optimal threshold to be applied on the ADC map of the whole ischemic hemisphere at baseline to predict total ischemic lesion volumes on ADC maps at 24 hours and final infarct volumes on T2-weighted imaging at 2 weeks was 70% as compared to the contralateral healthy hemisphere. This aligns with the reduction of ADC by 30% reported by Meng and colleagues. However, when expressed in an absolute value, the ADC threshold in our study was 439×10^{-6} mm^2/second, which is noticeably lower than the value in Meng's study [189]. This suggests that in future studies, when ADC thresholds are used to detect the penumbra or the ischemic core, absolute thresholds derived from prior studies should be applied cautiously. Instead, they

should be determined specifically for each research center, project or even study, based on control group data.

We could not find a suitable ADC threshold that could be used to predict the final infarct volume in the rats' striatum, likely because all animals ultimately developed a striatal infarct. A possible explanation for this could be that the striatum is supplied by penetrating arteries with poor collateral support. Together with its vulnerability to ischemia compared to the cerebral cortex [191], brain regions within the striatum could have resulted in irreversible ischemic tissue damage already at the timepoint of baseline diffusion MR scanning (about 39 minutes after filament occlusion of the middle cerebral artery) depending on the successfully occluded penetrating arteries.

The optimal threshold to be applied on baseline ADC maps for predicting cortical infarction in our study was 80% and thus higher than the optimal threshold for predicting the total infarct volume in the ischemic hemisphere. The neuroprotective effects of ICCI could have been potentially underrated if infarct volumes were not evaluated in a brain region-specific fashion. Specifically, the predicted cortical infarct volumes would have been smaller if the lower 70% threshold for total infarct volume prediction had been applied. Consequently, potential neuroprotective effects related to ICCI treatment (defined and calculated as the difference between predicted and actual infarct volume) would have been easier to overlook.

In this study, total infarct volumes that were observed in the ischemic hemisphere in the ICCI group at the 2-week timepoint were roughly one third smaller (~28%) than the predicted infarct volumes, which was mainly driven by a reduction of cortical infarct volume since no significant difference between predicted and measured infarct volume was observed in the striatum. The neuroprotective effects of ICCI that we observed in our study were at the lower end of the range of infarct volume reductions that were reported in previous studies by others which ranged between 29% and 77% (see **Table 2**).

Among these ICCI studies, a comparable duration of 15 minutes was administered only in one study conducted by Kurisu et al. [101]. Despite middle cerebral artery occlusion was maintained for twice as long (2 hours) in this study, a reduction of infarct volumes by 72% was observed [101]. Large differences of infusion parameters and/or poor transparency on key technical information (see **Table 2)** limit the comparability with our study results and can

therefore not be used to explain the lower neuroprotective effectiveness of ICCI that was observed in our study.

In summary, ICCI mediated neuroprotective effects on intra-individual ischemic core growth were observed in part III of our study when rats were exposed to 60 minutes of middle cerebral artery occlusion. Although selective brain hypothermia was achieved at an earlier timepoint (i.e., before reperfusion) and over a comparable or even longer duration, the neuroprotective effects were found to be less important as compared to those reported in the majority of previous studies (see **Table 1, Table 2**). The use of MRI for intra-individual assessment of ischemic core growth revealed that ICCI may mainly protect the ischemic penumbra in the better collateralized cortex from further evolving into infarct rather than impacting stroke progression in the more densely ischemic striatum. To achieve more reproducible ischemic core and penumbra, future ICCI studies that aim at optimizing infusion parameters should consider the clipping model of middle cerebral artery occlusion which leads to only cortical infarction with a better homogeneity, especially in case research groups have no access to image support.

ICCI related complications in middle cerebral artery occlusion rats

In accordance with both computational simulation and previous small animal studies, ICCI cooled the brain efficiently in our study. In contrast to whole-body cooling induced with intra-venous cold infusion which led to a decrease of core body temperature of about 2.5 °C, ICCI decreased core body temperature by only less than 0.7 °C. This difference in core body temperature decrease is surely partly due to the local heat exchange first in the ischemic target tissue, but also due to the fact that we used a peripheral heating system for stabilizing extracranial body temperature during ICCI. This peripheral heating system was turned off in rats undergoing treatment with intra-venous cold infusion in order not to counteract fast induction of systemic hypothermia.

Compared with whole-body cooling with an identical volume of intra-venous cold infusion, ICCI had less impact on blood gases, i.e., less severe acidosis, carbon dioxide retention, and decrease of arterial oxygen pressure. This may be related to the reduced breathing frequency and, consequently, pulmonary ventilation caused by more severe decreases in core body temperature that we observed in the intra-venous cold infusion group [192, 193]. But we did not monitor respiratory rate in our study and thus cannot confirm this

hypothesis. In both ventilated patients and rodents that were treated with intra-arterial cold infusion, the blood gases were reported to remain within the normal range [194, 195].

Another possible explanation could be a more pronounced effect of whole-body hypothermia on the gas binding ability of the blood including that of carbon dioxide and oxygen. Importantly, the hypothermia mediated left shift of the oxygen-hemoglobin binding curve could potentially result in a decreased oxygen delivery to the ischemic brain tissue. As we did not measure the cerebral metabolic rate of oxygen, we cannot conclude whether this effect is more pronounced during ICCI than during whole-body cooling with intra-venous cold infusion. Whole-body hypothermia may also lead to increased oxygen consumption due to cold shivering [196, 197], but it was not the case in our study for rats under anesthesia.

The death rate in ICCI treated rats was comparable to that observed in the control group and the other treatment groups, i.e., the intra-venous cold infusion group and the intra-carotid artery warm infusion group. Deaths were mainly caused by subarachnoid hemorrhage during filament insertion or retraction and thus, related to the middle cerebral artery occlusion approach rather than to any study (infusion) treatment. In ICCI treated rats (5 / 11) however the rate of hemorrhagic transformation observed on MRI was numerically higher as compared to the hemorrhagic transformation rate in the control group (2 / 10). Because we did not evaluate intra-carotid artery warm infusion in our MRI study, no conclusion can be made on whether the potentially higher hemorrhagic transformation rate was related to the intra-carotid artery infusion or the infusate's temperature. Because all cases of hemorrhagic transformation occurred beyond the assessment at 24 hours, one could even conclude that this effect was totally unrelated to study (infusion) treatment.

Hemorrhagic transformation is thought to result from blood brain barrier disruption caused by cerebral ischemia. Multiple mechanisms, such as a burst of reactive oxygen species after reperfusion, activation of neuroinflammation, or increased matrix metalloproteinase activity are involved in the process of blood brain barrier breakdown. However, in previous studies it has been widely reported that ICCI mediated local hypothermia inhibits those factors contributing to blood brain barrier breakdown [198-201] . This is further supported by the finding of our present study that ICCI mediated local hypothermia tends to alleviate cerebral edema (see **Figure 23**).

One potential reason accounting for the numerically higher rate of hemorrhagic transformation in the ICCI group as compared to the control group could be local hemodilution during infusion. This, together with hypothermia may have provoked local coagulopathy either by affecting plasmatic coagulation or platelet aggregation. Lower procoagulant platelet level and the use of antiplatelets especially in severe strokes have been reported to be related to increased hemorrhagic transformation [202-204] . In the infusion groups, systemic hemodilution with decreased hematocrit, hemoglobin and glucose was observed. Local hemodilution within the treated hemisphere during ICCI could be even more severe, as it is the first place where blood and infused fluid were mixed. The obvious transient drop in the laser Doppler flow curves observed during the pre-reperfusion phase in both the ICCI and the intra-carotid artery warm infusion groups (see **table 10**, **Table 11**), could be a possible reflection of local hemodilution. Since CCA was clipped in the phase of local saline infusion in our model, the hemodilution in the downstream arteries including collaterals through which the locally instilled infusate reached the target tissue - must have been significantly greater. This is due to the lack of blood mixing with the infusate before it reached the target tissue, unlike in the intra-venous cold infusion group.

Another factor that may contribute to hemorrhagic transformation could be cerebral hyperperfusion during ICCI treatment [205], especially when administered at high infusion rates. In our study, a maximal infusion rate of 2.0 mL/minute was used. This flow rate equals to about 50% of the physiological blood flow in the common carotid artery of rats [206]. In patients undergoing diagnostic angiography, even higher rates of up to 8 ml/second [147] are used for contrast injection into the internal carotid artery, which could correspond to 90% of the blood flow (see CCA flow table summarized by Nigel Ackroyd et al. [97]). However, it should be noted that the duration of contrast injection is only 1.5 seconds [147] while ICCI at the highest rate in our study lasted for 42 seconds.

Infusion rate is not only an important parameter that determines cooling efficacy in ICCI, but also safety. However, to our best knowledge, few local infusion studies investigated the impact of infusion rate on hemodilution and hemodynamics as we did, using continuous laser Doppler flowmetry throughout the experiment including infusion treatments. In our point of view, the maximal but safe infusion rate and duration in both rats with healthy and infarcted brain tissue should be determined before future ICCI studies are conducted.

Strength, Limitations

With this project, we were the first to establish a method for continuous pre- to post-reperfusion ICCI in rats, simulating the clinical scenario of endovascular mechanical thrombectomy using the large lumen guide catheter for infusion. As mentioned before, large animal studies would better resemble the clinical situation, but their application is obviously limited by related high costs and ethical considerations. Especially, optimal ICCI treatment variables such as timepoint of initiating ICCI, duration of treatment, fluid composition and their corresponding effects on local hemodilution and hemodynamic changes are at present not clear. By applying our experimental setup, those questions could be answered in generally more accepted and cost-effective small animal studies.

In comparison with existing intra-arterial cold infusion rodent studies, we did not only perform conventional arterial blood tests including blood gases, serum electrolytes, glucose and hematocrit, but also continuously monitored physiological parameters during treatment. However, results of blood tests, blood pressure and heart rate only reflect the systemic impact of treatments. Local infusion incurred downstream hemodilution and hemodynamic changes were not sufficiently evaluated in this study.

In the neuroprotection studies, to minimize the variability of baseline ischemia, we continuously monitored regional cerebral blood flow throughout the whole operation. Our approach was stricter in comparison with prior studies, in which regional cerebral blood flow was solely measured at the timepoints of filament insertion (baseline), filament removal (reperfusion) and in very few studies intermittently during ischemia [207-209]. Under continuous regional cerebral blood flow monitoring, rats with incomplete middle cerebral artery occlusion that may result from filament shift or autoregulation of cerebral arteries during ischemia were excluded. Despite these measures, the infarct volumes obtained in our study were highly variable as determined using standard TTC staining of whole brain slices at 24 hours after reperfusion.

To further reduce variability of infarcts and thereby enable more accurate detection of potential study treatment effects, we used serial MRI in the following study (part III) for both baseline control and intra-individual longitudinal evaluation of striatal and cortical infarct progression. With MRI, baseline ischemia control was more reliable and led to less exclusions as compared to laser Doppler flowmetry based selection. Moreover, due to the reduced

variability, intra-individual assessment of infarct progression could facilitate the evaluation of even smaller treatment effects as compared to an inter-individual stroke volume comparison. In contrast to previous studies evaluating intra-arterial cold infusion, to our best knowledge, our study was the first in which the striatum and cortex were evaluated separately. ICCI was found to reduce cortical infarction while having little treatment effect on the striatum. Moreover, hemorrhagic transformation was found to be more pronounced in the striatum.

Since we could not show neuroprotection in part II of the study using TTC staining at 24 hours, based on the 3R principle (replacement, reduction, and refinement), we focused in part III of the study on the main goal to evaluate the effects of ICCI and did not repeat experiments with intra-venous cold infusion and intra-carotid artery warm infusion. The question of whether cooling or just increased infusion rates during intra-carotid artery infusion facilitate hemorrhagic transformation can thus not be answered. Considering the small number of animals, these two findings should be further investigated in future larger sized randomized controlled animal studies.

For the worries of traumatic brain injury potentially mitigating neuroprotective effects, we did not perform brain temperature monitoring during treatment in the part II and III of the study. But the whole project was performed under the same experimental setup as well as infusion protocol that has been shown to have good reproducibility in part I which included continuous brain temperature assessment.

Future orientations

Endovascular mechanical thrombectomy has become a standard treatment for acute ischemic stroke since 2015 [17]. ICCI could be the optimal adjunct therapy to endovascular mechanical thrombectomy with the advantages of easy implementation into the routine workflow and low costs. Up to now, however, neuroprotective efficacy of ICCI could not be concluded from any existing clinical studies [94-96]. This is important to know when considering the history of translational failures during decades of neuroprotection research in acute ischemic stroke.

Enormous neuroprotection of both intra-arterial cold infusion as well as ICCI has consistently been reported in many rodent studies (**Table 1, Table 2**). Despite prolonging the duration of selective brain cooling and earlier induction in our setup, only mild neuroprotective

effects of ICCI were found in our study. To avoid unnecessary waste of time and resources by conducting large animal studies, repeating unsuccessful clinical studies, and/or putting patients in danger, small animal studies are still required for refining ICCI parameters.

Although brain temperature in previous small animal studies ranged between 30.5 °C and 36.5 °C, optimal target temperature that promotes most effective neuroprotection cannot be concluded from these studies, because none of these studies systematically investigated the impact of target temperature or any other parameter including infusion rate, treatment duration, time to target temperature and even the stroke model on infarct volume reduction. As discussed above, high infusion rates could result in local hemodilution that could potentially impair cerebral oxygenation and mitigate hypothermia mediated neuroprotection, and on the other hand could cause hyperperfusion which could potentially contribute to hemorrhagic transformation. Therefore, evaluating infusion rate dependent local hemodynamic changes and changes of blood composition in real time would be another important aspect which should be further investigated in rodents with or without middle cerebral artery occlusion. Ideally, rats that should be used in future studies should exhibit the same risk factors as ischemic stroke patients do, such as old age, hypertension or hyperglycemia. Moreover, ICCI needs to be tested in rats that also receive treatment with a common thrombolytic such as alteplase or tenecteplase.

Considering the inter-strain differences of cerebral blood supply and collaterals, studies investigating the optimal treatment variables should be conducted in a strain-specific manner. For example, in spontaneous hypertensive rats with poor collateral cerebral blood flow reserve [210], both cooling efficacy during the pre-reperfusion phase, when cold infusate indirectly reaches the target ischemic brain via collaterals, and the overall treatment effect might be compromised. To avoid the impact of ambient temperature on cortex, monitoring extracranial temperature at a normothermic level during the whole experiment should be also considered.

Cooling duration is another important factor that could critically impact the neuroprotective efficacy of ICCI. To achieve longer cooling duration with a fixed cold fluid volume, ICCI catheters equipped with closed-loop heat transfer balloons may be a promising solution. Currently, rodent-sized balloon catheters do not exist. This kind of catheter could only be tested in larger animals. But before that, all efforts should be made to determine the other favorable treatment variables of ICCI.

In future large animal studies, the main goal of applying balloon catheters should be to decrease infusion rate and fluid volume while achieving comparable cooling efficacy. The duration of ICCI should always be limited to that of the endovascular mechanical thrombectomy procedure, or at least not much longer. Prolonged stay in the catheter laboratory or neuro intensive care unit due to catheter retention would inevitably compromise the translational significance of ICCI.

Conclusion

In our studies, we put forward a guide catheter approach for continuous cold fluid delivery from before to after reperfusion, which could easily be implemented into the clinical procedure of endovascular mechanical thrombectomy of proximal vessel occlusion in acute ischemic stroke. It enables not only much earlier local hypothermia induction of the ischemic hemisphere compared to other intra-arterial cooling approaches and even more compared to whole-body cooling, but also avoids cooling interruption or delay of reperfusion as it was the case in previous animal studies and in the three clinical studies that tested intra-arterial cold infusion for neuroprotection in ischemic stroke. To confirm its neuroprotective capability, which is the prerequisite of initiating further studies in large animals and humans, we successfully simulated continuous ICCI in the middle cerebral artery occlusion rat model using a custom-made experimental setup. With the detailed description of experimental procedures provided in this thesis, this setup could be easily replicated.

Our data suggest that ICCI was neuroprotective, but the effect is not as robust as reported in most of the previous preclinical studies. Due to the large diversity of treatment variables applied in existing reports, as well as the fact that many aspects were only partially described or monitored, underlying reasons for this compromised effect could not be concluded from this study. ICCI had a minor impact on physiological parameters, serum electrolytes, blood gases but could be related with a higher rate of hemorrhagic transformation.

To facilitate large animal studies and prospective clinical translation, rodent studies are still warranted. Specifically, treatment variables that promote more effective neuroprotection, along with their impact on local hemodilution and hemodynamics, need to be investigated to optimize the efficacy and safety of ICCI.

References

1. Collaborators GBDS. Global, regional, and national burden of stroke and its risk factors, 1990-2019: A systematic analysis for the global burden of disease study 2019. *Lancet Neurol*. 2021;20:795-820
2. Collaborators GBDS. Global, regional, and national burden of stroke, 1990-2016: A systematic analysis for the global burden of disease study 2016. *Lancet Neurol*. 2019;18:439-458
3. Dirnagl U, Iadecola C, Moskowitz MA. Pathobiology of ischaemic stroke: An integrated view. *Trends Neurosci*. 1999;22:391-397
4. Wu TC, Grotta JC. Hypothermia for acute ischaemic stroke. *Lancet Neurol*. 2013;12:275-284
5. Gonzalez-Ibarra FP, Varon J, Lopez-Meza EG. Therapeutic hypothermia: Critical review of the molecular mechanisms of action. *Front Neurol*. 2011;2:4
6. Leker RR, Shohami E. Cerebral ischemia and trauma-different etiologies yet similar mechanisms: Neuroprotective opportunities. *Brain Res Brain Res Rev*. 2002;39:55-73
7. Durukan A, Tatlisumak T. Acute ischemic stroke: Overview of major experimental rodent models, pathophysiology, and therapy of focal cerebral ischemia. *Pharmacol Biochem Behav*. 2007;87:179-197
8. Gidday JM, Gasche YG, Copin JC, Shah AR, Perez RS, Shapiro SD, et al. Leukocyte-derived matrix metalloproteinase-9 mediates blood-brain barrier breakdown and is proinflammatory after transient focal cerebral ischemia. *Am J Physiol Heart Circ Physiol*. 2005;289:H558-568
9. Yang Y, Estrada EY, Thompson JF, Liu W, Rosenberg GA. Matrix metalloproteinase-mediated disruption of tight junction proteins in cerebral vessels is reversed by synthetic matrix metalloproteinase inhibitor in focal ischemia in rat. *J Cereb Blood Flow Metab*. 2007;27:697-709
10. Guglielmo MA, Chan PT, Cortez S, Stopa EG, McMillan P, Johanson CE, et al. The temporal profile and morphologic features of neuronal death in human stroke resemble those observed in experimental forebrain ischemia: The potential role of apoptosis. *Neurol Res*. 1998;20:283-296
11. Sairanen T, Karjalainen-Lindsberg ML, Paetau A, Ijas P, Lindsberg PJ. Apoptosis dominant in the periinfarct area of human ischaemic stroke--a possible target of antiapoptotic treatments. *Brain*. 2006;129:189-199
12. Saver JL. Time is brain--quantified. *Stroke*. 2006;37:263-266
13. Baron JC. Protecting the ischaemic penumbra as an adjunct to thrombectomy for acute stroke. *Nat Rev Neurol*. 2018;14:325-337
14. Saini V, Guada L, Yavagal DR. Global epidemiology of stroke and access to acute ischemic stroke interventions. *Neurology*. 2021;97:S6-S16
15. Saqqur M, Uchino K, Demchuk AM, Molina CA, Garami Z, Calleja S, et al. Site of arterial occlusion identified by transcranial doppler predicts the response to intravenous thrombolysis for stroke. *Stroke*. 2007;38:948-954
16. Riedel CH, Zimmermann P, Jensen-Kondering U, Stingele R, Deuschl G, Jansen O. The importance of size: Successful recanalization by intravenous thrombolysis in acute anterior stroke depends on thrombus length. *Stroke*. 2011;42:1775-1777

17. Goyal M, Menon BK, van Zwam WH, Dippel DW, Mitchell PJ, Demchuk AM, et al. Endovascular thrombectomy after large-vessel ischaemic stroke: A meta-analysis of individual patient data from five randomised trials. *Lancet*. 2016;387:1723-1731
18. Nogueira RG, Jadhav AP, Haussen DC, Bonafe A, Budzik RF, Bhuva P, et al. Thrombectomy 6 to 24 hours after stroke with a mismatch between deficit and infarct. *N Engl J Med*. 2018;378:11-21
19. Albers GW, Marks MP, Kemp S, Christensen S, Tsai JP, Ortega-Gutierrez S, et al. Thrombectomy for stroke at 6 to 16 hours with selection by perfusion imaging. *N Engl J Med*. 2018;378:708-718
20. Sarraj A, Kleinig TJ, Hassan AE, Portela PC, Ortega-Gutierrez S, Abraham MG, et al. Association of endovascular thrombectomy vs medical management with functional and safety outcomes in patients treated beyond 24 hours of last known well: The select late study. *JAMA Neurol*. 2023;80:172-182
21. Yoshimura S, Sakai N, Yamagami H, Uchida K, Beppu M, Toyoda K, et al. Endovascular therapy for acute stroke with a large ischemic region. *N Engl J Med*. 2022;386:1303-1313
22. Yang P, Zhang Y, Zhang L, Zhang Y, Treurniet KM, Chen W, et al. Endovascular thrombectomy with or without intravenous alteplase in acute stroke. *N Engl J Med*. 2020;382:1981-1993
23. Coutinho JM, Liebeskind DS, Slater LA, Nogueira RG, Clark W, Davalos A, et al. Combined intravenous thrombolysis and thrombectomy vs thrombectomy alone for acute ischemic stroke: A pooled analysis of the swift and star studies. *JAMA Neurol*. 2017;74:268-274
24. Tao C, Nogueira RG, Zhu Y, Sun J, Han H, Yuan G, et al. Trial of endovascular treatment of acute basilar-artery occlusion. *N Engl J Med*. 2022;387:1361-1372
25. Jovin TG, Li C, Wu L, Wu C, Chen J, Jiang C, et al. Trial of thrombectomy 6 to 24 hours after stroke due to basilar-artery occlusion. *N Engl J Med*. 2022;387:1373-1384
26. Toyoda K. Tenecteplase versus alteplase in stroke thrombolysis: The last piece of the puzzle? *Lancet Neurol*. 2024
27. Meretoja A, Keshtkaran M, Saver JL, Tatlisumak T, Parsons MW, Kaste M, et al. Stroke thrombolysis: Save a minute, save a day. *Stroke*. 2014;45:1053-1058
28. Meretoja A, Keshtkaran M, Tatlisumak T, Donnan GA, Churilov L. Endovascular therapy for ischemic stroke: Save a minute-save a week. *Neurology*. 2017;88:2123-2127
29. Evenson KR, Foraker RE, Morris DL, Rosamond WD. A comprehensive review of prehospital and in-hospital delay times in acute stroke care. *Int J Stroke*. 2009;4:187-199
30. Walter S, Kostopoulos P, Haass A, Keller I, Lesmeister M, Schlechtriemen T, et al. Diagnosis and treatment of patients with stroke in a mobile stroke unit versus in hospital: A randomised controlled trial. *Lancet Neurol*. 2012;11:397-404
31. Ebinger M, Winter B, Wendt M, Weber JE, Waldschmidt C, Rozanski M, et al. Effect of the use of ambulance-based thrombolysis on time to thrombolysis in acute ischemic stroke: A randomized clinical trial. *JAMA*. 2014;311:1622-1631
32. Zhao H, Coote S, Easton D, Langenberg F, Stephenson M, Smith K, et al. Melbourne mobile stroke unit and reperfusion therapy: Greater clinical impact of thrombectomy than thrombolysis. *Stroke*. 2020;51:922-930

33. Navi BB, Audebert HJ, Alexandrov AW, Cadilhac DA, Grotta JC, Group PW. Mobile stroke units: Evidence, gaps, and next steps. *Stroke*. 2022;53:2103-2113
34. O'Collins VE, Macleod MR, Donnan GA, Horky LL, van der Worp BH, Howells DW. 1,026 experimental treatments in acute stroke. *Ann Neurol*. 2006;59:467-477
35. Chamorro A, Dirnagl U, Urra X, Planas AM. Neuroprotection in acute stroke: Targeting excitotoxicity, oxidative and nitrosative stress, and inflammation. *Lancet Neurol*. 2016;15:869-881
36. Chamorro A, Lo EH, Renu A, van Leyen K, Lyden PD. The future of neuroprotection in stroke. *J Neurol Neurosurg Psychiatry*. 2021;92:129-135
37. Hill MD, Goyal M, Menon BK, Nogueira RG, McTaggart RA, Demchuk AM, et al. Efficacy and safety of nerinetide for the treatment of acute ischaemic stroke (escape-na1): A multicentre, double-blind, randomised controlled trial. *Lancet*. 2020;395:878-887
38. Hagerdal M, Harp J, Nilsson L, Siesjo BK. The effect of induced hypothermia upon oxygen consumption in the rat brain. *J Neurochem*. 1975;24:311-316
39. Bernard SA, Gray TW, Buist MD, Jones BM, Silvester W, Gutteridge G, et al. Treatment of comatose survivors of out-of-hospital cardiac arrest with induced hypothermia. *N Engl J Med*. 2002;346:557-563
40. Hypothermia after Cardiac Arrest Study G. Mild therapeutic hypothermia to improve the neurologic outcome after cardiac arrest. *N Engl J Med*. 2002;346:549-556
41. Jacobs SE, Morley CJ, Inder TE, Stewart MJ, Smith KR, McNamara PJ, et al. Whole-body hypothermia for term and near-term newborns with hypoxic-ischemic encephalopathy: A randomized controlled trial. *Arch Pediatr Adolesc Med*. 2011;165:692-700
42. van der Worp HB, Sena ES, Donnan GA, Howells DW, Macleod MR. Hypothermia in animal models of acute ischaemic stroke: A systematic review and meta-analysis. *Brain*. 2007;130:3063-3074
43. Esposito E, Ebner M, Ziemann U, Poli S. In cold blood: Intraarteral cold infusions for selective brain cooling in stroke. *J Cereb Blood Flow Metab*. 2014;34:743-752
44. Kammersgaard LP, Rasmussen BH, Jorgensen HS, Reith J, Weber U, Olsen TS. Feasibility and safety of inducing modest hypothermia in awake patients with acute stroke through surface cooling: A case-control study: The copenhagen stroke study. *Stroke*. 2000;31:2251-2256
45. Testori C, Sterz F, Behringer W, Spiel A, Firbas C, Jilma B. Surface cooling for induction of mild hypothermia in conscious healthy volunteers - a feasibility trial. *Crit Care*. 2011;15:R248
46. De Georgia MA, Krieger DW, Abou-Chebl A, Devlin TG, Jauss M, Davis SM, et al. Cooling for acute ischemic brain damage (cool aid): A feasibility trial of endovascular cooling. *Neurology*. 2004;63:312-317
47. Georgiadis D, Schwarz S, Kollmar R, Schwab S. Endovascular cooling for moderate hypothermia in patients with acute stroke: First results of a novel approach. *Stroke*. 2001;32:2550-2553
48. Guluma KZ, Hemmen TM, Olsen SE, Rapp KS, Lyden PD. A trial of therapeutic hypothermia via endovascular approach in awake patients with acute ischemic stroke: Methodology. *Acad Emerg Med*. 2006;13:820-827

49. Lyden P, Hemmen T, Grotta J, Rapp K, Ernstrom K, Rzesiewicz T, et al. Results of the ictus 2 trial (intravascular cooling in the treatment of stroke 2). *Stroke*. 2016;47:2888-2895
50. Schwab S, Georgiadis D, Berrouschot J, Schellinger PD, Graffagnino C, Mayer SA. Feasibility and safety of moderate hypothermia after massive hemispheric infarction. *Stroke*. 2001;32:2033-2035
51. Poli S, Purrucker J, Priglinger M, Ebner M, Sykora M, Diedler J, et al. Rapid induction of cooling in stroke patients (icool1): A randomised pilot study comparing cold infusions with nasopharyngeal cooling. *Crit Care*. 2014;18:582
52. Li J, Wang D, Tao W, Dong W, Zhang J, Yang J, et al. Early consciousness disorder in acute ischemic stroke: Incidence, risk factors and outcome. *BMC Neurol*. 2016;16:140
53. Jarvis JL, Panchal AR, Lyng JW, Bosson N, Donofrio-Odmann JJ, Braude DA, et al. Evidence-based guideline for prehospital airway management. *Prehosp Emerg Care*. 2024;28:545-557
54. Hemmen TM, Raman R, Guluma KZ, Meyer BC, Gomes JA, Cruz-Flores S, et al. Intravenous thrombolysis plus hypothermia for acute treatment of ischemic stroke (ictus-l): Final results. *Stroke*. 2010;41:2265-2270
55. Geurts M, Petersson J, Brizzi M, Olsson-Hau S, Luijckx GJ, Algra A, et al. Coolist (cooling for ischemic stroke trial): A multicenter, open, randomized, phase ii, clinical trial. *Stroke*. 2017;48:219-221
56. van der Worp HB, Macleod MR, Bath PM, Bathula R, Christensen H, Colam B, et al. Therapeutic hypothermia for acute ischaemic stroke. Results of a european multicentre, randomised, phase iii clinical trial. *Eur Stroke J*. 2019;4:254-262
57. Huh PW, Belayev L, Zhao W, Koch S, Busto R, Ginsberg MD. Comparative neuroprotective efficacy of prolonged moderate intraischemic and postischemic hypothermia in focal cerebral ischemia. *J Neurosurg*. 2000;92:91-99
58. Wallner B, Schenk B, Hermann M, Paal P, Falk M, Strapazzon G, et al. Hypothermia-associated coagulopathy: A comparison of viscoelastic monitoring, platelet function, and real time live confocal microscopy at low blood temperatures, an in vitro experimental study. *Front Physiol*. 2020;11:843
59. Watts DD, Trask A, Soeken K, Perdue P, Dols S, Kaufmann C. Hypothermic coagulopathy in trauma: Effect of varying levels of hypothermia on enzyme speed, platelet function, and fibrinolytic activity. *J Trauma*. 1998;44:846-854
60. Piironen K, Tiainen M, Mustanoja S, Kaukonen KM, Meretoja A, Tatlisumak T, et al. Mild hypothermia after intravenous thrombolysis in patients with acute stroke: A randomized controlled trial. *Stroke*. 2014;45:486-491
61. Just B, Delva E, Camus Y, Lienhart A. Oxygen uptake during recovery following naloxone. Relationship with intraoperative heat loss. *Anesthesiology*. 1992;76:60-64
62. Flickinger KL, Weissman A, Elmer J, Coppler PJ, Guyette FX, Repine MJ, et al. Metabolic manipulation and therapeutic hypothermia. *Ther Hypothermia Temp Manag*. 2023
63. Bay J, Nunn JF, Prys-Roberts C. Factors influencing arterial po2 during recovery from anaesthesia. *Br J Anaesth*. 1968;40:398-407
64. JONES HD, MCLAREN CAB. Postoperative shivering and hypoxaemia after halothane, nitrous oxide and oxygen anaesthesia. *BJA: British Journal of Anaesthesia*. 1965;37:35-41

65. Togo M, Akazawa Y, Akashi T, Yamashita R, Yoshitomi I, Ohba K, et al. Comprehensive prospective analysis of the factors contributing to aspiration pneumonia following endoscopic submucosal dissection in patients with early gastric neoplasms. *Acta Med Okayama*. 2020;74:407-413
66. Hoffmann S, Harms H, Ulm L, Nabavi DG, Mackert BM, Schmehl I, et al. Stroke-induced immunodepression and dysphagia independently predict stroke-associated pneumonia - the predict study. *J Cereb Blood Flow Metab*. 2017;37:3671-3682
67. Chamorro A, Amaro S, Vargas M, Obach V, Cervera A, Torres F, et al. Interleukin 10, monocytes and increased risk of early infection in ischaemic stroke. *J Neurol Neurosurg Psychiatry*. 2006;77:1279-1281
68. Yenari MA, Han HS. Neuroprotective mechanisms of hypothermia in brain ischaemia. *Nat Rev Neurosci*. 2012;13:267-278
69. Laupland KB, Zahar JR, Adrie C, Minet C, Vesin A, Goldgran-Toledano D, et al. Severe hypothermia increases the risk for intensive care unit-acquired infection. *Clin Infect Dis*. 2012;54:1064-1070
70. Martins PN, Schlegel A, Ghinolfi D. Cold or not so cold?-static organ preservation at 10 degrees c may prolong organ preservation and facilitate transplant logistics. *Transplantation*. 2022;106:427-429
71. Faberowski N, Stefansson E, Davidson RC. Local hypothermia protects the retina from ischemia. A quantitative study in the rat. *Invest Ophthalmol Vis Sci*. 1989;30:2309-2313
72. Mowlavi A, Neumeister MW, Wilhelmi BJ, Song YH, Suchy H, Russell RC. Local hypothermia during early reperfusion protects skeletal muscle from ischemia-reperfusion injury. *Plast Reconstr Surg*. 2003;111:242-250
73. Otake H, Shite J, Paredes OL, Shinke T, Yoshikawa R, Tanino Y, et al. Catheter-based transcoronary myocardial hypothermia attenuates arrhythmia and myocardial necrosis in pigs with acute myocardial infarction. *J Am Coll Cardiol*. 2007;49:250-260
74. Wang F, Luo Y, Ling F, Wu H, Chen J, Yan F, et al. Comparison of neuroprotective effects in ischemic rats with different hypothermia procedures. *Neurol Res*. 2010;32:378-383
75. Zhao J, Mu H, Liu L, Jiang X, Wu D, Shi Y, et al. Transient selective brain cooling confers neurovascular and functional protection from acute to chronic stages of ischemia/reperfusion brain injury. *J Cereb Blood Flow Metab*. 2019;39:1215-1231
76. Tauchi M, Tejada de Rink MM, Fujioka H, Okayama S, Nakamura KI, Dietel B, et al. Targeted temperature management: Peltier's element-based focal brain cooling protects penumbra neurons from progressive damage in experimental cerebral ischemia. *Ther Hypothermia Temp Manag*. 2018;8:225-233
77. Wang H, Olivero W, Lanzino G, Elkins W, Rose J, Honings D, et al. Rapid and selective cerebral hypothermia achieved using a cooling helmet. *J Neurosurg*. 2004;100:272-277
78. Poli S, Purrucker J, Priglinger M, Diedler J, Sykora M, Popp E, et al. Induction of cooling with a passive head and neck cooling device: Effects on brain temperature after stroke. *Stroke*. 2013;44:708-713
79. Andrews PJ, Harris B, Murray GD. Randomized controlled trial of effects of the airflow through the upper respiratory tract of intubated brain-injured patients on brain temperature and selective brain cooling. *Br J Anaesth*. 2005;94:330-335

80. Harris BA, Andrews PJ, Murray GD. Enhanced upper respiratory tract airflow and head fanning reduce brain temperature in brain-injured, mechanically ventilated patients: A randomized, crossover, factorial trial. *Br J Anaesth*. 2007;98:93-99
81. Poli S, Purrucker J, Priglinger M, Sykora M, Diedler J, Rupp A, et al. Safety evaluation of nasopharyngeal cooling (rhinochill(r)) in stroke patients: An observational study. *Neurocrit Care*. 2014;20:98-105
82. Lu H, Lam LCW, Ning Y. Scalp-to-cortex distance of left primary motor cortex and its computational head model: Implications for personalized neuromodulation. *CNS Neurosci Ther*. 2019;25:1270-1276
83. McCalley DM, Hanlon CA. Regionally specific gray matter volume is lower in alcohol use disorder: Implications for noninvasive brain stimulation treatment. *Alcohol Clin Exp Res*. 2021;45:1672-1683
84. Nowak K, Mix E, Gimsa J, Strauss U, Sriperumbudur KK, Benecke R, et al. Optimizing a rodent model of parkinson's disease for exploring the effects and mechanisms of deep brain stimulation. *Parkinsons Dis*. 2011;2011:414682
85. Galiakhmetova D, Dremin V, Koviarov A, Stoliarov D, Ngum N, Murugesan RC, et al. Ultra-short laser pulses propagation through mouse head tissues: Experimental and computational study. *IEEE Journal of Selected Topics in Quantum Electronics*. 2023;29:1-11
86. Wang H, Wang B, Normoyle KP, Jackson K, Spitler K, Sharrock MF, et al. Brain temperature and its fundamental properties: A review for clinical neuroscientists. *Front Neurosci*. 2014;8:307
87. Ghassemi M, Shahidian A. Chapter 3 - biosystems heat and mass transfer. In: Ghassemi M, Shahidian A, eds. *Nano and bio heat transfer and fluid flow*. Oxford: Academic Press; 2017:31-56.
88. Abou-Chebl A, Sung G, Barbut D, Torbey M. Local brain temperature reduction through intranasal cooling with the rhinochill device: Preliminary safety data in brain-injured patients. *Stroke*. 2011;42:2164-2169
89. Williams LR, Leggett RW. Reference values for resting blood flow to organs of man. *Clin Phys Physiol Meas*. 1989;10:187-217
90. Cattaneo G, Schumacher M, Wolfertz J, Jost T, Meckel S. Combined selective cerebral hypothermia and mechanical artery recanalization in acute ischemic stroke: In vitro study of cooling performance. *AJNR Am J Neuroradiol*. 2015;36:2114-2120
91. Cattaneo G, Schumacher M, Maurer C, Wolfertz J, Jost T, Buchert M, et al. Endovascular cooling catheter for selective brain hypothermia: An animal feasibility study of cooling performance. *AJNR Am J Neuroradiol*. 2016;37:885-891
92. Cattaneo GF, Herrmann AM, Eiden SA, Wieser M, Kellner E, Doostkam S, et al. Selective intra-carotid blood cooling in acute ischemic stroke: A safety and feasibility study in an ovine stroke model. *J Cereb Blood Flow Metab*. 2021;41:3097-3110
93. Choi JH, Marshall RS, Neimark MA, Konstas AA, Lin E, Chiang YT, et al. Selective brain cooling with endovascular intracarotid infusion of cold saline: A pilot feasibility study. *AJNR Am J Neuroradiol*. 2010;31:928-934
94. Peng X, Wan Y, Liu W, Dan B, Lin L, Tang Z. Protective roles of intra-arterial mild hypothermia and arterial thrombolysis in acute cerebral infarction. *Springerplus*. 2016;5:1988

95. Chen J, Liu L, Zhang H, Geng X, Jiao L, Li G, et al. Endovascular hypothermia in acute ischemic stroke: Pilot study of selective intra-arterial cold saline infusion. *Stroke*. 2016;47:1933-1935
96. Wu C, Zhao W, An H, Wu L, Chen J, Hussain M, et al. Safety, feasibility, and potential efficacy of intraarterial selective cooling infusion for stroke patients treated with mechanical thrombectomy. *J Cereb Blood Flow Metab*. 2018;38:2251-2260
97. Ackroyd N, Gill R, Griffiths K, Kossoff G, Appleberg M. Quantitative common carotid artery blood flow: Prediction of internal carotid artery stenosis. *J Vasc Surg*. 1986;3:846-853
98. Konstas AA, Neimark MA, Laine AF, Pile-Spellman J. A theoretical model of selective cooling using intracarotid cold saline infusion in the human brain. *J Appl Physiol (1985)*. 2007;102:1329-1340
99. Slotboom J, Kiefer C, Brekenfeld C, Ozdoba C, Remonda L, Nedeltchev K, et al. Locally induced hypothermia for treatment of acute ischaemic stroke: A physical feasibility study. *Neuroradiology*. 2004;46:923-934
100. Song W, Wu YM, Ji Z, Ji YB, Wang SN, Pan SY. Intra-carotid cold magnesium sulfate infusion induces selective cerebral hypothermia and neuroprotection in rats with transient middle cerebral artery occlusion. *Neurol Sci*. 2013;34:479-486
101. Kurisu K, Abumiya T, Nakamura H, Shimbo D, Shichinohe H, Nakayama N, et al. Transarterial regional brain hypothermia inhibits acute aquaporin-4 surge and sequential microvascular events in ischemia/reperfusion injury. *Neurosurgery*. 2016;79:125-134
102. Ji YB, Wu YM, Ji Z, Song W, Xu SY, Wang Y, et al. Interrupted intracarotid artery cold saline infusion as an alternative method for neuroprotection after ischemic stroke. *Neurosurg Focus*. 2012;33:E10
103. Ji Y, Hu Y, Wu Y, Ji Z, Song W, Wang S, et al. Therapeutic time window of hypothermia is broader than cerebral artery flushing in carotid saline infusion after transient focal ischemic stroke in rats. *Neurol Res*. 2012;34:657-663
104. Duan Y, Wu D, Huber M, Shi J, An H, Wei W, et al. New endovascular approach for hypothermia with intrajugular cooling and neuroprotective effect in ischemic stroke. *Stroke*. 2020;51:628-636
105. Kurisu K, Abumiya T, Ito M, Gekka M, Osanai T, Shichinohe H, et al. Transarterial regional hypothermia provides robust neuroprotection in a rat model of permanent middle cerebral artery occlusion with transient collateral hypoperfusion. *Brain Res*. 2016;1651:95-103
106. Ding Y, Yao B, Zhou Y, Park H, McAllister JP, 2nd, Diaz FG. Prereperfusion flushing of ischemic territory: A therapeutic study in which histological and behavioral assessments were used to measure ischemia-reperfusion injury in rats with stroke. *J Neurosurg*. 2002;96:310-319
107. Ding Y, Li J, Rafols JA, Phillis JW, Diaz FG. Prereperfusion saline infusion into ischemic territory reduces inflammatory injury after transient middle cerebral artery occlusion in rats. *Stroke*. 2002;33:2492-2498
108. Ding Y, Li J, Luan X, Lai Q, McAllister JP, 2nd, Phillis JW, et al. Local saline infusion into ischemic territory induces regional brain cooling and neuroprotection in rats with transient middle cerebral artery occlusion. *Neurosurgery*. 2004;54:956-964; discussion 964-955

109. Luan X, Li J, McAllister JP, 2nd, Diaz FG, Clark JC, Fessler RD, et al. Regional brain cooling induced by vascular saline infusion into ischemic territory reduces brain inflammation in stroke. *Acta Neuropathol*. 2004;107:227-234
110. Li J, Luan X, Lai Q, Clark JC, McAllister JP, 2nd, Fessler R, et al. Long-term neuroprotection induced by regional brain cooling with saline infusion into ischemic territory in rats: A behavioral analysis. *Neurol Res*. 2004;26:677-683
111. Zhao WH, Ji XM, Ling F, Ding YC, Xing CH, Wu H, et al. Local mild hypothermia induced by intra-arterial cold saline infusion prolongs the time window of onset of reperfusion injury after transient focal ischemia in rats. *Neurol Res*. 2009;31:43-51
112. Chen J, Fredrickson V, Ding Y, Cheng H, Wang N, Ling F, et al. Enhanced neuroprotection by local intra-arterial infusion of human albumin solution and local hypothermia. *Stroke*. 2013;44:260-262
113. Chen J, Fredrickson V, Ding Y, Jiang L, Luo Y, Ji X. The effect of a microcatheter-based selective intra-arterial hypothermia on hemodynamic changes following transient cerebral ischemia. *Neurol Res*. 2015;37:263-268
114. Wei W, Wu D, Duan Y, Elkin KB, Chandra A, Guan L, et al. Neuroprotection by mesenchymal stem cell (msc) administration is enhanced by local cooling infusion (lci) in ischemia. *Brain Res*. 2019;1724:146406
115. Corey S, Abraham DI, Kaneko Y, Lee JY, Borlongan CV. Selective endovascular cooling for stroke entails brain-derived neurotrophic factor and splenic il-10 modulation. *Brain Res*. 2019;1722:146380
116. Wang B, Wu D, Dornbos Iii D, Shi J, Ma Y, Zhang M, et al. Local cerebral hypothermia induced by selective infusion of cold lactated ringer's: A feasibility study in rhesus monkeys. *Neurol Res*. 2016;38:545-552
117. Wu D, Chen J, Hussain M, Wu L, Shi J, Wu C, et al. Selective intra-arterial brain cooling improves long-term outcomes in a non-human primate model of embolic stroke: Efficacy depending on reperfusion status. *J Cereb Blood Flow Metab*. 2020;40:1415-1426
118. Wu D, Fu Y, Wu L, Huber M, Chen J, Yao T, et al. Reperfusion plus selective intra-arterial cooling (si-ac) improve recovery in a nonhuman primate model of stroke. *Neurotherapeutics*. 2020;17:1931-1939
119. Caroff J, King RM, Mitchell JE, Marosfoi M, Licwinko JR, Gray-Edwards HL, et al. Focal cooling of brain parenchyma in a transient large vessel occlusion model: Proof-of-concept. *J Neurointerv Surg*. 2020;12:209-213
120. Raoult H, Eugene F, Ferre JC, Gentric JC, Ronziere T, Stamm A, et al. Prognostic factors for outcomes after mechanical thrombectomy with solitaire stent. *J Neuroradiol*. 2013;40:252-259
121. Hussein HM, Saleem MA, Qureshi AI. Rates and predictors of futile recanalization in patients undergoing endovascular treatment in a multicenter clinical trial. *Neuroradiology*. 2018;60:557-563
122. Emberson J, Lees KR, Lyden P, Blackwell L, Albers G, Bluhmki E, et al. Effect of treatment delay, age, and stroke severity on the effects of intravenous thrombolysis with alteplase for acute ischaemic stroke: A meta-analysis of individual patient data from randomised trials. *Lancet*. 2014;384:1929-1935
123. Wu L, Wu D, Yang T, Xu J, Chen J, Wang L, et al. Hypothermic neuroprotection against acute ischemic stroke: The 2019 update. *J Cereb Blood Flow Metab*. 2020;40:461-481

124. Benali F, van der Leij C, Staals J, van Zwam WH. Use of heparinized saline flush during endovascular thrombectomy for acute ischemic stroke; a survey of clinical practice in the netherlands. *CVIR Endovasc*. 2021;4:76
125. Winningham MJ, Haussen DC, Nogueira RG, Liebeskind DS, Smith WS, Lutsep HL, et al. Periprocedural heparin use in acute ischemic stroke endovascular therapy: The trevo 2 trial. *J Neurointerv Surg*. 2018;10:611-614
126. Roth C, Papanagiotou P, Behnke S, Walter S, Haass A, Becker C, et al. Stent-assisted mechanical recanalization for treatment of acute intracerebral artery occlusions. *Stroke*. 2010;41:2559-2567
127. Castano C, Dorado L, Guerrero C, Millan M, Gomis M, Perez de la Ossa N, et al. Mechanical thrombectomy with the solitaire ab device in large artery occlusions of the anterior circulation: A pilot study. *Stroke*. 2010;41:1836-1840
128. Kang DH, Park J. Endovascular stroke therapy focused on stent retriever thrombectomy and direct clot aspiration: Historical review and modern application. *J Korean Neurosurg Soc*. 2017;60:335-347
129. Pederson JM, Reierson NL, Hardy N, Touchette JC, Medam S, Barrett A, et al. Comparison of balloon guide catheters and standard guide catheters for acute ischemic stroke: A systematic review and meta-analysis. *World Neurosurg*. 2021;154:144-153 e121
130. Ojha V, Raju SN, Deshpande A, Ganga KP, Kumar S. Catheters in vascular interventional radiology: An illustrated review. *Diagn Interv Radiol*. 2023;29:138-145
131. Papanagiotou P, Ntaios G. Endovascular thrombectomy in acute ischemic stroke. *Circ Cardiovasc Interv*. 2018;11:e005362
132. Mattingly TK, Denning LM, Siroen KL, Lehrbass B, Lopez-Ojeda P, Stitt L, et al. Catheter based selective hypothermia reduces stroke volume during focal cerebral ischemia in swine. *J Neurointerv Surg*. 2016;8:418-422
133. Alawieh A, Vargas J, Fargen KM, Langley EF, Starke RM, De Leacy R, et al. Impact of procedure time on outcomes of thrombectomy for stroke. *J Am Coll Cardiol*. 2019;73:879-890
134. Charbonnier G, Bonnet L, Bouamra B, Vuillier F, Vitale G, Moulin T, et al. Does intravenous thrombolysis influence the time of recanalization and success of mechanical thrombectomy during the acute phase of cerebral infarction? *Cerebrovasc Dis Extra*. 2020;10:28-35
135. Kidwell CS, Saver JL, Carneado J, Sayre J, Starkman S, Duckwiler G, et al. Predictors of hemorrhagic transformation in patients receiving intra-arterial thrombolysis. *Stroke*. 2002;33:717-724
136. Honig A, Percy J, Sepehry AA, Gomez AG, Field TS, Benavente OR. Hemorrhagic transformation in acute ischemic stroke: A quantitative systematic review. *J Clin Med*. 2022;11
137. Lee HB, Blaufox MD. Blood volume in the rat. *J Nucl Med*. 1985;26:72-76
138. Paxinos G, Watson C, Pennisi M, Topple A. Bregma, lambda and the interaural midpoint in stereotaxic surgery with rats of different sex, strain and weight. *J Neurosci Methods*. 1985;13:139-143
139. Paxinos G. The rat brain in stereotaxic coordinates. 2004
140. Kuts R, Frank D, Gruenbaum BF, Grinshpun J, Melamed I, Knyazer B, et al. A novel method for assessing cerebral edema, infarcted zone and blood-brain barrier breakdown in a single post-stroke rodent brain. *Front Neurosci*. 2019;13:1105

141. Chen J, Sanberg PR, Li Y, Wang L, Lu M, Willing AE, et al. Intravenous administration of human umbilical cord blood reduces behavioral deficits after stroke in rats. *Stroke*. 2001;32:2682-2688
142. Schaar KL, Brenneman MM, Savitz SI. Functional assessments in the rodent stroke model. *Exp Transl Stroke Med*. 2010;2:13
143. Gharbawie OA, Whishaw PA, Whishaw IQ. The topography of three-dimensional exploration: A new quantification of vertical and horizontal exploration, postural support, and exploratory bouts in the cylinder test. *Behav Brain Res*. 2004;151:125-135
144. Sheth SA, Jahan R, Gralla J, Pereira VM, Nogueira RG, Levy EI, et al. Time to endovascular reperfusion and degree of disability in acute stroke. *Ann Neurol*. 2015;78:584-593
145. Merrill TL, Mitchell JE, Merrill DR. Heat transfer analysis of catheters used for localized tissue cooling to attenuate reperfusion injury. *Med Eng Phys*. 2016;38:758-766
146. Baz RA, Scheau C, Niscoveanu C, Bordei P. Morphometry of the entire internal carotid artery on ct angiography. *Medicina (Kaunas)*. 2021;57
147. Raz E. Dsa imaging protocol and technique. In: Saba L, Raz E, eds. *Neurovascular imaging: From basics to advanced concepts*. New York, NY: Springer New York; 2016:67-84.
148. Choi J MS, Barone F, Novotney C, Lin E, Pile-Spellman J. Rapid and selective brain cooling and maintenance of selective cooling with intra-carotid cold fluid infusion is feasible and safe. *European Stroke Journal*. 2016;1:3-612
149. Faber JE, Storz JF, Cheviron ZA, Zhang H. High-altitude rodents have abundant collaterals that protect against tissue injury after cerebral, coronary and peripheral artery occlusion. *J Cereb Blood Flow Metab*. 2021;41:731-744
150. Pastor G, Jimenez-Gonzalez M, Plaza-Garcia S, Beraza M, Padro D, Ramos-Cabrer P, et al. A general protocol of ultra-high resolution mr angiography to image the cerebro-vasculature in 6 different rats strains at high field. *J Neurosci Methods*. 2017;289:75-84
151. He Z, Yang SH, Naritomi H, Yamawaki T, Liu Q, King MA, et al. Definition of the anterior choroidal artery territory in rats using intraluminal occluding technique. *J Neurol Sci*. 2000;182:16-28
152. Mangla S, Choi JH, Barone FC, Novotney C, Libien J, Lin E, et al. Endovascular external carotid artery occlusion for brain selective targeting: A cerebrovascular swine model. *BMC Res Notes*. 2015;8:808
153. Kim F, Nichol G, Maynard C, Hallstrom A, Kudenchuk PJ, Rea T, et al. Effect of prehospital induction of mild hypothermia on survival and neurological status among adults with cardiac arrest: A randomized clinical trial. *JAMA*. 2014;311:45-52
154. Caro AC, Hankenson FC, Marx JO. Comparison of thermoregulatory devices used during anesthesia of c57bl/6 mice and correlations between body temperature and physiologic parameters. *J Am Assoc Lab Anim Sci*. 2013;52:577-583
155. Roche M, Chaigneau E, Rungta RL, Boido D, Weber B, Charpak S. In vivo imaging with a water immersion objective affects brain temperature, blood flow and oxygenation. *Elife*. 2019;8

156. Liu CW, Wang EY, Wang HL, Liao KH, Chen HY, Chen HS, et al. Blood-brain barrier disruption in preclinical mouse models of stroke can be an experimental artifact caused by craniectomy. *eNeuro*. 2022;9
157. Sokolowski JD, Soldozy S, Sharifi KA, Norat P, Kearns KN, Liu L, et al. Preclinical models of middle cerebral artery occlusion: New imaging approaches to a classic technique. *Front Neurol*. 2023;14:1170675
158. Sommer CJ. Ischemic stroke: Experimental models and reality. *Acta Neuropathol*. 2017;133:245-261
159. Zhang L, Zhang RL, Jiang Q, Ding G, Chopp M, Zhang ZG. Focal embolic cerebral ischemia in the rat. *Nat Protoc*. 2015;10:539-547
160. Li Y, Zhang J. Animal models of stroke. *Animal Model Exp Med*. 2021;4:204-219
161. Wang R, Wang H, Liu Y, Chen D, Wang Y, Rocha M, et al. Optimized mouse model of embolic mcao: From cerebral blood flow to neurological outcomes. *J Cereb Blood Flow Metab*. 2022;42:495-509
162. Koizumi J. Experimental studies of ischemic brain edema. 1. A new experimental model of cerebral embolism in rats in which recirculation can be introduced in the ischemic area. *Jpn. J. Stroke.* 1986;8:1-8
163. Longa EZ, Weinstein PR, Carlson S, Cummins R. Reversible middle cerebral artery occlusion without craniectomy in rats. *Stroke*. 1989;20:84-91
164. Guglielmi V, Quaranta D, Masone Iacobucci G, Citro S, Scala I, Genovese D, et al. Basal ganglia ischaemic infarction after thrombectomy: Cognitive impairment at acute stage. *Eur J Neurol.* 2023;30:3772-3779
165. Smith HK, Russell JM, Granger DN, Gavins FN. Critical differences between two classical surgical approaches for middle cerebral artery occlusion-induced stroke in mice. *J Neurosci Methods*. 2015;249:99-105
166. Morris GP, Wright AL, Tan RP, Gladbach A, Ittner LM, Vissel B. A comparative study of variables influencing ischemic injury in the longa and koizumi methods of intraluminal filament middle cerebral artery occlusion in mice. *PLoS One*. 2016;11:e0148503
167. Strom JO, Ingberg E, Theodorsson A, Theodorsson E. Method parameters' impact on mortality and variability in rat stroke experiments: A meta-analysis. *BMC Neurosci*. 2013;14:41
168. Taninishi H, Jung JY, Izutsu M, Wang Z, Sheng H, Warner DS. A blinded randomized assessment of laser doppler flowmetry efficacy in standardizing outcome from intraluminal filament mcao in the rat. *J Neurosci Methods*. 2015;241:111-120
169. Cuccione E, Padovano G, Versace A, Ferrarese C, Beretta S. Cerebral collateral circulation in experimental ischemic stroke. *Exp Transl Stroke Med*. 2016;8:2
170. Hungerhuber E, Zausinger S, Westermaier T, Plesnila N, Schmid-Elsaesser R. Simultaneous bilateral laser doppler fluxmetry and electrophysiological recording during middle cerebral artery occlusion in rats. *J Neurosci Methods*. 2006;154:109-115
171. Esposito E, Hayakawa K, Ahn BJ, Chan SJ, Xing C, Liang AC, et al. Effects of ischemic post-conditioning on neuronal vegf regulation and microglial polarization in a rat model of focal cerebral ischemia. *J Neurochem*. 2018;146:160-172
172. Popp A, Jaenisch N, Witte OW, Frahm C. Identification of ischemic regions in a rat model of stroke. *PLoS One*. 2009;4:e4764

173. Wang J, Zhang P, Tang Z. Animal models of transient ischemic attack: A review. *Acta Neurol Belg*. 2020;120:267-275
174. Hedna VS, Ansari S, Shahjouei S, Cai PY, Ahmad AS, Mocco J, et al. Validity of laser doppler flowmetry in predicting outcome in murine intraluminal middle cerebral artery occlusion stroke. *J Vasc Interv Neurol*. 2015;8:74-82
175. Ingberg E, Dock H, Theodorsson E, Theodorsson A, Strom JO. Effect of laser doppler flowmetry and occlusion time on outcome variability and mortality in rat middle cerebral artery occlusion: Inconclusive results. *BMC Neurosci*. 2018;19:24
176. Riva M, Pappada GB, Papadakis M, Cuccione E, Carone D, Menendez VR, et al. Hemodynamic monitoring of intracranial collateral flow predicts tissue and functional outcome in experimental ischemic stroke. *Exp Neurol*. 2012;233:815-820
177. Liu S, Zhen G, Meloni BP, Campbell K, Winn HR. Rodent stroke model guidelines for preclinical stroke trials (1st edition). *J Exp Stroke Transl Med*. 2009;2:2-27
178. Gerriets T, Stolz E, Walberer M, Muller C, Rottger C, Kluge A, et al. Complications and pitfalls in rat stroke models for middle cerebral artery occlusion: A comparison between the suture and the macrosphere model using magnetic resonance angiography. *Stroke*. 2004;35:2372-2377
179. Albers GW. Expanding the window for thrombolytic therapy in acute stroke. The potential role of acute mri for patient selection. *Stroke*. 1999;30:2230-2237
180. Ebinger M, De Silva DA, Christensen S, Parsons MW, Markus R, Donnan GA, et al. Imaging the penumbra - strategies to detect tissue at risk after ischemic stroke. *J Clin Neurosci*. 2009;16:178-187
181. Albach FN, Brunecker P, Usnich T, Villringer K, Ebinger M, Fiebach JB, et al. Complete early reversal of diffusion-weighted imaging hyperintensities after ischemic stroke is mainly limited to small embolic lesions. *Stroke*. 2013;44:1043-1048
182. Scheldeman L, Wouters A, Bertels J, Dupont P, Cheng B, Ebinger M, et al. Reversibility of diffusion-weighted imaging lesions in patients with ischemic stroke in the wake-up trial. *Stroke*. 2023;54:1560-1568
183. Back T, Hoehn-Berlage M, Kohno K, Hossmann KA. Diffusion nuclear magnetic resonance imaging in experimental stroke. Correlation with cerebral metabolites. *Stroke*. 1994;25:494-500
184. Hoehn-Berlage M, Norris DG, Kohno K, Mies G, Leibfritz D, Hossmann KA. Evolution of regional changes in apparent diffusion coefficient during focal ischemia of rat brain: The relationship of quantitative diffusion nmr imaging to reduction in cerebral blood flow and metabolic disturbances. *J Cereb Blood Flow Metab*. 1995;15:1002-1011
185. Busch E, Kruger K, Allegrini PR, Kerskens CM, Gyngell ML, Hoehn-Berlage M, et al. Reperfusion after thrombolytic therapy of embolic stroke in the rat: Magnetic resonance and biochemical imaging. *J Cereb Blood Flow Metab*. 1998;18:407-418
186. Fiehler J, Foth M, Kucinski T, Knab R, von Bezold M, Weiller C, et al. Severe adc decreases do not predict irreversible tissue damage in humans. *Stroke*. 2002;33:79-86
187. Oppenheim C, Grandin C, Samson Y, Smith A, Duprez T, Marsault C, et al. Is there an apparent diffusion coefficient threshold in predicting tissue viability in hyperacute stroke? *Stroke*. 2001;32:2486-2491
188. Wetterling F, Chatzikonstantinou E, Tritschler L, Meairs S, Fatar M, Schad LR, et al. Investigating potentially salvageable penumbra tissue in an in vivo model of

transient ischemic stroke using sodium, diffusion, and perfusion magnetic resonance imaging. *BMC Neurosci*. 2016;17:82
189. Meng X, Fisher M, Shen Q, Sotak CH, Duong TQ. Characterizing the diffusion/perfusion mismatch in experimental focal cerebral ischemia. *Ann Neurol*. 2004;55:207-212
190. Purushotham A, Campbell BC, Straka M, Mlynash M, Olivot JM, Bammer R, et al. Apparent diffusion coefficient threshold for delineation of ischemic core. *Int J Stroke*. 2015;10:348-353
191. Payabvash S, Souza LC, Wang Y, Schaefer PW, Furie KL, Halpern EF, et al. Regional ischemic vulnerability of the brain to hypoperfusion: The need for location specific computed tomography perfusion thresholds in acute stroke patients. *Stroke*. 2011;42:1255-1260
192. Blair E, Fellows J. Pulmonary ventilation in hypothermia. *J Thorac Cardiovasc Surg*. 1960;39:305-311
193. McNicol MW. Respiratory failure and acid-base status in hypothermia. *Postgrad Med J*. 1967;43:674-676
194. Ren Y, Hashimoto M, Pulsinelli WA, Nowak TS, Jr. Hypothermic protection in rat focal ischemia models: Strain differences and relevance to "reperfusion injury". *J Cereb Blood Flow Metab*. 2004;24:42-53
195. Aslami H, Binnekade JM, Horn J, Huissoon S, Juffermans NP. The effect of induced hypothermia on respiratory parameters in mechanically ventilated patients. *Resuscitation*. 2010;81:1723-1725
196. Frank SM, Fleisher LA, Olson KF, Gorman RB, Higgins MS, Breslow MJ, et al. Multivariate determinants of early postoperative oxygen consumption in elderly patients. Effects of shivering, body temperature, and gender. *Anesthesiology*. 1995;83:241-249
197. Ralley FE, Wynands JE, Ramsay JG, Carli F, MacSullivan R. The effects of shivering on oxygen consumption and carbon dioxide production in patients rewarming from hypothermic cardiopulmonary bypass. *Can J Anaesth*. 1988;35:332-337
198. Ceulemans AG, Zgavc T, Kooijman R, Hachimi-Idrissi S, Sarre S, Michotte Y. The dual role of the neuroinflammatory response after ischemic stroke: Modulatory effects of hypothermia. *J Neuroinflammation*. 2010;7:74
199. Hamann GF, Burggraf D, Martens HK, Liebetrau M, Jager G, Wunderlich N, et al. Mild to moderate hypothermia prevents microvascular basal lamina antigen loss in experimental focal cerebral ischemia. *Stroke*. 2004;35:764-769
200. Tang XN, Liu L, Koike MA, Yenari MA. Mild hypothermia reduces tissue plasminogen activator-related hemorrhage and blood brain barrier disruption after experimental stroke. *Ther Hypothermia Temp Manag*. 2013;3:74-83
201. Kurisu K, Yenari MA. Therapeutic hypothermia for ischemic stroke; pathophysiology and future promise. *Neuropharmacology*. 2018;134:302-309
202. Prodan CI, Stoner JA, Cowan LD, Dale GL. Lower coated-platelet levels are associated with early hemorrhagic transformation in patients with non-lacunar brain infarction. *J Thromb Haemost*. 2010;8:1185-1190
203. Whiteley WN, Slot KB, Fernandes P, Sandercock P, Wardlaw J. Risk factors for intracranial hemorrhage in acute ischemic stroke patients treated with recombinant tissue plasminogen activator: A systematic review and meta-analysis of 55 studies. *Stroke*. 2012;43:2904-2909

204. Thomas SE, Plumber N, Venkatapathappa P, Gorantla V. A review of risk factors and predictors for hemorrhagic transformation in patients with acute ischemic stroke. *Int J Vasc Med*. 2021;2021:4244267
205. Huang J, Hao P, Chen Z, Deng K, Liu B, Xu Y. Quantitative assessment of hyperperfusion using arterial spin labeling to predict hemorrhagic transformation in acute ischemic stroke patients with mechanical endovascular therapy. *Eur Radiol*. 2024;34:579-587
206. Kenwright DA, Thomson AJ, Hadoke PW, Anderson T, Moran CM, Gray GA, et al. A protocol for improved measurement of arterial flow rate in preclinical ultrasound. *Ultrasound Int Open*. 2015;1:E46-52
207. Yang GY, Betz AL. Reperfusion-induced injury to the blood-brain barrier after middle cerebral artery occlusion in rats. *Stroke*. 1994;25:1658-1664; discussion 1664-1655
208. Lu X, Dong J, Zheng D, Li X, Ding D, Xu H. Reperfusion combined with intraarterial administration of resveratrol-loaded nanoparticles improved cerebral ischemia-reperfusion injury in rats. *Nanomedicine*. 2020;28:102208
209. Vigil TM, Frieler RA, Kilpatrick KL, Wang MM, Mortensen RM. Aconitate decarboxylase 1 suppresses cerebral ischemia-reperfusion injury in mice. *Exp Neurol*. 2022;347:113902
210. Coyle P, Heistad DD. Blood flow through cerebral collateral vessels in hypertensive and normotensive rats. *Hypertension*. 1986;8:II67-71

Statement of Contributions

Within the scope of the research conducted in the laboratory of Prof. Dr. med. Sven Poli, this project focused on using a guide catheter for continuous cold fluid delivery into the ischemic brain from pre- to post-reperfusion, aiming to achieve localized hypothermia. The experimental design and subsequent modifications were independently developed by the PhD candidate under the guidance of Prof. Sven Poli. Technical aspects of the project, including the combination of two brain thermoprobes into a single unit, the development of a rodent-specific intra-carotid artery infusion port, and the modification of the cooling system, were also carried out by the PhD candidate.

Under the direct quality control and close scientific supervision of Prof. Poli, and with scientific advice from the two advisory board members, Prof. Dr. rer. nat. Jonas Neher (Biomedical Center (BMC), Biochemistry, Faculty of Medicine, LMU Munich, Munich, Germany) and Prof. Dr. med. Simone Di Giovanni (Faculty of Medicine, Department of Brain Sciences, Imperial College London, London, UK), the majority of the research work for this project was conducted by the PhD candidate. This included all animal surgeries, brain harvesting, slicing and staining, infarct volume measurements, neurofunctional experiments (training and performance), and MRI image processing and analysis. Experimental data were collected by the candidate and interpreted together with Prof. Poli. The thesis was written independently by the candidate and revised in accordance with comments from Prof. Poli.

Further support during the animal experiments (e.g., animal transfer, research equipment/material preparation, and rating of neurofunctional scores) was provided by Mr. Xueyu Yang (MD candidate from the research group of Prof. Poli). MRI scanning during the long-term survival experiments was conducted by Dr. Kristin Patzwaldt with support from Dr. med. Salvador G. Castaneda-Vega (both from the research group of Prof. Dr. Bernd Pichler at the Werner Siemens Imaging Center, University of Tübingen, Tübingen, Germany).

Acknowledgments

First of all, I would like to thank my PhD supervisor (*auf Deutsch: Doktorvater*), Prof. Dr. med. Sven Poli, for his consistent support, guidance throughout this project, and his encouragement when things went wrong. The encouraging moments when we together addressed some kind of technical challenges will remain some of my happiest recollections. I would like to thank Prof. Dr. med. Ulf Ziemann (Director of the Department of Neurology, University Hospital of Tübingen, Tübingen, Germany) for providing me with this amazing platform to conduct this project.

I would also like to say "thank you" to my two co-supervisors, Prof. Dr. Jonas Neher (Biomedical Center (BMC), Biochemistry, Faculty of Medicine, LMU Munich, Munich, Germany) and Prof. Dr. med. Simone Di Giovanni (Faculty of Medicine, Department of Brain Sciences, Imperial College London, London, UK). Without their kind and thoughtful advice, this project could not be completed smoothly.

Further, I would like to express my sincere gratitude to Dr. med. Salvador G. Castaneda-Vega and Dr. Kristin Patzwaldt from the research group of Prof. Dr. Bernd Pichler at Werner Siemens Imaging Center, University of Tübingen, Tübingen, Germany for their outstanding work on the MRI scanning and later on advice on image analysis of this project. Besides, I would like to thank my colleague Mr. Xueyu Yang for his help during the animal experiments, Mrs. M.A. Julia Zeller (Study Coordinator at the Neurovascular Study Center, University Hospital of Tübingen) and Mrs. Gabriele Kuebart for their administrative support throughout this project.

Finally, I would like to thank my wife, Mrs. Dr. Liunan Song, and our four parents for their unconditional support. I would also like to thank, of course, my three kids for the constant happiness, occasional surprises, and rare troubles they bring me, which make my life feel more real.

Appendix

Abbreviations

ADC: Apparent Diffusion Coefficient

BGA: Blood Gas Analysis

BP: Blood Pressure

Bpm: Beats per minute

CCA: Common Carotid Artery

CT: Computed Tomography

CTRL: Control group

DALYs: Stroke-rated disability-adjusted-life-years

DICOM: Digital Imaging and Communications in Medicine

EVT: Endovascular Thrombectomy

HCO^{3-}: Hydrogen Carbonate

HR: Heart Rate

ICCI: Intra-Carotid Artery Cold Infusion

ICWI: Intra-Carotid Artery Warm Infusion group

IVCI: Intra-Venous Cold Infusion group

LDF: Laser Doppler Flowmetry

MAP: Mean Arterial Pressure

MCA: Middle Cerebral Artery

mNSS: modified Neurological Severity Score

MRI: Magnetic Resonance Imaging

NIfTI : Neuroimaging Informatics Technology Initiative

pCO2: Partial Pressure of Carbon dioxide

pO2: Partial Pressure of Oxygen

rCBF: Regional Cerebral Blood Flow

sO2: Oxygen Saturation.

T2-MRI: T2-weighted Magnetic Resonance Image

TTC: 2, 3, 5 - Triphenyltetrazolium Chloride

VOI: Volume of Interest

Macro code for batch measurement of brain regions on TTC staining pictures

```
//// ROI measurement

title = "Choose a Directory for importing images";
 msg = "Please choose a directory containing images";
 waitForUser(title,msg);

OriginDir = getDirectory("Choose a Directory");
FileArray = getFileList(OriginDir);
title = "Directory for saving the output images";
 msg = "Please choose a directory for saving output image";
 waitForUser(title, msg);

SaveDir = getDirectory("Choose a Directory")

run("Set Measurements...", "area standard area_fraction redirect = None decimal = 3");
length = lengthOf(FileArray);

for (i = 0; i < length; i++) {
//        threshold
          open(OriginDir + "/" + FileArray[i]);
          run("Make Binary");
          run("Analyze Particles...", "size = 10-Infinity show = Nothing display summarize");
          saveAs("PNG", SaveDir + FileArray[i]+".PNG");
          close("*");
}
```